2019

Multimodal Strategies of Host-Seeking Mosquitoes

Molly Zhen Liu

MULTIMODAL STRATEGIES OF HOST-SEEKING MOSQUITOES

A Thesis Presented to the Faculty of

The Rockefeller University

in Partial Fulfillment of the Requirements for

the degree of Doctor of Philosophy

by

Molly Zhen Liu

June 2019

MULTIMODAL STRATEGIES OF HOST-SEEKING MOSQUITOES

Molly Zhen Liu, Ph.D.

The Rockefeller University 2019

Mosquitoes use multiple sensory modalities, including olfaction, thermosensation, and vision, to hunt human hosts and obtain a blood-meal for egg production. Any individual sensory cue is an incomplete signal of a human host, and so a mosquito must integrate multimodal sensory information before committing to approaching and biting a person. Mosquito host-seeking behavior is thus a particularly fruitful model for studying multimodal integration because of its robustness, intricacy, and public health importance.

Using tethered and free flight assays, we have teased apart responses to attractive visual and thermal cues in female *Aedes aegypti*, the yellow fever mosquito, uncovering their contributions to host-seeking decisions and distinctions in how they modulate their responses to those cues depending on CO_2, the most salient cue in human breath. We show that mosquitoes orient towards visual contrast in flight, regardless of CO_2 concentration, and then sense CO_2 to unlock thermotaxis towards potential hosts.

Mosquitoes across their evolutionary lineage display an impressive variety of host choices, from mammals to cold-blooded frogs to leeches and earthworms, and the algorithms they use to weigh sensory host cues likely vary just as much. Our results illustrate how such weighting is performed in one species, providing a first glimpse into how general and contingent cues are integrated to produce host-seeking behavior in

mosquitoes. With the rapid development of genetic and neuroscience tools in mosquitoes, we are poised to uncover the neuronal mechanisms underlying multimodal integration in these charismatic and deadly insects.

In memory of BJ Kittredge, 郑用熙, and 关英.

For my parents, Pan Zheng and Yang Liu, who paved my path;

&

For my qtpoc siblings, to the path we'll make together.

ACKNOWLEDGEMENTS

The work of this thesis was done on the traditional lands of the Lenape, Canarsie, and Matinecock.

I’d like to thank the *Aedes aegypti* mosquitoes who made this work possible. Their intricate behaviors sparked new questions every day, and I feel honored to have spent my graduate school years watching them.

The people in the Vosshall lab made this work joyful. Leslie Vosshall, your choice to establish modern-day mosquito neurogenetics has inspired me and your shrewd mentorship has steadied me. I thank you for your support as I wandered into the wild blue yonder of mosquito vision. Ben Matthews and Laura Duvall first mentored me when I rotated in the lab and have continued to be forces of wisdom since. It’s a funny coincidence to be leaving at the same time as you, and I look forward to our collective move to the “west coast.” I can’t wait to see the brilliant work that will come out of your labs! Josh Zeng, my first graduate school friend, it was wonderful to share time with you in lab. Ben Matthews, Román Corfas, Trevor Sorrells, and Takeshi Morita helped and delighted me in my perpetual wrangling of behavioral assays. Meg Younger, it was so cool to set up shop in the two-photon room and watch you start up mosquito neuroscience. Ellen De Obaldia, it was an honor to wear the nylons, and thank you for being such a considerate and funny bay neighbor. Gloria Gordon, Libby Mejia, Isabel Gutierrez, and Barbara Ghelardi accomplished heroic feats every day in keeping this lab running so impeccably. I especially thank Gloria and Libby for raising mosquitoes and for the company and music across my bay. Nipun Basrur, Veronica Jove, Margo Herre,

Anjali Pandey, and Krithika Venkataraman: Thank you for your scientific illuminations and your dear companionship.

I feel inestimably lucky to have a committee composed of Vanessa Ruta and Gaby Maimon. Vanessa, your brilliance and thoughtfulness inspired and supported me. My long rotation with Gaby Maimon was to pattern the rest of my investigations at Rockefeller. Gaby, thank you for hosting my very first magnotether experiments, for the depth and clarity of your thoughts, and for always making time to talk science and life. The insights I gained in conversation with you have stayed with me throughout graduate school. I also thank Michael Reiser for being my external advisor. You have supported my scientific training since I was an undergraduate, and I am so honored to have you at my graduate thesis defense.

I give my deep gratitude to the invertebrate neuroscience community at Rockefeller. The monthly BSVMRKYZ meeting has the most stimulating science and the most delightfully unpronounceable name on campus. Buck Trible, my brother in bugs, thank you for the bug walks and the vodka twists. Aylesse Sordillo, Itzel Ishida, and May Dobosiewicz: Our lunches (and nights out) sustained me throughout graduate school. Lisa Fenk, thank you for being a vision scientist inspiration and for traipsing through Central Park with me, sticking our hands into tree holes. T Hart, thank you for being a fellow scientist-artist, and here’s to Comics Retreat. Kunal Shah, Jim Petrillo, Jonathan Hirokawa, and Kris Fonselius helped me at crucial points in my inadvertent engineering career. Thank you to my fellow board members at People at Rockefeller Identifying as Sexual/Gender minorities (PRISM): Devon Collins, Aaron Mertz, Gabriella Spitz-Becker, Josh Zeng, and now Mariano Cardenas, Aylesse Sordillo, Trevor Sorrells, and Tom Wiley. It has been such a pleasure to work alongside with you to make Rockefeller a better place and then leave the organization in your capable hands.

I was nurtured by numerous New York City institutions. Undiscovered Countries gave me a community and the inspiration to draw. I thank Alton Alburo, Barbara Begley, Kaela Mei-Shing Garvin, and Adin Lenahan for their artistry, curation, and friendship. Gandor Chorale, comprising Cameron Toy, Caroline Kittredge Faustine, and Cris Neglia, soundtracked my labwork. Thank you for the music, companionship, and also a car. Yellow Brown Power Hour and the performance/hotpot crew Regal Eagles showed me the possibilities of radical Asian-American art. My abiding gratitude to Wo Chan, Adrien Weibgen, Lara Lorenzo, Ryan Wong, Victory Matsui, and Rob Rusli. Last, I would like to thank the 67th St New York Public Library. The 10-minute walk from Rockefeller always cleared my head after a frustrating experiment. Thank you to the NYPL hold system and the innumerable books it gave me.

I somehow arrived in New York with an entourage of friends from Chicago. Thank you to Alex Laas, James Salazar, Abhinav Shrestha, and most of all Rob Jaslow for six years of roommates. Andrew Fan, Kelsey Ganser, and Jean Baptiste Point du Sable (“JB”): Your monthly phone calls and annual hospitality were perpetual balms, and I am so lucky for your friendship. Kira McDonald and Hye Yun Park, thank you for your friendships. You’ve sustained me at the finish line of graduate school.

This thesis is dedicated to the memory of three family members who passed away during my time in graduate school: BJ Kittredge, my mother-in(-common)-law, and my maternal grandparents, Zheng Yongxi and Guan Ying. I dedicate this thesis to my parents, Pan Zheng and Yang Liu. As scientists all, you made me possible. Thank you to my family: Cheng Liqing, Liu Guisong, Shuang Cai, Paul Faustine, and most of all Jonathan Liu.

As another New Yorker wrote, I came to this city to seek my fortune, and I found it in you, Caroline Kittredge Faustine. Thank you for the home that we have created with Jack Daniels (the cat). I am so excited for our next adventure.

TABLE OF CONTENTS

LIST OF FIGURES

Chapter 1: Introduction

1.1 Organizing multisensory behavior

All animals act according to sensory information gleaned from their external environment. These sensory cues are fundamentally uncertain, both in their intrinsic structure and in their reception by an animal's sensory organs. A hungry flying insect trying to find food using odor alone must confront not only the uncertainty of the stochastic structure of a three-dimensional odor plume, but also the uncertain probability of an odor molecule binding to her olfactory receptors. One method of increasing certainty is to combine information from multiple sensory systems. So, our exemplary flying insect does not rely solely on smelling food to determine the location of a food source. She assumes that the airborne food scent is traveling in the same direction as the wind, and she senses wind direction to orient flight properly. In flight, she gauges her flight direction by observing the direction that her visual world is moving.

This navigation is thus a multisensory behavior, for it takes input from multiple sensory modalities (olfaction, mechanosensation, and vision) to increase certainty about an important fact (location of food) and produce the appropriate motor output (flight towards the food). Other behaviors are more reflexively unimodal because they respond to sensory cues which signal more certain benefits or threats, such as a sudden visual loom that, even in the absence of other sensory cues, will trigger rapid escape in an insect that believes itself to be threatened by a predator attack.

To understand the neural basis of a complex behavior, we must understand how that behavior is organized. Complex behaviors can be decomposed into a cascade of simpler behaviors: an initiating sensory stimulus causes an animal to react in a way that generates a second stimulus, which then causes another reaction, and onwards until the animal performs the entire sequence. If the whole behavioral cascade relies on multiple sensory stimuli, does each step require integrating cues from one or more sensory modalities ("cross-modal stimuli")? Or does the multisensory nature of the behavior arise from the sequence of multiple reactions, each triggered by a single cue?

The truth for each specific behavior lies in a different place between those two extremes. Yet the precise balance is important to determine because each unique solution implies different underlying neural and genetic architectures. If the smallest effective behavioral unit in a sequence integrates cross-modal inputs, then that integration likely occurs within the smallest effective neural unit and is inherited in a linked genetic unit. In this section, I will use examples from across the animal kingdom to investigate the modularity of complex behavior and how neurons can integrate cross-modal stimuli within these modules. After this broad survey, I will turn to mosquito host-seeking behavior as a promising model for studying multisensory sequential behavior.

1.1.1 Complex behavior as a series of simpler modules

We humans perceive that we act according to conscious decisions made using a holistic map of the world around us. However, animals can behave according to much simpler stimuli. Founder of ethology Niko Tinbergen [Tinbergen, 1951] observed for male stickleback fish to begin courting, they needed only to see the swollen belly of a receptive female fish. All other sensory stimuli, such as odor or coloration, could be absent or different, and males would still proceed with the invariant motor program of courtship. Tinbergen termed the swollen belly a “sign stimulus,” and the resulting stereotyped courtship movement a “fixed action pattern.” He and his collaborator Konrad Lorenz would go on to characterize these simple sensorimotor modules in behaviors such as brooding in graylag geese, dove courtship, and more [Lorenz, 1981].

How can these simple fixed action patterns be built up to create more complex behavior? An example is mud wasps constructing their nest, classically investigated by Smith [Smith, 1978]. Australian mud wasps (*Paralastor* sp.) dig narrow holes where they keep their larvae and provision them with food. At the entrance of the hole, the wasps construct an elaborate bell-shaped funnel out of mud, hypothesized to protect the larvae from parasitic wasps. While the overall behavior is quite complex, Smith was able to demonstrate through a series of ingenious perturbations that construction can be

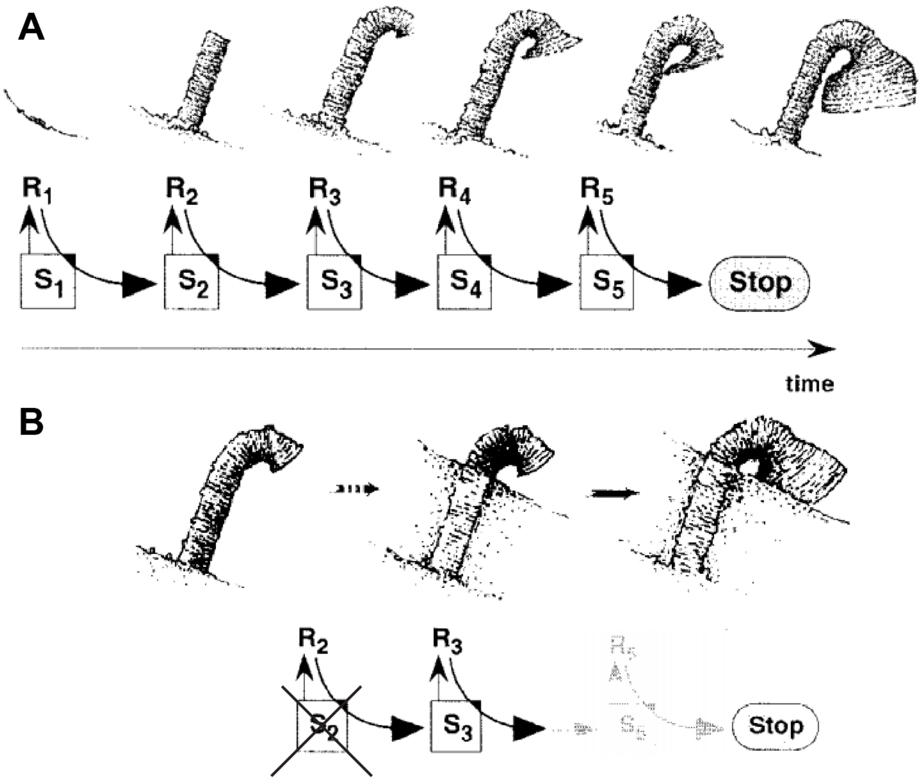

Figure 1.1 Serial fixed action patterns in mud wasp *Paralastor* sp. nest construction. (A) Standard five steps undertaken by mud wasps to construct their nests. **(B)** Results of an experimental perturbation. Modified from Theraulaz & Bonabeau, 1999 and Smith, 1978.

divided into five steps. Each step depends only on sensing a single local cue, regardless of the overall shape of the nest. Upon sensing a round hole (S_1), wasps build a long straight stem (R_1). Once the stem reaches a certain height (S_2), wasps begin to curve the stem (R_2). After the stem is sufficiently curved (S_3), wasps begin to build the funnel (R_3) (Fig 1.1A). If a nest was altered mid-construction, wasps only changed their behavior if it affected the local cue of their current step. For example, if a nest during R_3 had its stem shortened (disrupted S_2) but its curve preserved (normal S_3), construction proceeded normally, even though the finished funnel dragged against the ground (Fig 1.1B). Wasps build not by carrying through a unified vision of the finished nest, but by serially executing small, independent modules that create the conditions needed to move onto the next.

Smith separated this complex sequence into simple modules by carefully altering the sensory cues available to animals at different time points. More recently, researchers are parsing sequential behavior by using high-throughput genomic techniques to elucidate steps with different underlying genetic architectures [Weber et al., 2013; Kowalko et al., 2013; Greenwood et al., 2013]. A particularly fruitful platform for the genetic modularity of behavior has been the natural variation in nest construction between interfertile species of *Peromyscus* mice [reviewed in Hu & Hoekstra, 2017]. *Peromyscus polionotus* mice are specialized to life on open exposed fields. They dig three-part burrows comprised of a long entrance tunnel, a nest, and a long escape tunnel with a thin wall to the outside world which can be easily knocked down should a predator block the entrance tunnel. In contrast, mice of their sister species *Peromyscus maniculatus* live in a variety of habitats and dig simple, single-tunnel burrows.

What do genetic differences between the two species illuminate about the structure of complex burrow-digging? A team of scientists led by Weber and Hoekstra [Weber et al., 2013] demonstrated that mice from two generations of hybrid crosses of *P. polionotus* and *P. maniculatus* dug tunnels of intermediate and variable phenotypes. They dug entrance tunnels that ranged from typical short *P. maniculatus* to long *P. polionotus* lengths, and about half of them dug *P. polionotus*-typical escape tunnels. Notably, the tendency to dig a long entrance tunnel was only weakly correlated with the tendency to dig an escape tunnel, indicating that *P. polionotus* burrowing behavior is made up of at least two modules under separate genetic control. Indeed, mapping the genetic architecture of the behaviors revealed that three chromosomal regions contribute to variation in entrance tunnel length, and escape tunnel construction is associated with another single region. Weber et al. thus show that separate behavioral modules are correlated with separate genetic regions, an organization that facilitates the rapid evolution of behaviors as the genomes of succeeding generations mix and match the modules of their ancestors.

Not only are behavioral modules in a sequence under separate genetic control, they are also controlled by separate neural circuits. To describe this by example, it is useful to turn to model organism in which neural circuits can be precisely labeled and controlled: the vinegar fly, *Drosophila melanogaster.* The courtship of female flies by males involves a complex sequence of behavior, recognized as taking in multimodal olfactory, tactile, and visual cues since its first description in 1915 [Sturtevant, 1915]. Courtship occurs in three main phases [Bastock & Manning, 1955]. First, a male fly approaches and orients towards a female, visually maintaining a steady angle behind her [Markow, 1987; Agrawal et al., 2014; Ribeiro et al., 2018]. Second, he extends one wing and vibrates it in a stereotyped courtship song. Hearing the song, a receptive female signals interest by slowing down and pausing to allow him to make contact [Sturtevant, 1915; Bussell et al., 2014; Clemens et al., 2018]. Once he touches her, the third phase of engagement actions begin. The male taps and licks, the female opens her abdominal plates, and the sequence ends in copulation [Bastock & Manning, 1955; McKellar et al., 2019].

Each phase requires different sensory stimuli and is controlled by separate neural circuits. The second phase, courtship song, has been especially well-studied, with its different steps mapped to the level of single neurons. Male flies pattern their songs by rapidly switching between three stereotyped modes, named after the shape of their acoustic waveforms: fast pulse, slow pulse, and sine song [Clemens et al., 2017]. Interestingly, each mode appears to be a separate behavioral module, under unique sensory, neural, and motor control. While initiation and persistence of all parts of song require chemosensory stimuli [Agrawal et al., 2014; Kohatsu & Yamamoto, 2015], encoded and integrated by a sexually dimorphic circuit [Datta et al., 2008; Ruta et al., 2010; Clowney et al., 2015], only pulse mode qualities are modulated by a visual estimation of the female's distance [Coen et al., 2016]. Sine and pulse modes are encoded by separate neurons in the fly brain [Philipsborn et al., 2011; Clemens et al., 2018], controlled by different muscles of the fly wing [Shirangi et al., 2013; O'Sullivan et al., 2018], and perhaps even programmed by different genetic elements [Ding et al., 2016]. Successful *Drosophila melanogaster* males combine these modules to sing varied songs. His evolutionary cousins across the *Drosophila* tree sing modified songs that adapt pulses into clacks or change timing parameters of sine song, and so modification of each module appears to provide fertile ground for sexual selection and speciation [Cowling & Burnet, 1981; Ding et al., 2017].

These examples from fish, insects, and rodents illustrate an overall principle: Complex sequential behavior can be constructed by linking together simple sensorimotor modules. This idea has been widely used to program artificial intelligences to complete tasks, from efficiently vacuuming a room [Jones, 2006] to winning Ms. Pac-Man games [Schrum & Miikkulainen, 2014]. Further, the modularity of these behaviors corresponds to modularity in the genetic and neural architectures which program them. By elucidating the number and nature of modules within a complex behavior, we can learn how many neural transformations lie between sensory input to motor output, as well as which inputs are required at each step. Because these modules are inherited, we gain insight into how behaviors can diverge between species in the grand process of evolution.

1.1.2 Neural implementation of multisensory modules

When a single behavioral module requires cross-modal sensory input, what is the smallest effective neural unit that can integrate those stimuli? Neurons that responded to cross-modal stimuli were first described in the cat superior colliculus (SC) [Meredith & Stein, 1983; reviewed in Stein & Stanford, 2008]. Meredith and Stein found SC neurons which responded to stimuli in both visual (a moving dark bar) and auditory (a static tone) modalities. Though the neurons spiked in response to each modality alone, presenting them synchronously greatly amplified the spike rate, a phenomenon termed multisensory enhancement. Importantly, the receptive fields for both modalities spatially overlapped. Thus, multisensory enhancement depends on the two modalities being bound together in time and space, thus increasing the likelihood that they come from the same source. This finding demonstrated that single neurons can represent responses to cross-modal stimuli.

However, at least in large-brained vertebrates, network properties may determine the degree of multisensory enhancement. Further experiments [Jiang et al., 2001] revealed that multisensory enhancement in the cat SC is regulated by inputs from the anterior ectosylvian sulcus (AES), which itself does not have cross-modal responders. Abolishing those inputs did not disturb the ability of SC neurons to respond to visual and auditory stimuli, but the neurons were no longer able to *amplify* their responses to cross-modal stimuli. The same manipulation impaired a cat’s ability to orient towards and approach a combined audiovisual stimulus, although it did not have any defects in approaching unimodal stimuli [Wilkinson, 1996].

Neuronal populations appear to be particularly important for noisy sensory decisions, which is when we might expect multisensory integration to be most important for reducing uncertainty. Experiments by a team led by Raposo and Churchland [Raposo et al., 2012; Raposo et al., 2014] showed that both rats and humans can integrate visual and auditory stimuli over time to make decisions about the total rate of stimuli. In rats, these decisions are mediated by a varying population of cortical neurons that can be flexibly recoded to different modalities as the task changes. This experimental finding is supported by theoretical models demonstrating that sensory cues can be optimally integrated by simply summing neuronal population activities [Fetsch et al., 2013; Seilheimer et al., 2014].

Do smaller invertebrate brains also use population codes to enhance responses to multimodal stimuli? So far, a general principle has not emerged, and it is likely that the size of an effective neural unit depends on the specific behavioral task. The innate and stereotyped behavior of courting *Drosophila melanogaster* males relies on the sustained activation of approximately 20 male-specific interneurons, called P1. The population of P1 neurons receives direct feedforward input from both gustatory and olfactory channels, and the summation of those channels drives continued courtship [Clowney et al., 2015]. It is not yet known if individual neurons within the P1 cluster respond in distinct and fixed ways, or if they can be flexibly recoded like rat cortical neurons.

Because this population activity leads to fixed action patterns of song and courtship, these multiple interneurons must eventually converge to motor neurons. This has been elegantly shown in another system with an even more reduced nervous system, *Drosophila melanogaster* larvae [Ohyama et al., 2015]. Larval nervous systems consist of ~10,000 neurons, an order of magnitude smaller than the ~135,000-neuron adult brain. Despite this small size, larvae integrate touch and pain stimuli to roll away from putative predator attacks. These cross-modal stimuli simultaneously activate two circuits, one in the brain and the other in the nerve cord. Both streams integrate touch and pain stimuli at first-order multisensory interneurons. These interneurons combine information once again at later layers before both streams converge at a set of premotor neurons that command the motor pattern of rolling. These complex and seemingly redundant layers of multisensory processing distinguish even “simple” nervous systems.

Further, multisensory information is likely carried through means besides synaptic wiring of neurons. The ~302-neuron nervous system of *Caenorhabditis elegans* worms makes decisions to balance cross-modal appetitive food and aversive olfactory stimuli by biasing network properties with differential neuromodulator release [Harris et al., 2019]. Neuromodulators may represent yet another hidden repository of multisensory information [Bargmann, 2012].

Let us conclude this section with a few experimental principles drawn from this survey of neural systems. First, because even simple modules of multisensory integration have complex neural implementations with population-dependent properties, it is especially necessary to focus on small brains and behaviors that can be broken down into separate modules. Second, natural innate behaviors, such as courting or escape, have been useful in probing integration because they seem more likely to make use of populations with defined sensory inputs. The subject of this thesis, host-seeking of female *Aedes aegypti* mosquitoes, is a robust natural behavior in a small brain that promises to not only illuminate strategies of multisensory integration, but also impact human public health.

1.2 Mosquito host-seeking as a model sequence of multisensory behavior

Female mosquitoes transmit deadly pathogens from person to person because of their remarkable drive to seek out and bite human hosts. *Aedes aegypti* is the main vector of arborviruses that infect and sicken humans, such as dengue, Zika, yellow fever, and chikungunya [Bhatt et al., 2013; Kuehn, 2014; Matthews et al., 2019]. Because the blood meal provides protein crucial for egg development, female mosquitoes must find hosts to reproduce. While most blood-seeking mosquito species are generalists who drink from large classes of animals, such as all birds or all mammals, *Ae. aegypti* and a few other mosquitoes specialize on seeking humans. Much to our detriment, these human specialist mosquitoes have been effectively domesticated by us. Their adaptations include a distinct attraction toward humans over other animals [reviewed in McBride, 2016], as well as altered egg-laying behavior. While all mosquitoes lay their eggs in or along water upon the eggs' blood-nourished maturation, *Aedes aegypti* have evolved a preference for laying eggs on surfaces close to clean freshwater, environments which humans have created abundantly in the form of water containers and discarded tires [Matthews et al., 2018].

Mosquito host-seeking is highly relevant to human public health, and also serves as a model for robust, multisensory sequential behavior. *Ae. aegypti* female mosquitoes are nature's human-seeking missiles, using a combination of carbon dioxide from our breath, odor and heat from our skin, and contrast from our visual signature to find us (Fig 1.2). By studying the steps of host-seeking, we can better understand how small

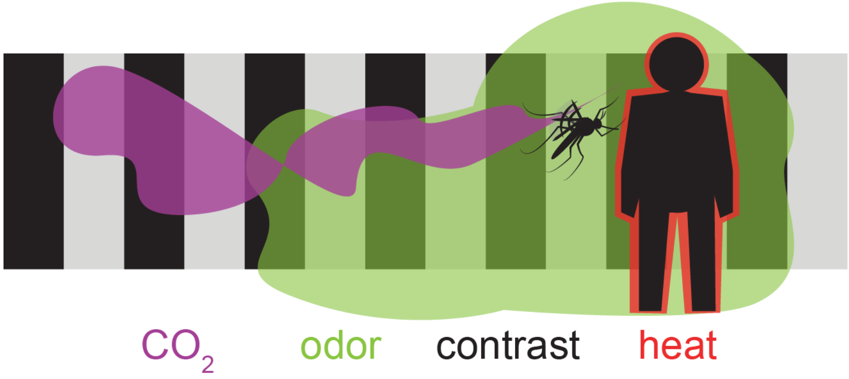

Figure 1.2 Schematic of sensory cues used by female *Ae. aegypti* to find hosts.

brains combine and process sensory information. We will begin by exploring the steps of host-seeking, each of which takes defined sensory inputs.

1.2.1 Takeoff and activation

A female mosquito begins her search for a host by initiating flight, or taking off. *Ae. aegypti* fly most in morning and evening [Taylor & Jones, 1968]. During these times, "roving flights" of *Aedes* mosquitoes have been reported, supposedly so that they may disperse and increase the range over which they can encounter hosts [Wellington, 1974]. While mosquitoes spontaneously take off, they take off most robustly in response to one particular sensory cue: carbon dioxide (CO_2). CO_2 is highly volatile and enriched in exhaled breath (approximately 4-5% of human exhalations vs. 0.04% in the atmosphere [Gillies, 1980]), making it a potent long-range signal of potential hosts. After exposure to elevated CO_2, female mosquitoes dramatically increase flight initiation [Daykin et al., 1965; reviewed in Gillies, 1980].

In addition to its role in initiating flight, CO_2 increases overall locomotor activity in female mosquitoes, an activity called "activation." Female mosquitoes are more likely to re-initiate flight [Daykin et al., 1965] and fly longer distances for over 2 minutes after a single increase in CO_2 concentration (Fig 1.3, from McMeniman et al., 2014). Male mosquitoes are also activated by CO_2, though to a much lesser degree [McMeniman et al., 2014]. Because males do not seek hosts, this has been speculated to be vestigial, or as a way to ensure that males can actively congregate near female attractants to mate. Further, CO_2 sensitizes mosquitoes to skin odors to enable further tracking [Dekker et al., 2005]. CO_2 is a uniquely potent host signal [Dekker & Carde, 2011;

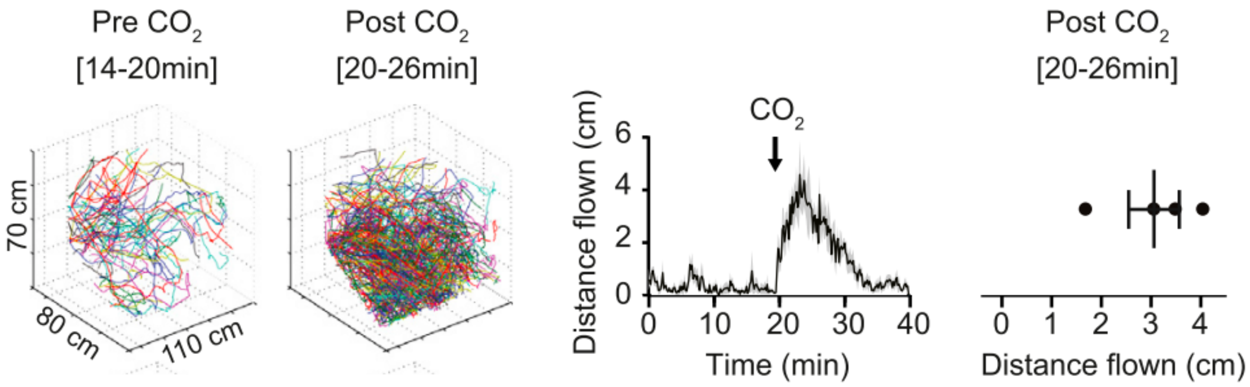

Figure 1.3 Female mosquitoes dramatically increase flight after exposure to elevated CO_2. (A) Raw 3D trajectories of 20 female mosquitoes before and after a 1000 ppm puff of CO_2 introduced at 20 minutes. **(B)** Quantification of mean distance flown per mosquito in the population. Line indicates mean, fill indicates standard error of the mean. **(C)** Mean distance flown during 6 minutes after introduction of CO_2. Adapted from McMeniman et al., 2014.

Gillies, 1980]. Just as the sign stimulus of a swollen stickleback female belly releases male stickleback courtship, the sign stimulus of CO_2 induces female mosquitoes to initiate and sustain host-seeking flight.

1.2.2 Orienting in flight

After CO_2 primes mosquitoes to take off and fly, mosquitoes must fly towards the source of that CO_2. Mosquitoes fly towards both CO_2 and human skin odor blends [Dekker & Carde, 2011], as well as some single odorants that have been identified from human blends, such as lactic acid and 1-octen-3-ol [reviewed in Bowen, 1991; Takken, 1991]. These odor blends vary between individual humans and between species, and likely largely determine the preferences *Ae. aegypti* have between different mammalian hosts [Verhulst et al., 2013; McBride et al., 2014]. As is typical for flying insects, mosquitoes track attractive odor plumes to their source by flying upwind [Cardé & Willis, 2008].

In addition to olfaction and wind sensation, mosquitoes use vision to navigate towards an odor source. As befits a species active at dawn and dusk, *Aedes aegypti* eyes are exquisitely well-adapted to low-light conditions. Insect compound eyes are composed of facets, or ommatidia. Each ommatidium includes several photoreceptor cells which are clustered into a tube called the rhabdom. Unlike the open rhabdoms of most flies, in which each of the photoreceptor cells in an ommatidium receives light from a different region in space, host-seeking mosquitoes pool information from the entire rhabdom to increase their sensitivity to light. Host-seeking mosquito rhabdoms are shaped as cones, instead of the usual tube, to focus light while sampling larger areas of space (Fig 1.4) [Land et al., 1999].

These adaptations to sensitivity come at a high cost to the mosquito's ability to resolve sharp images, for the large ommatidial area needed to maximize capture of light also averages an image across that area. *Ae. aegypti* have a visual acuity of ~12.3° predicted by anatomy [Muir et al., 1992], compared to ~9.3° in *Drosophila melanogaster* [Hecht & Wald, 1934] and ~0.2° in the human fovea [Hirsch & Curcio, 1989], and resulting image from each ommatidia has been termed "a wide circle of confusion" [Land et al., 1999]. Yet *Aedes aegypti* still use this substandard vision to pursue hosts.

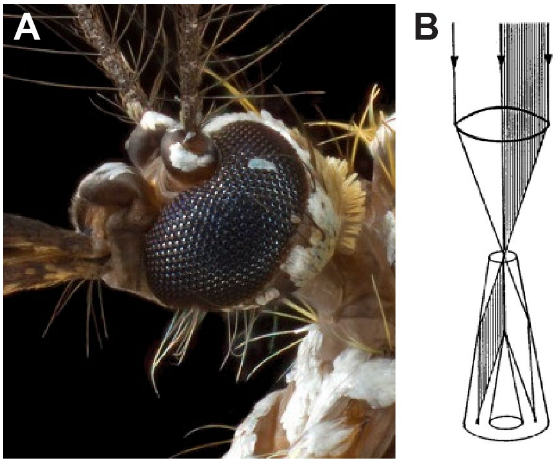

Figure 1.4 The *Ae. aegypti* eye is adapted for sensitivity in low-light conditions. (A) Photograph of the mosquito head. Note the large ommatidia. From Alex Wild. **(B)** Diagram of the conical structure of the mosquito ommatidium, indicating how the cone allows for a wider capture of light. From Land et al., 1999.

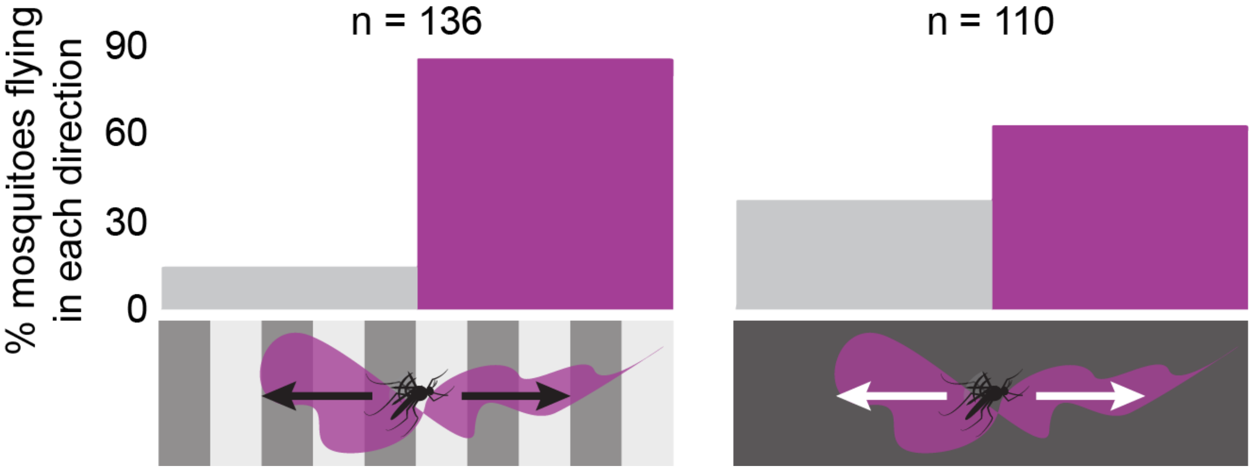

Figure 1.5 Mosquitoes do not correctly track a CO_2 plume in the dark. A CO_2 plume was introduced in a wind tunnel from the direction indicated as right, and the numbers of mosquitoes that flew towards (purple) or away (gray) were noted. Only when the wind tunnel was illuminated with a low-contrast stripe pattern (left column) were the majority of mosquitoes capable of flying towards the source. Adapted from Kennedy, 1940.

Mosquitoes fail to fly upwind in a dark chamber (Fig 1.5). Conversely, in the absence of wind, mosquitoes will reflexively fly ahead of stripes moving across the floor, visual motion that mosquitoes would expect to see if going upwind. These experiments suggest that visual feedback is necessary and sufficient for an upwind tracking response [Kennedy, 1940]. Mosquitoes use a combination of olfaction, wind sensation, and vision to fly towards their hosts.

1.2.3 Short-range attraction and landing

In addition to the visual cues that aid mosquito navigation in odor plumes, mosquitoes may also use visual cues to hone in on hosts when they become close enough to resolve. Host-seeking female *Ae. aegypti* mosquitoes are more attracted to a moving host in a transparent airtight cage than one in an opaque perforated cage, implying they may prioritize visual cues over olfactory ones [Sippell & Brown, 1953]. Visual properties important to mosquitoes may include color intensity, contrast, and movement. Mosquitoes generally prefer landing on low-intensity or dark colors [Holmes, 1911; Allan et al., 1987], although color wavelength does not seem to matter [Clements, 1999]. Mosquitoes attend to both the degree of contrast, preferentially landing on higher-contrast patterns [Clements, 1999], and the sign of contrast, fixating on dark stripes on light backgrounds but not light stripes on dark backgrounds [Kennedy, 1940]. And mosquitoes are more attracted to moving hosts than motionless ones in the laboratory and in the field, indicating that they respond to motion [Sippell & Brown, 1953; Allan et al., 1987].

Ae. aegypti prefer warm-blooded hosts and thus also are attracted to host heat. Because heat dissipates rapidly over distance in air, this warmth becomes most relevant to mosquitoes at short range [van Breugel et al., 2015]. Upon sensitization by human odor or CO2, mosquitoes robustly fly towards warmth approximating human skin temperature (Fig 1.6) [Burgess, 1959; McMeniman et al., 2014; van Breugel et al., 2015]. *Ae. aegypti* fly towards relatively warmer temperatures (>2-5°C above ambient) and avoid cooler than ambient and absolutely hot temperatures (>50°C) [Corfas & Vosshall, 2015]. Humidity, correlated with warmth in natural environments and

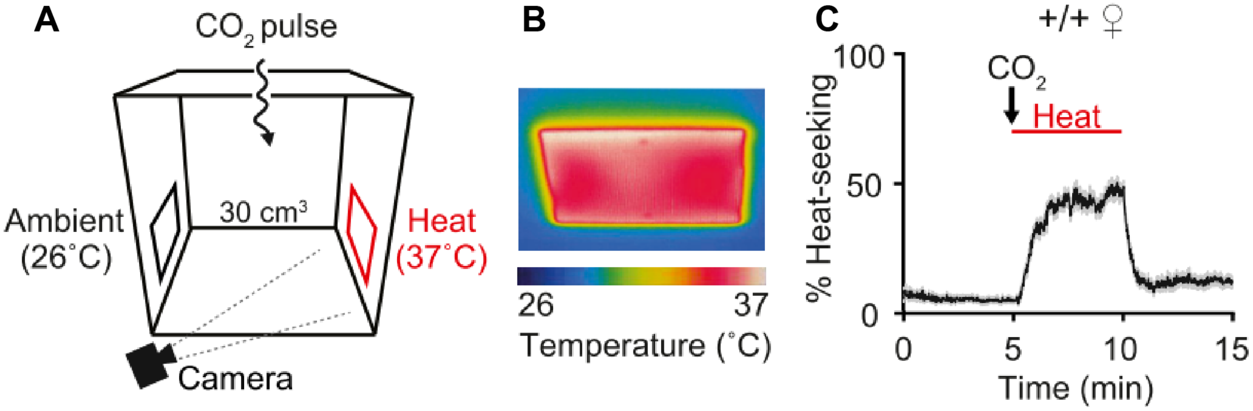

Figure 1.6 Mosquitoes fly towards heat approximating human skin temperatures. (A) Enclosure to study heat-seeking behavior. **(B)** Thermal image of the test surface, warmed to 37°C. **(C)** Mosquitoes robustly land on the Peltier when warmed to 37°C with concurrent puff of CO_2. Adapted from McMeniman et al., 2014.

vertebrate breath, may also be an attractive host cue [Burgess 1959; Daykin et al., 1965; van Breugel et al., 2015].

In isolation, single cues are dispensable for short-range attraction; together, they robustly induce host-seeking. No single sensory modality is necessary or sufficient for host-seeking. When *Ae. aegypti* mosquitoes are genetically modified to be deficient at sensing human odors or CO_2, the mutants still find and bite hosts at rates similar to wild type [DeGennaro et al., 2013; McMeniman et al., 2014]. Instead, mosquitoes integrate at least two cues in any combination, such as human odor and carbon dioxide or human odor and heat, to seek a host (Fig 1.7) [Mayer & James, 1969; Takken, 1991; McMeniman et al., 2014].

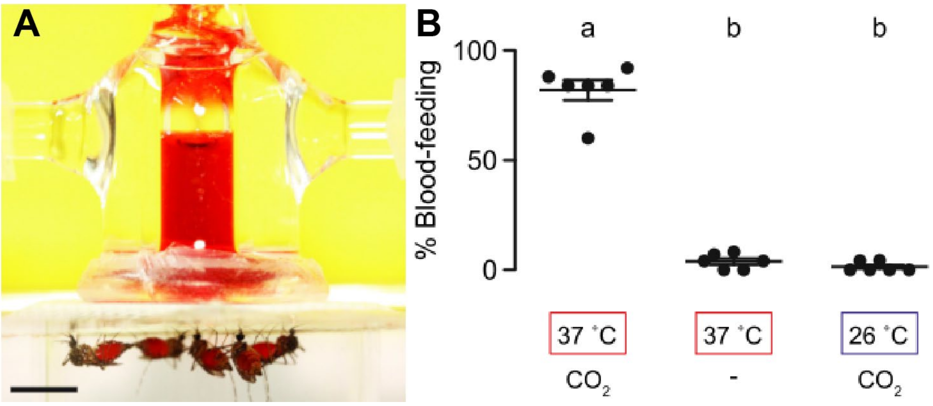

Figure 1.7 Mosquitoes require at least two cues to feed at a membrane feeder. (A) Assay with membrane feeder. **(B)** Percentage of mosquitoes fed at each combination of cues: heat and CO_2, heat alone, and CO2 alone. Letters indicate statistically different groups ($p < 0.05$), tested with one-way ANOVA and post-hoc Tukey's HSD test. Adapted from McMeniman et al., 2014.

1.2.4 Probing and biting

After landing on a host, female mosquitoes must bite and engorge on blood. Mosquitoes appear to prepare for biting at probing at a candidate surface. Although the exact relationship of probing to biting is unclear, probing can be activated with heat alone [Corfas, 2015]. Skin tastants and texture may also be involved, but as far as we know this has not yet been studied systematically.

Mosquitoes pierce the skin using a specialized needle-like structure called the stylet, usually sheathed in the larger mouthpart structure of the labium. The human-preferring malaria mosquito *Anopheles gambiae* possesses a stylet that, videotaped within veined skin, moves and searches for blood vessels [Choumet et al., 2012]. It is yet unknown whether this is a passive process or if the stylet actively senses multimodal stimuli such as heat, touch, or taste to direct itself towards a blood vessel. *Ae. aegypti* stylets possess chemosensory and mechanosensory innervations, and so may also be capable of such an active search [Lee & Craig, 1983]. *Ae. aegypti* female mosquitoes may use their stylets to decide to engorge on a blood meal, for female mosquitoes engorge only on solutions that contain ATP [Galun et al., 1963; Duvall et al., 2019], and stylet is the only organ that directly contacts blood before feeding [Choumet et al., 2012]. Little is known about the sensory cues that underlie a mosquito's final decision to bite and engorge, and so this will be a fruitful area for further study outside the scope of this thesis.

1.3 Conclusion: Parsing sensory requirements in short-range attraction

Mosquito host-seeking is a beautifully multifaceted and multisensory behavior. The work described in the thesis uses behavior to investigate sensory interdependence within short-range attraction. What behavioral modules exist to explain how mosquitoes home towards a potential host, and what are their sensory requirements? We begin by demonstrating that visual attraction to dark contrast is not affected by elevated CO_2 or the internal nutritional and reproductive states of the animal, showing the generality of visual response (**Chapter 2**). Despite the independence of visual responses, we go on to show that this general visual attraction to dark contrast does enhance host-related thermotaxis (**Chapter 3**). Lastly, we use this general attraction to reveal that mosquitoes actually find host heat aversive unless they are concurrently exposed to elevated CO_2 (**Chapter 4**). Unlike visual attraction, mosquito thermotaxis is tightly coupled to sensation of CO_2. We conclude with a discussion of the circuit implications of this behavioral work, as well as opportunities for further investigation (**Chapter 5**).

Chapter 2: Visual responses of tethered flying mosquitoes are not altered by host-seeking status

2.1 The magnetic tether quantifies orientation of flying insects to visual stimuli

In the natural world, mosquitoes fly freely in a visual panorama that changes complexly according to the 3D movement of mosquitoes. To begin studying mosquito vision, we needed to simplify the mosquito's visual environment to identify specific cues that she responded to. We looked for methods that would allow us present those simple, specific cues rapidly and with precise spatial and temporal control.

We thus decided to tether mosquitoes, keeping her position fixed so that the visual cues we presented could not be altered by translational motion. Mosquito vision was first studied by loosely tethering a mosquito to a freely rotating silk string and observing orientation towards a stripe [Kennedy, 1940] (Fig 2.1). A modern analog to this loose tether is the magnetic tether preparation pioneered in *Drosophila* [Bender & Dickinson, 2006; Weir & Dickinson, 2012]. Here, a flying insect is tethered by her upper thorax to a steel pin (Fig 2.2) and suspended in a vertically aligned magnetic field, which

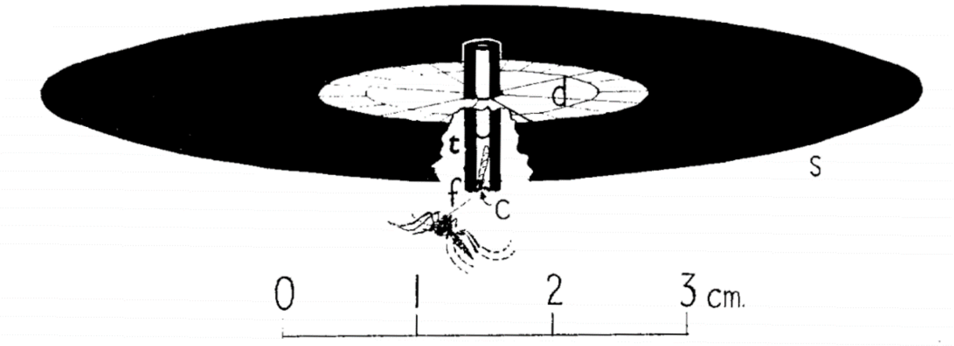

Arrangement for observation of orientation of mosquitoes suspended and in flight. *s*, circular sheet of celluloid (partly cut away), painted black except at the centre; *d*, transparent centre portion of *s*, with an orientation dial marked out; *t*, glass tube projecting through the centre of *d*; *c*, short length of sewing cotton, held in the tube by oil; *f*, silk fibre attaching mosquito to *c* by dabs of enamel paint. The mosquito was viewed through the dial from directly over the suspension tube.

Figure 2.1 First system for tethering living flying insects. From Kennedy, 1940.

Figure 2.2 Magnetically tethering mosquitoes. (A) Mosquitoes are tethered by anesthetizing on ice. **(B)** After anesthesia, mosquitoes are transferred to a chill table with forceps. With a micromanipulator and UV-curing glue, a steel pin is glued to the head such that the proboscis points -30-45° below horizontal. **(C)** Mosquitoes are then allowed in a humid enclosure with their legs resting on mesh for at least 1 hour before testing.

keeps the insect in a fixed position while allowing her to rotate freely. Free rotation within the magnotether allows animals to control their own flight turns naturalistically, avoiding the confounds that arise from rigid-tether closed-loop experiments where the gains of visual feedback are arbitrarily chosen [Fenk et al., 2014].

To present visual stimuli, we surrounded the insect with a fully programmable panoramic LED array [Reiser & Dickinson, 2008] (Fig 2.3). Each LED occupies ~2° of visual space, well under the minimum acuity of 6.4° measured in the *Ae. aegypti* eye. *Ae. aegypti* photoreceptors are maximally sensitive to green, the color of the LEDs, so the array allowed us to present to the mosquito a seamless panorama that spans the

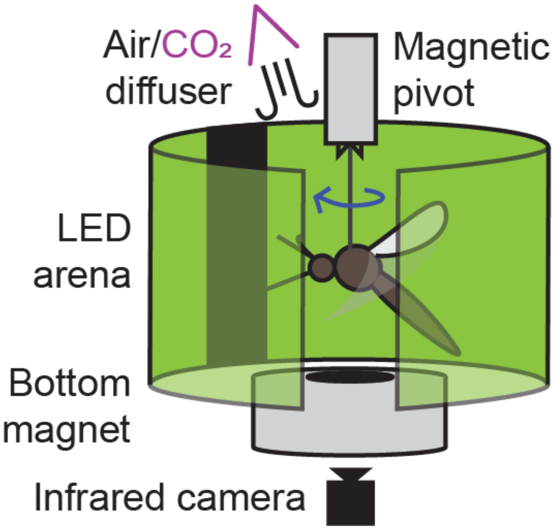

Figure 2.3 Magnotether schematic. Not to scale.

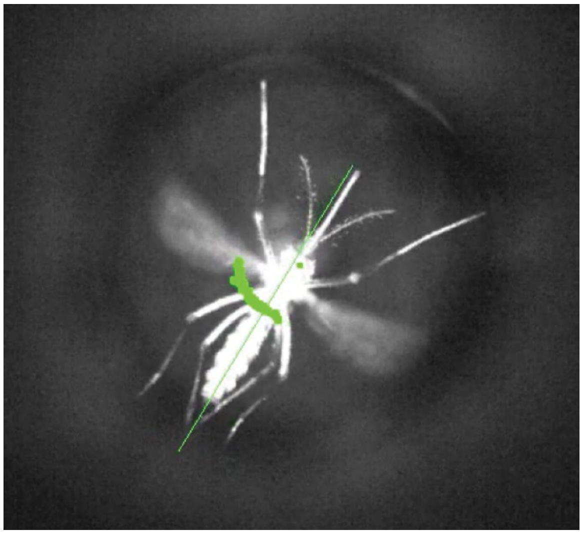

Figure 2.4 Camera image of the mosquito. Illumination by IR lights. Green line is calculated orientation.

mosquito's visual intensity range. [Muir et al., 1992; Clements, 1999] Raw data are high-speed videos from a camera pointed at the underside of the insect (Fig 2.4). Orientation of the insect is computed from the video by FView software in real time [Straw & Dickinson, 2009] (Fig 2.5). Because animals must be flying to be assayed in the magnotether, we focused solely on orientation in flight.

In each trial, we showed an individually tethered animal a shape, such as a long dark stripe (Fig 2.6A), recorded the animal's orientation over time (Fig 2.6B), computed the offset between the stimulus and animal position (Fig 2.6C) and calculated the proportion of time spent with an offset within ±45° to obtain "fixation" (expected ~1.00 for attractive shapes, Fig 2.6D). As controls, we presented animals with trials where only a

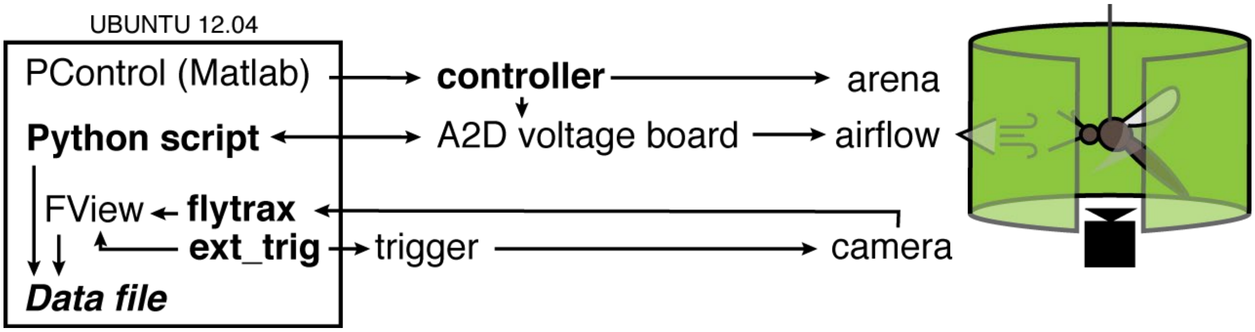

Figure 2.5 Software controlling magnotether components and recording data.

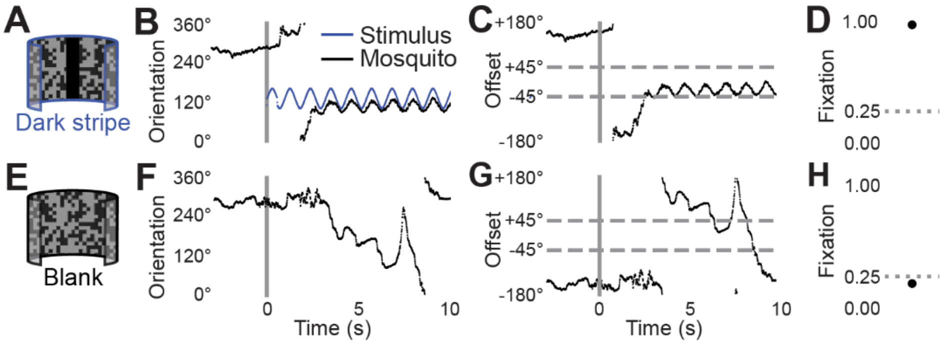

Figure 2.6 Processing magnotether data. (A, E) Example shapes shown to mosquitoes. **(B, F)** Raw traces from a single trial. **(C, G)** Offset of mosquito orientation from stimulus center position. Dotted lines indicate bounds for calculating fixation. Solid lines indicate time of stimulus onset. **(D, H)** Fixation. Dotted lines indicate null expectation of 0.25.

static background was shown ("blank") and computed offset and fixation relative to a randomly assigned fictive stimulus position (expected ~0.25, Fig 2.6E-H).

2.2 Flies exhibit object responses in the magnotether

To test that our magnotether could accurately capture object responses, we presented female *Drosophila melanogaster* flies with simple dark shapes that had known response profiles in rigid-tether and free flight (Fig 2.7A). Both free flying

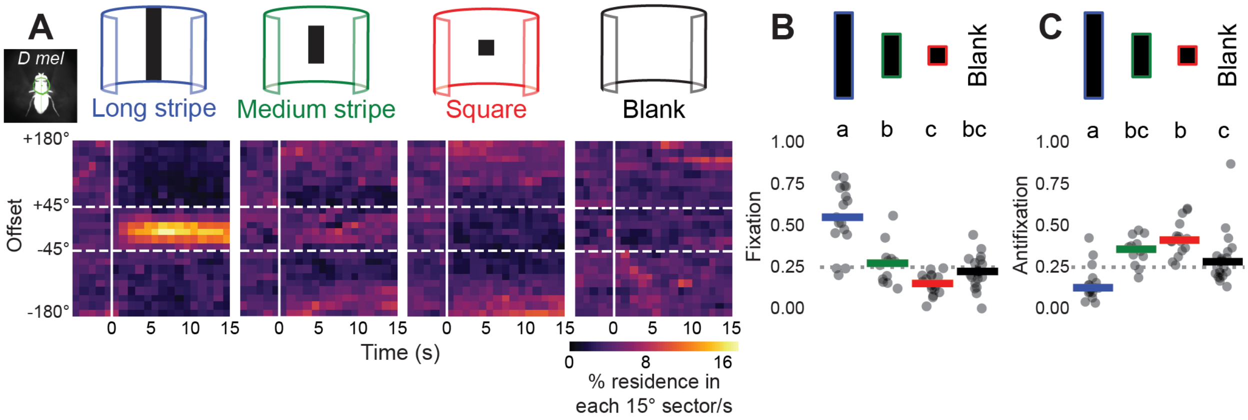

Figure 2.7 Magnotethered *Drosophila melanogaster* flies orient towards long stripes and away from squares. Each trial corresponds to a single female. **(A)** Heat maps of offset, parsed by shape of stimulus, long stripe (n = 17), medium stripe (n = 12), square (n = 16), and blank (n = 21). Dotted lines indicate bounds used to calculate fixation. Solid lines indicate stimulus onset. **(B)** Fixation, parsed by shape. **(C)** Anti-fixation, calculated similarly to fixation but with an offset window >±135°. **(B-C)** Letters indicate statistically significant different groups ($p < 0.05$), tested with Kruskal-Wallis test and post hoc Mann-Whitney U test with Bonferroni correction.

[Maimon et al., 2008] and tethered [Gotz, 1986; Maimon et al., 2008; Mongeau & Frye, 2017] flies respond to dark thin shapes with strong tuning to the tallness of the shape: they fixate on long stripes, thought to represent possible landing locations [Dickinson, 2014]; avoid small squares, which may indicate a flying predator [Maimon et al., 2008; Mongeau et al., 2019; Theobald et al., 2004]; and behave ambiguously towards stripes of intermediate heights. We replicated these results using our magnotether. The fixation score of flies towards the bar was significantly higher than those of other shapes (Fig 2.7B), and their antifixation score (calculated by looking at offsets >±135°, or opposite to fixation) towards the small square was significantly higher ($p < 0.05$) than those towards the long stripe and the blank (Fig. 2.7C). Interestingly, flies may respond bimodally towards the medium stripe, with slight, nonsignificant elevations of attraction and aversion visible in the heat maps.

These results confirm that flies exhibit well-known object responses in the magnotether, and that our method of analysis can statistically distinguish those object responses. We then sought to apply this assay to a novel problem: whether mosquito visual responses are altered by elevating an important host cue, CO_2.

2.3 Mosquito visual responses do not change upon elevation of CO_2

Because we observed strong responses to simple shapes in magnotethered *Drosophila*, we reasoned that mosquitoes might also respond to the same shapes. Previous reports indicated that loosely tethered mosquitoes orient towards long dark stripes, but not towards long bright stripes or blank control stimuli [Kennedy 1940]. Because mosquitoes paid attention to sign of contrast in those experiments, we altered the stimuli presented to *Drosophila* by replacing the bright uniform background (maximal contrast with dark shapes, but no ability to present bright shapes) with a patterned low-light background. The intermediate contrast of the new background allowed us to examine mosquito responses to both bright and dark shapes.

Both non-directionally [McMeniman et al., 2014] and as a plume [Dekker et al., 2005], CO_2 is a potent signature of host breath that amplifies responses to other host cues. We hypothesized that, in line with a previous report and both olfactory and thermal host cues, mosquitoes would become more attracted to visual cues after

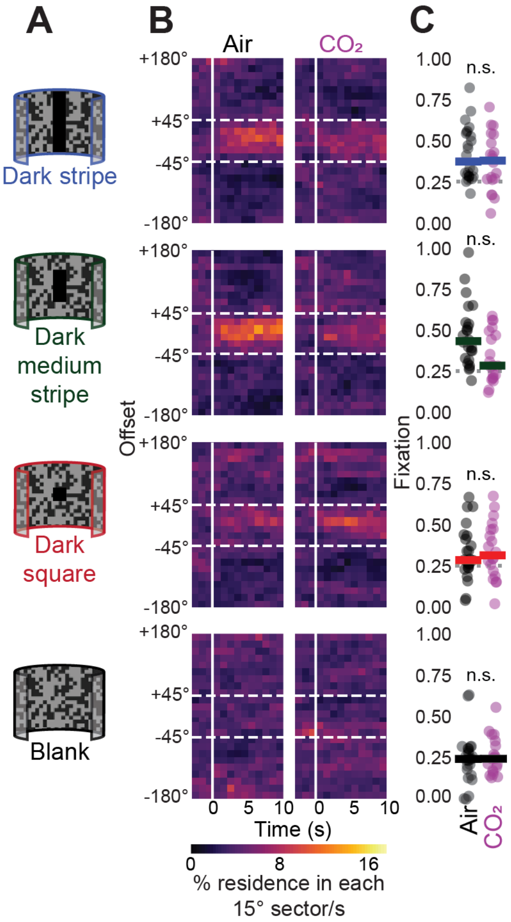

Figure 2.8 Visual responses to dark shapes are not affected by concentration of CO_2. (A) Dark magnotether stimuli. **(B)** Heat maps of offset, parsed by shape of stimulus, from mosquitoes tested in air (n = 24) or CO_2 (n = 20). Each trial corresponds to a single female. Dotted lines indicate the bounds used to calculate fixation. Solid lines indicate onset of visual stimulus. **(C)** Fixation, parsed by shape. n.s.: not significant ($p > 0.05$), Mann-Whitney U test with Bonferroni correction. Dotted lines indicate null expectation of 0.25.

increased CO_2. We applied non-directional pulses of CO_2 in the magnotether while presenting dark shapes to mosquitoes.

However, in contrast to a previous report [van Breugel et al., 2015], we could not detect differences in the visual orientation responses towards dark long stripes, medium stripes, squares, or blank stimuli in mosquitoes flying in air (~1000 ppm CO_2) compared different mosquitoes flying after increasing CO_2 by 1250 ppm (“CO_2”, Fig 2.8), a concentration previously shown to potentiate increased attraction to thermal and olfactory cues. We found the same negative result when we presented bright long

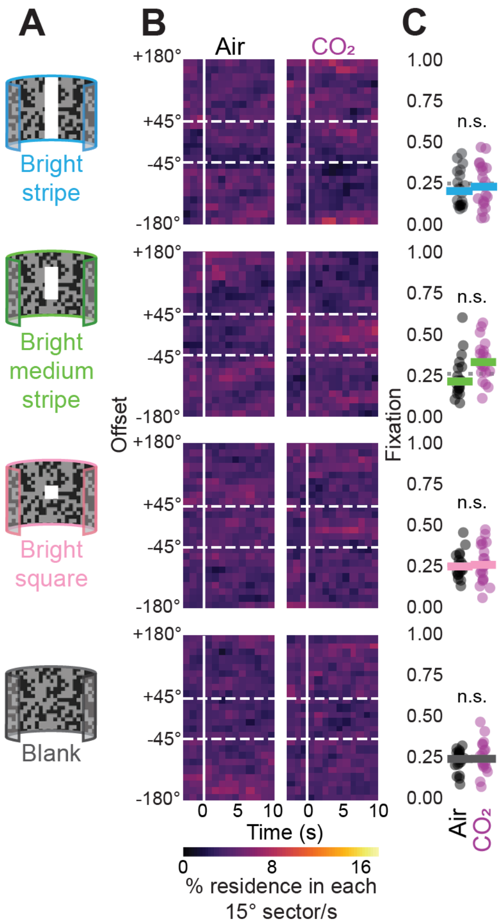

Figure 2.9 Visual responses to light shapes are not altered by concentration of CO_2. (A) Light magnotether stimuli. **(B)** Heat maps of offset, parsed by shape of stimulus, from mosquitoes tested in air (n = 20) or CO_2 (n = 21). Each trial corresponds to a single female. Dotted lines indicate the bounds used to calculate fixation. Solid lines indicate onset of visual stimulus. **(C)** Fixation, parsed by shape. n.s.: not significant ($p > 0.05$), Mann-Whitney U test with Bonferroni correction. Dotted lines indicate null expectation of 0.25.

stripes, medium stripes, squares, or blank stimuli to mosquitoes flying in air and in CO_2 (Fig 2.9).

We believe that this apparent conflict with previous results is resolved if attraction to dark contrast depends on flight, regardless of CO_2 levels. Instead of CO_2 potentiating visual attraction, as previously proposed [van Breugel et al., 2015], CO_2 plumes may cause freely moving mosquitoes to increase approach to visual stimuli through by potently activating their flight. Without activation by CO_2, mosquitoes in a free flight arena are less likely to take off [McMeniman et al., 2014], and thus do not fly to visual stimuli. Conversely, tethered mosquitoes are always flying, and so introducing CO_2 has no effect on their propensity to fly towards dark contrast. Our results are replicated by a recent study [Vinauger et al., 2019] in which rigidly tethered mosquitoes track a dark stripe and dark square of analogous size to those studied here. In that study, while an effect was found with a very small square (subtending ~3.75°, as opposed to the ~15° subtended by the square used here), adding a plume of CO_2 did not significantly change fidelity of tracking to these larger shapes. We thus propose that elevated CO_2 increases visual attraction in freely moving mosquitoes through increasing flight probability, not through changing the attractiveness of the visual stimulus.

2.4 Mosquito visual responses do not change after ingestion of a blood meal

In addition to the external environment, attraction to host cues is also modulated by internal state. After a blood meal, mosquitoes suppress host-seeking until they lay eggs, 3-5 days later [Klowden, 1995; Liesch et al., 2013]. As part of this suppression, mosquitoes inhibit their responses to host cues while preserving or heightening responses to sensory stimuli unrelated to hosts. Although host-seeking female mosquitoes exhibit a robust increase in flight activity in response to CO_2, blood-fed mosquitoes do not show any increase in activity [Matthews et al., 2016]. This suppression of chemosensory response is specific to the host cue CO_2, for blood-fed mosquitoes will preserve or increase their responses to other chemosensory stimuli, such as humidity, which signifies an appropriate egg-laying substrate [Matthews et al., 2018]. Thermosensory responses undergo similar modulation. Blood-fed mosquitoes fail to probe at host-like heat, but both host-seeking and blood-fed mosquitoes rapidly leave surfaces warmed to noxious temperatures (>45°C) at the same rate [Corfas, 2015]. These results from chemosensory and thermosensory cues suggest that if mosquitoes use visual host cues, their responses should also be specifically suppressed after a blood meal. Conversely, mosquitoes fed a saline meal will engorge similarly, but then continue to be attracted to hosts.

To examine the effect of blood-feeding on visual responses, we took a group of female mosquitoes born and raised at the same time, and used artificial feeders to feed half of them saline and the other half sheep's blood (Fig 2.10). We expected that mosquitoes 48 hours after a blood meal would suppress all their responses, as they do for CO2, heat, and human odor. We compared visual orientation behaviors of

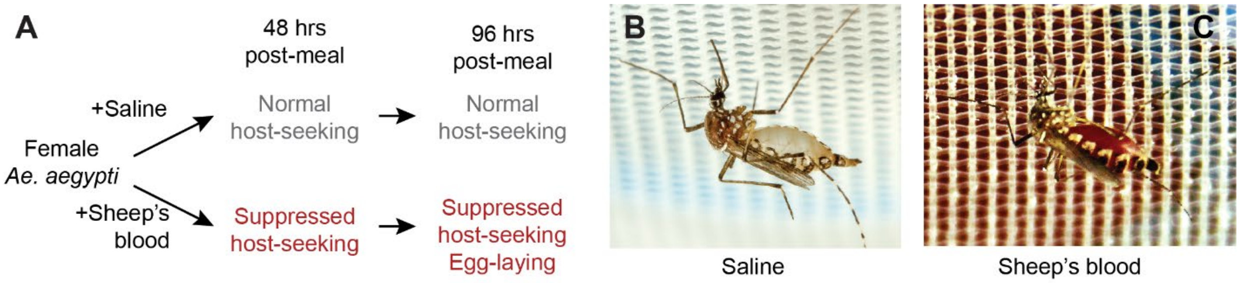

Figure 2.10 Testing effect of fed state on visual responses. (A) Schematic of experimental setup. **(B)** Mosquito engorging on saline from an artificial feeder. Photo: Alex Wild. **(C)** Mosquito engorging on sheep's blood from an artificial feeder. Photo: Molly Liu.

mosquitoes after 48 hours after ingestion of blood or saline, and were not able to detect any suppression of visual responses in blood-fed animals (Fig 2.11).

We also tested mosquitoes 96 hours after a blood meal. Because female mosquitoes have at that time finished developing eggs and are searching for suitable egg-laying sites, we might expect to see elevation of responses related to water-

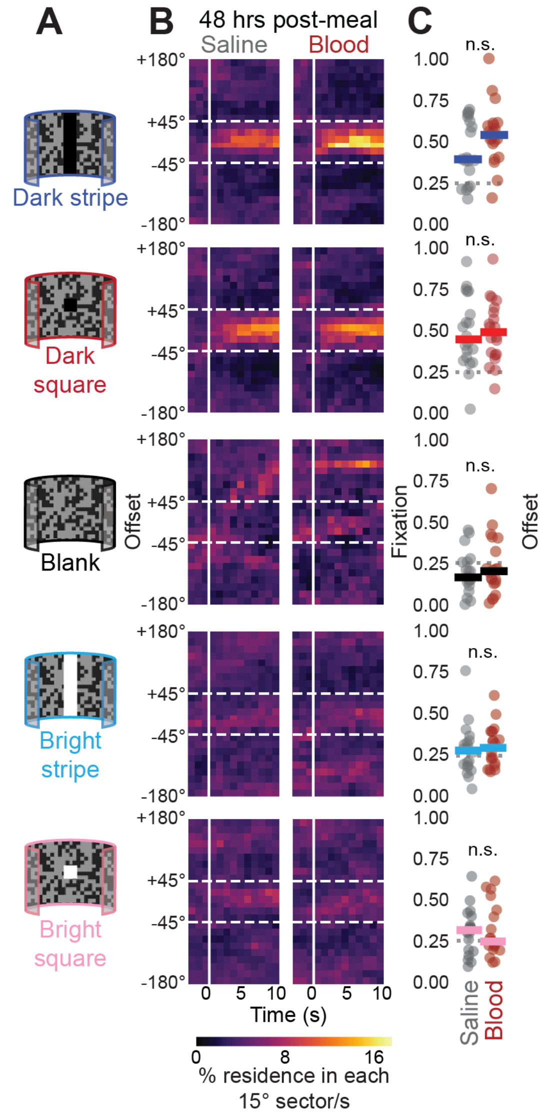

Figure 2.11 Visual responses do not change 48 hours after a blood meal. (A) Magnotether stimuli. **(B)** Heat maps of offset, parsed by shape of stimulus, from mosquitoes tested 48 hours after being fed a meal of saline (n = 20) or sheep's blood (n = 20). Each trial corresponds to a single female. Dotted lines indicate the bounds used to calculate fixation. Solid lines indicate onset of visual stimulus. **(C)** Fixation, parsed by shape. n.s.: not significant ($p > 0.05$), Mann-Whitney U test with Bonferroni correction. Dotted lines indicate null expectation of 0.25.

seeking. However, we were similarly unable to detect a difference in visual orientation for any shape tested (Fig 2.12).

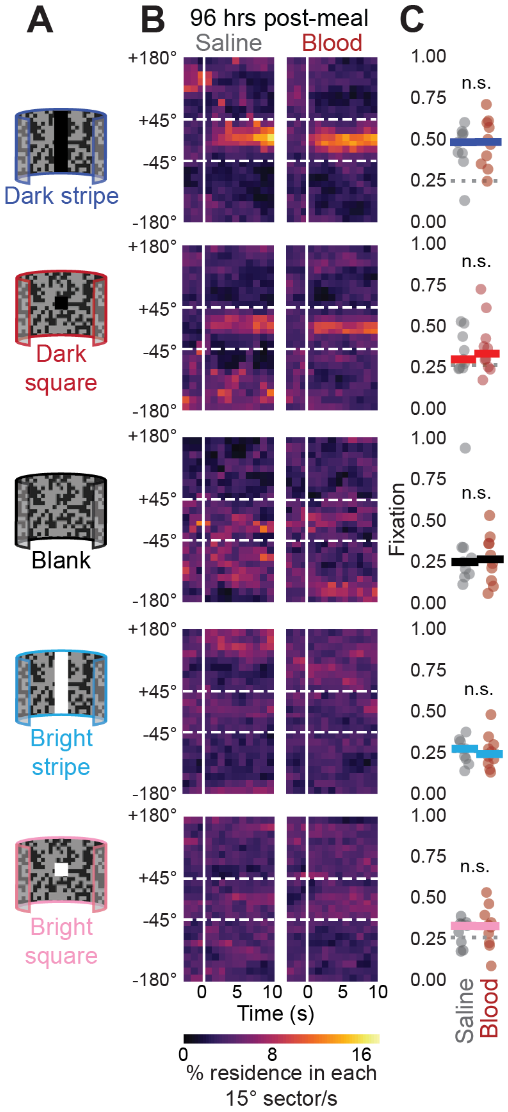

Figure 2.12 Visual responses do not change 96 hours after a blood meal. (A) Magnotether stimuli. **(B)** Heat maps of offset, parsed by shape of stimulus, from mosquitoes tested 96 hours after being fed a meal of saline (n = 9) or sheep's blood (n = 10). Each trial corresponds to a single female. Dotted lines indicate the bounds used to calculate fixation. Solid lines indicate onset of visual stimulus. **(C)** Fixation, parsed by shape. n.s.: not significant ($p > 0.05$), Mann-Whitney U test with Bonferroni correction. Dotted lines indicate null expectation of 0.25.

2.5 Mosquito visual responses may not be tuned by object size

To investigate the relationship between fixation and shape height, we pooled data from statistically indistinguishable trials to increase the power of our comparisons. In the dark trials, we can compare the strength of response according to the height of the stimulus (Fig 2.13A). We find that long stripes and medium stripes are both statistically different from the blank, whereas the square is not statistically distinguishable from either the stripes or the blank (Fig 2.13B, C). While we cannot make direct comparisons to *Drosophila* because of numerous differences in the experimental design, these results do suggest that mosquitoes lack the aversion characteristic of *Drosophila* responses to small squares.

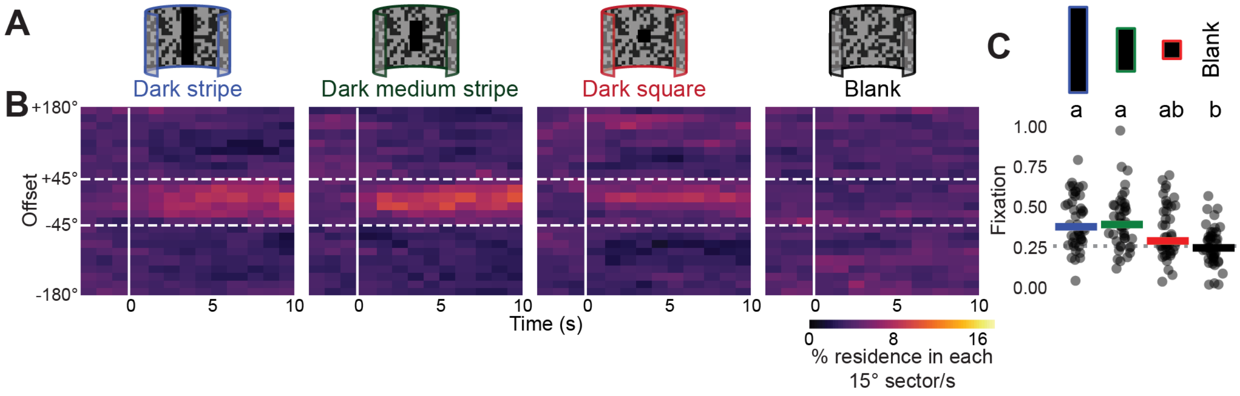

Figure 2.13 Mosquito responses to dark shapes may or may not depend on stimulus shape. (A) Dark magnotether stimuli. **(B)** Heat maps of offset, parsed by shape of stimulus, pooled from mosquitoes tested in air and CO2 (n = 44). Each trial corresponds to a single female. Dotted lines indicate the bounds used to calculate fixation. Solid lines indicate onset of visual stimulus. **(C)** Fixation, parsed by shape. n.s.: not significant ($p > 0.05$), Mann-Whitney U test with Bonferroni correction. Dotted lines indicate null expectation of 0.25.

Mosquitoes do not respond to bright shapes, regardless of their shape. This may reflect a previously documented negative phototactic response [Kennedy, 1940]. *Ae. aegypti* hunt during dawn and dusk, and so they likely rarely encounter objects which are brighter than the twilight sky.

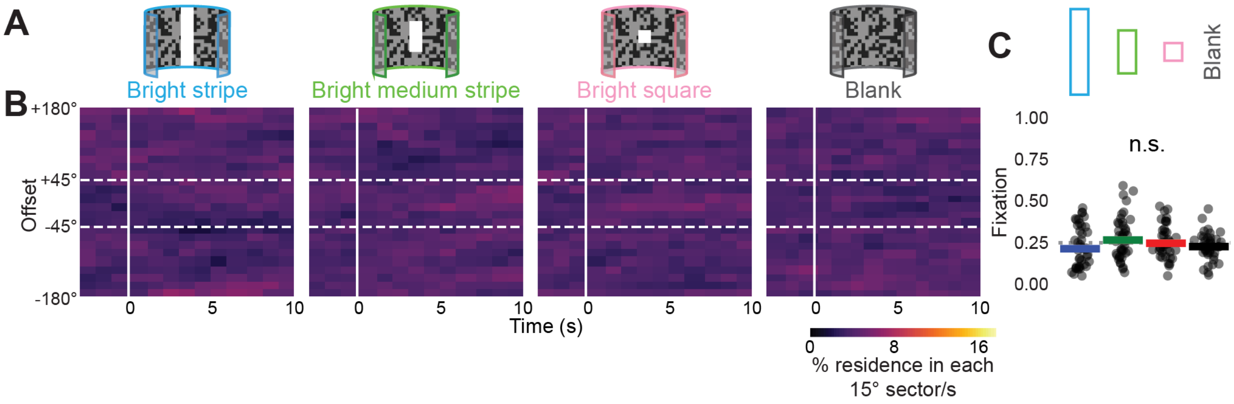

Figure 2.14 Mosquito responses to bright shapes do not depend on stimulus shape. (A) Bright magnotether stimuli. **(B)** Heat maps of offset, parsed by shape of stimulus, pooled from mosquitoes tested in air and CO2 (n = 42). Each trial corresponds to a single female. Dotted lines indicate the bounds used to calculate fixation. Solid lines indicate onset of visual stimulus. **(C)** Fixation, parsed by shape. n.s.: not significant ($p > 0.05$), Mann-Whitney U test with Bonferroni correction. Dotted lines indicate null expectation of 0.25.

2.6 Mosquito visual responses are tuned to contrast polarity

To look more rigorously at the effect of contrast polarity on mosquito responses, we pooled data from blood-fed and saline trials. While this seems counterintuitive, these were the only mosquitoes in this experimental setup that were shown both dark and bright shapes in the same trial, and we believe that the saline-fed mosquitoes (and by extension the statistically indistinguishable blood-fed mosquitoes) should have the visual responses of non-fed mosquitoes. Replicating results indicating that mosquitoes pay attention to contrast polarity [Kennedy, 1940; van Breugel et al., 2015], 48 hours after a meal, mosquitoes are attracted to dark shapes and not light shapes or blanks (Fig 2.15). Responses to dark long stripes and dark spots were statistically distinct from responses to light shapes or blanks.

One odd divergence is that dark squares seem more attractive overall to this group of mosquitoes than they were to the groups of mosquitoes tested in previous experiments. While dark square responses were always indistinguishable from those of

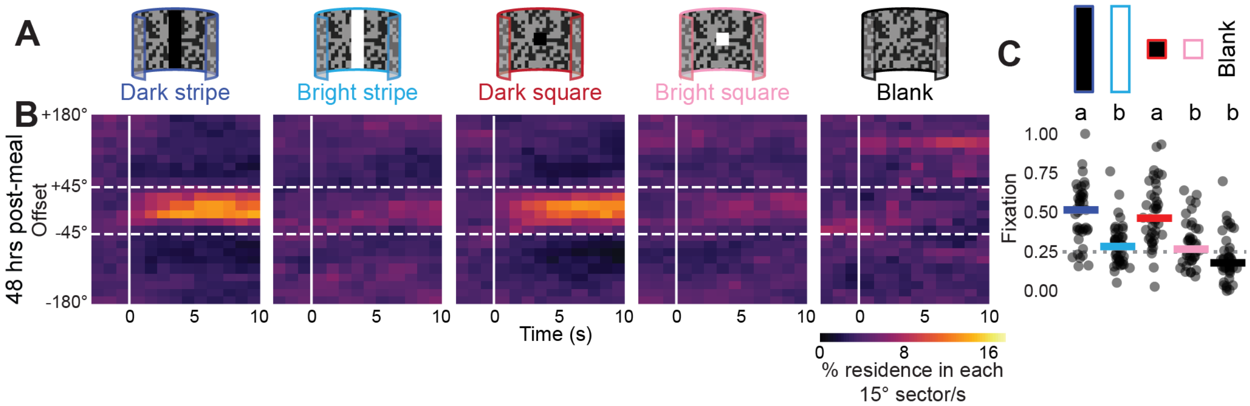

Figure 2.15 Mosquitoes orient towards dark shapes, but not bright shapes, 48 hours after a saline or blood meal. (A) Magnotether stimuli. **(B)** Heat maps of offset, parsed by shape of stimulus, pooled from mosquitoes 48 hours after being fed a meal of saline or sheep's blood (n = 40). Each trial corresponds to a single female. Dotted lines indicate the bounds used to calculate fixation. Solid lines indicate onset of visual stimulus. **(C)** Fixation, parsed by shape. n.s.: not significant ($p > 0.05$), Mann-Whitney U test with Bonferroni correction. Dotted lines indicate null expectation of 0.25.

dark stripes, they were also indistinguishable from blank controls except 48 hours post-meal. As mosquitoes 48 hours after a saline meal behave like non-fed mosquitoes in other assays [Duvall et al., 2019], we speculate that this is due to behavioral variation in the assay.

We found similar results looking at pooled mosquitoes 96 hours after a blood or saline meal (Fig 2.16). Because of the smaller sample size, statistical distinctions were not as clear as with larger groups of mosquitoes. Nevertheless, fixation scores towards dark long stripes are statistically distinct from those of bright shapes. Fixation towards dark spots and blanks were statistically indistinguishable from other shapes.

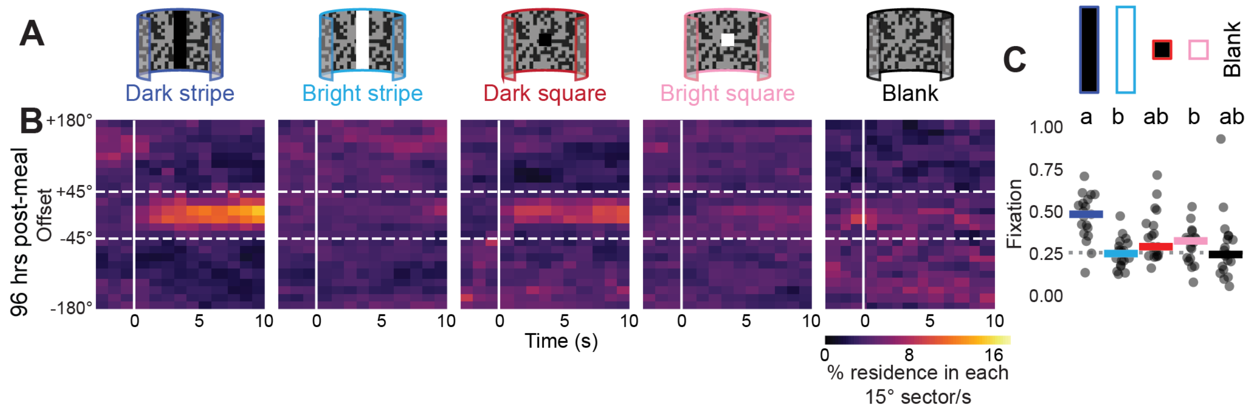

Figure 2.16 Mosquitoes orient towards dark shapes, but not bright shapes, 96 hours after a saline or blood meal. (A) Magnotether stimuli. **(B)** Heat maps of offset, parsed by shape of stimulus, pooled from mosquitoes 96 hours after being fed a meal of saline or sheep's blood (n = 19). Each trial corresponds to a single female. Dotted lines indicate the bounds used to calculate fixation. Solid lines indicate onset of visual stimulus. **(C)** Fixation, parsed by shape. n.s.: not significant ($p > 0.05$), Mann-Whitney U test with Bonferroni correction. Dotted lines indicate null expectation of 0.25.

2.7 Conclusion: Mosquitoes are generally attracted to dark visual contrast

From these magnotether experiments, we conclude that flying mosquitoes are attracted to dark visual contrast, and this attraction is modulated by neither CO_2 concentration nor blood-fed state. Because of this general attraction, we suggest that dark visual contrast signals potential landing sites, as has been proposed for *Drosophila* [Dickinson, 2014; Maimon et al., 2008].

Chapter 3:Visual contrast enhances mosquito thermotaxis

3.1 Adapting a free flight heat-seeking assay to study visual and thermal integration

Given that responses to visual cues in the magnotether are not modulated by CO_2 or blood-feeding, we asked a reciprocal question: how do visual cues affect mosquito responses to a signature host cue, such as human skin temperature? To test this, we adapted a previously described free flight thermotaxis assay [Corfas & Vosshall, 2015] that measures mosquito occupancy on a temperature-controlled Peltier in the presence of CO_2.

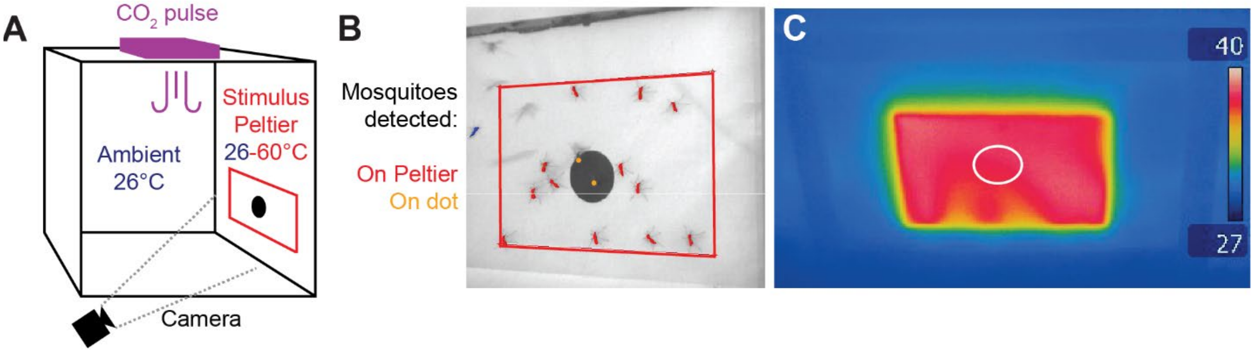

Figure 3.1 Assay to test the effect of visual contrast on mosquito thermotaxis. (A) Schematic of heat-seeking assay with 2 cm diameter black dot as visual cue. **(B)** Camera image, showing mosquitoes on Peltier (red outline) sampled at 1 Hz. **(C)** Thermal image of the Peltier set to 40°C. White outline shows boundary of black dot.

We modified the Peltier by affixing a 2 cm black circle ("dot") to its center (Fig 3.1A). We chose this visual stimulus because it was previously shown to attract mosquitoes and be modulated by heat in free flight [van Breugel et al., 2015]. We tracked the two-dimensional location of mosquitoes while setting the internal temperature of the Peltier to various temperatures (Fig 3.1B). The dot did not present a detectably different thermal signature from the rest of the Peltier (Fig 3.1C), meaning that any differences in occupancy should be due to visual features of the dot.

To test the effect of the visual mark on heat-seeking, we presented the same thermal ramp as in [Corfas & Vosshall, 2015] to groups of 45-50 mosquitoes with either the dot or a blank stimulus placed on the Peltier (Fig 3.2A).

3.2 Dark visual contrast attracts mosquitoes at ambient temperature

As was demonstrated in a previous study [Corfas & Vosshall, 2015], mosquitoes did not occupy the blank Peltier between heat bouts, showing that mosquitoes are not interested in blank white backgrounds. However, when the Peltier was marked with a dot, mosquitoes occupied the unheated Peltier at high rates when it was set to ambient temperature (26°C) between heat bouts and before pulses of CO_2 (Fig 3.2B). We quantified this by averaging the percentage of the mosquito population that landed on

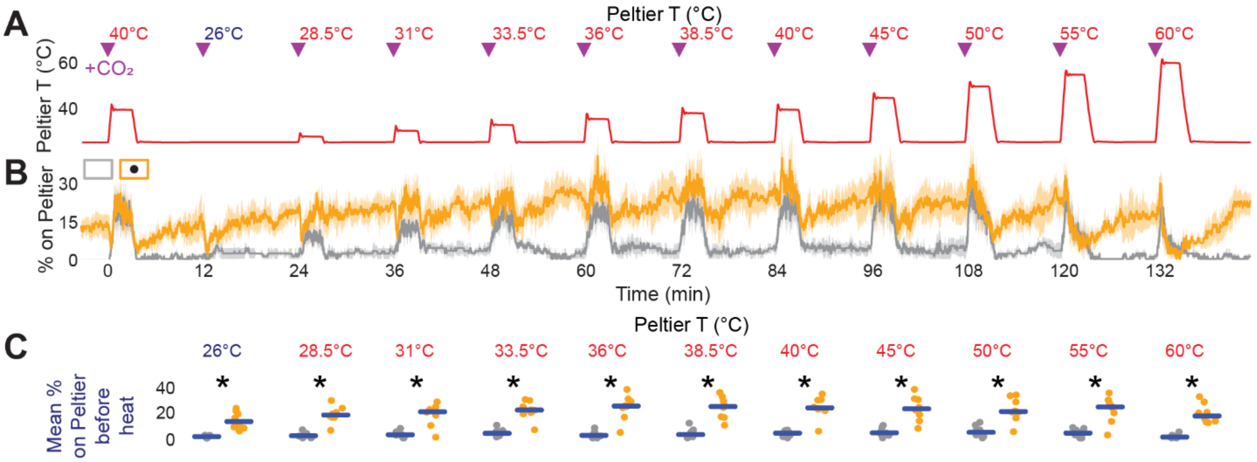

Figure 3.2 Mosquitoes reside on visually marked Peltier at ambient heat. (A) Peltier temperature. CO_2 was pulsed in for 20 s at onset of each heat bout (purple triangle). **(B)** Median % of a population of 45-50 mosquitoes on Peltier over entire experiment ± median absolute deviation, blank (gray, n = 8) or visual cue (orange, n = 8). **(C)** Median % of mosquitoes on the Peltier 90-0 s before onset of heat (“before heat”). * $p < 0.05$, Mann-Whitney U test with Bonferroni correction.

the Peltier across the 90 seconds before onset of heat and CO_2, and found statistically significant differences before all heat bouts (Fig 3.2B).

These results demonstrate that mosquitoes are attracted to areas of dark contrast at ambient temperatures, as shown in the magnotether. Even after mosquitoes have been swept off the Peltier by bouts of noxiously high temperatures (>50°C), they reaccumulate over the 9-minute inter-bout interval when the Peltier is reset to ambient. Because we never set the Peltier to stay at ambient for more than 9 minutes, we do not know how high this accumulation would become if the Peltier were to remain at ambient temperatures indefinitely. We speculate that the concentration of mosquitoes on the Peltier would eventually reach a steady state between their visual attraction to the dot and some aversion to crowding.

3.3 Dark visual contrast enhances mosquito thermotaxis to moderate heat

We examined the effect of the dot on thermotaxis by analyzing the mean occupancy of mosquitoes on the Peltier during the heat bout. Consistent with a previous study [Corfas & Vosshall, 2015], mosquito occupancy on the Peltier increased as the temperature heated to 28.5-50°C, then decreased as it heated to 55-60°C (Fig 3.3). Mosquitoes also took off from the dot at ambient temperature after a pulse of CO_2, consistent with findings that CO_2 promotes take-off [McMeniman et al., 2015]. The dot

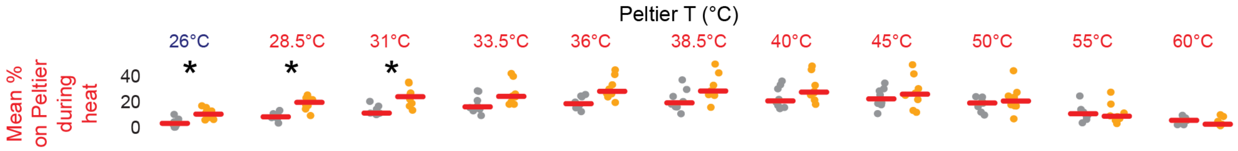

Figure 3.3 Mosquitoes are attracted to lower temperatures on a visually marked Peltier. Median % of mosquitoes on the Peltier 90-180 s after onset of heat ("during heat"). Blank (gray, n = 8) or visual cue (orange, n = 8). * $p < 0.05$, Mann-Whitney U test with Bonferroni correction.

only enhanced total levels of mosquito occupancy on the Peltier at temperatures warmer than ambient, but cooler than human skin (Peltier temperatures: 28.5-31°C). We speculate that at higher, more host-like temperatures, thermotaxis has reached a ceiling and cannot be further aided by the visual cue.

The thermocouple used to measure temperature here is embedded within the Peltier, which the mosquitoes cannot access. Instead, what mosquitoes experience is the air temperature at the surface of the Peltier. We measured the air temperature 2 mm from the surface of the Peltier during several behaviorally salient temperatures (Fig 3.4). 28.5°C is more attractive to mosquitoes when the Peltier is marked with a dot, and varies from 26.3-28.4°C, so perhaps indistinguishable from ambient in some trials. 36°C approximates human skin temperature and is attractive to mosquitoes. 50°C is the highest temperature to which mosquitoes are attracted. 60°C is a high temperature from which mosquitoes are repulsed. Thus, the attractive range of the Peltier (air temperatures of 27.9-32.2°C) approximates the temperature range of human skin, 29-35°C [Yao et al., 2008].

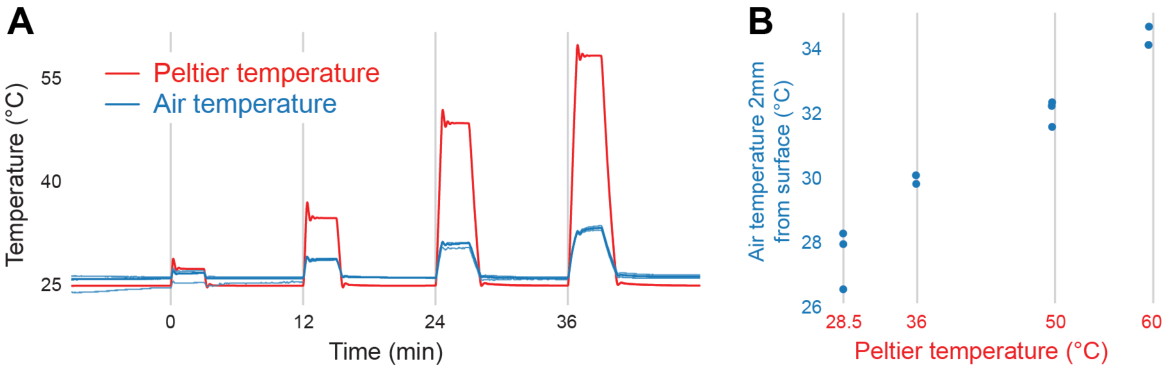

Figure 3.4 Mosquitoes likely experience air temperatures lower than reported internal temperatures of the Peltier during heat bouts. (A) Peltier temperature (red, internal temperature of the Peltier as measured by a thermocouple) and air temperature measured by a thermocouple placed 2 mm from the Peltier surface (blue), n = 3. Thick lines indicate median temperatures, and thin translucent lines indicate temperature of individual trials. **(B)** Air temperature graphed as a function of Peltier temperature.

3.4 Dark visual contrast redistributes mosquito occupancy at all attractive temperature

To examine the effect of the dot more closely, we compared mosquito locations with and without the visual cue during thermotaxis (Fig 3.5A). With the visually blank Peltier, mosquitoes spread themselves evenly across the warm Peltier, with a slight bias towards the bottom edge. However, when the dot was present, mosquitoes aggregated on and around the dot at all non-noxious temperatures (Peltier temperatures: 26-50°C, Fig 3.5B). The presence of the visual cue thus redistributed mosquito occupancy, shifting it from the bottom of the Peltier to the center. As the dot is thermally indistinguishable from the rest of the Peltier, the mosquitoes are likely aggregating on the dot because of visual attraction.

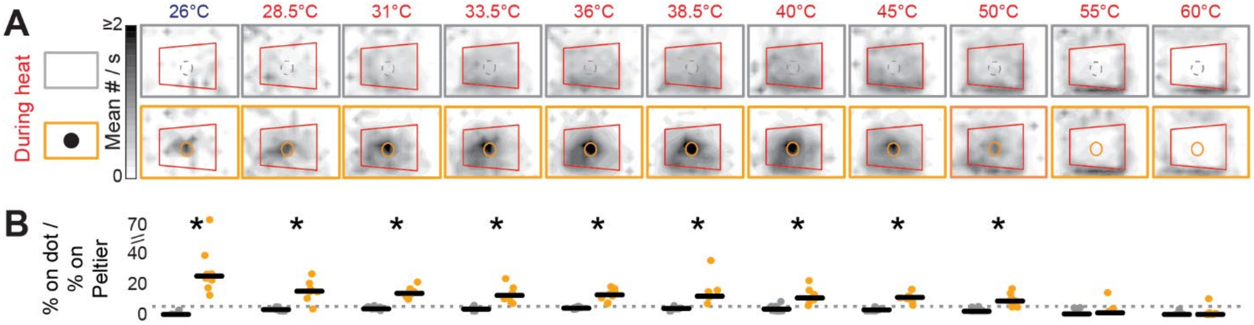

Figure 3.5 Mosquitoes preferentially land on the dot at all non-noxious temperatures. (A) Heat maps showing mean mosquito occupancy on the Peltier (red line) and surrounding area during seconds 90-180 of heat. Orange line indicates visual stimulus position on dot trials, and gray dotted outline indicates equivalent position on blank trials. **(B)** Ratio of the % of mosquitoes on the area of the dot over the % of mosquitoes on the entire area of the Peltier during 90-180 s of heat. Dotted line indicates expected value from a uniform spatial distribution (5.42%, or the area of the dot over the area of the Peltier).

3.5 Are thermotactic and visual attractions additive?

Peltier occupancy in this assay is multisensory, affected by visual, thermal, and CO_2 cues. Combining thermal and CO_2 cues results in multisensory enhancement, in which occupancy in response to the cues combined is much greater than occupancy in response to the cues presented singly [McMeniman et al., 2014]. Does combining visual cues with thermal and CO_2 cues result in a similar enhancement?

We can estimate the effect of visual and CO_2 cues alone by taking the occupancy of mosquitoes on the visually marked Peltier at 26°C. If we subtract this “visual” occupancy from the “visual and thermal” traces represented by occupancy on the dot-marked Peltier at higher than ambient temperatures, we obtain traces which are superficially remarkably similar to those of “thermal” traces of occupancy on the blank Peltier for non-noxious temperatures (Fig 3.6). Interestingly, this overlap lessens at 55 and 60°C, implying that noxious heat and visual stimuli do not sum linearly together. This initial look is qualitative but provokes interesting questions to investigate further. Since these experiments are performed in a population of mosquitoes, do these additive effects represent two subpopulations, one motivated by visual cues and the other by thermal cues? Or are individual mosquitoes summing the two sensory drives? These questions could be answered in an assay with the ability to present the same populations of mosquitoes with a Peltier with and without visual stimuli, as could be with a projection or LED system instead of paper stimuli, and the ability to track individual mosquitoes.

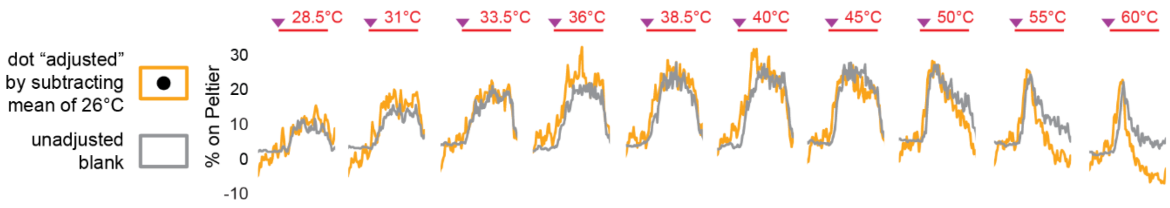

Figure 3.6 Thermotactic and visual attractions may be additive without enhancement. Subtracting “vision and CO_2 alone” from occupancy traces of the dot-marked Peltier leads to surprising overlap between the dot-marked (orange, n = 8) and blank (gray, n = 8) mean % traces for all non-noxious temperatures. Data from Figure 3.2C. Red line indicates the time the Peltier is heated. Purple triangle is the 20 s pulse of CO_2.

3.6 Enhancing of thermotaxis by visual contrast does not depend on order of presentation

Similar results as in sections 3.2-4 were obtained when we randomized the order of the Peltier temperatures (Fig 3.7A, B). Mosquitoes occupied the dot at ambient temperatures before all heat bouts (Fig 3.7C). In an interesting divergence from the ordered heat bouts, total mosquito occupancy was greater on the visually marked Peltier at all non-noxious heat bouts, except for 33.5°C, the first heat bout presented

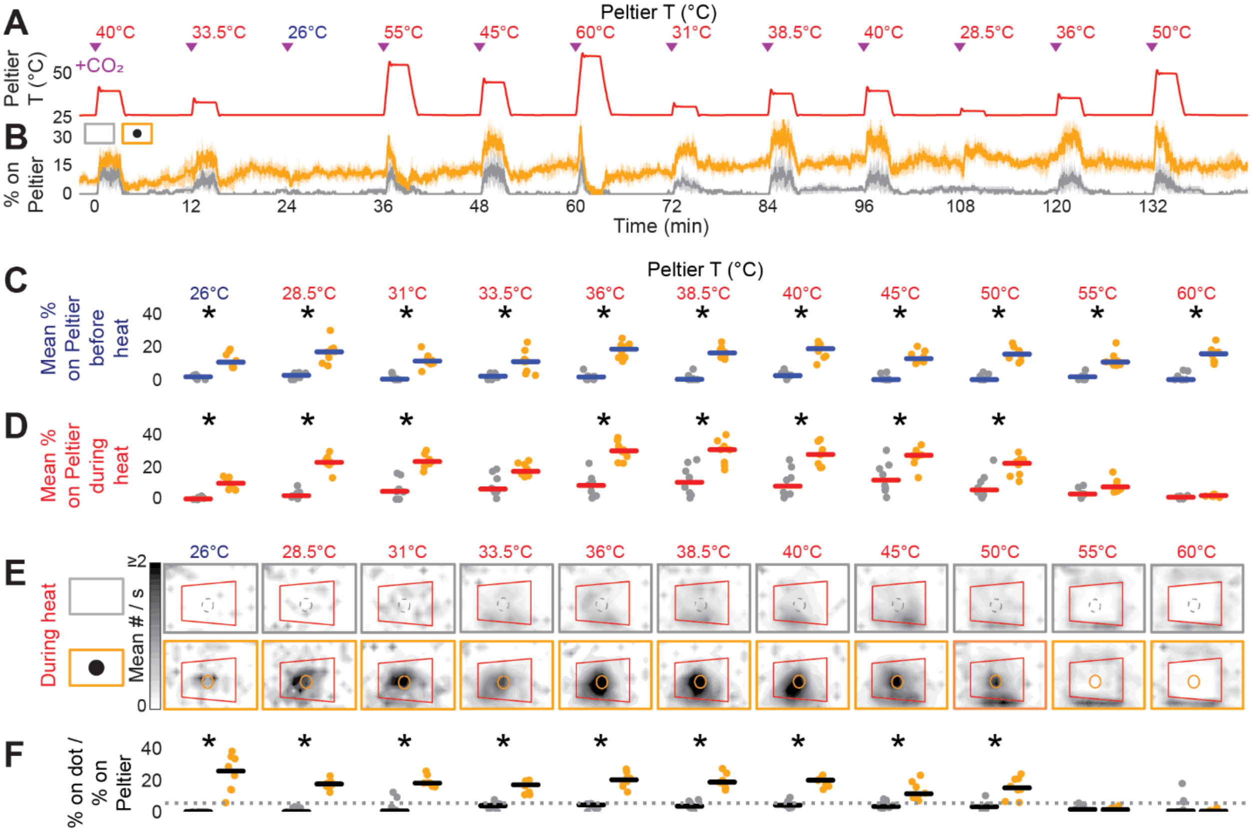

Figure 3.7 Visual cue enhances mosquito thermotaxis to moderate heat presented in shuffled order and to areas of contrast. (A) Peltier temperature. CO_2 was pulsed in for 20 s at onset of each heat bout (purple triangle). **(B)** Median ± median absolute deviation % of populations of 45-50 mosquitoes on Peltier, blank (gray, n = 8) or marked with circle (orange, n = 8). **(C,D,F)** Median % of mosquitoes on the Peltier (C) 90-0 s before onset of heat, **(D)** 90-180 s after onset of heat, and (F) on the dot 90-180 s after onset of heat, normalized by median % of mosquitoes anywhere on the Peltier**.** Dotted line in (F) indicates expected value from a uniform spatial distribution. *p < 0.05, Mann-Whitney U test with Bonferroni correction. (E) Smoothed histograms of mosquito positions during heat, boundaries of Peltier (red) and blank (gray) or visual cue (orange).

(Fig 3.7D). Perhaps this indicates a slight acclimation over the course of the assay. The significant difference between the visually marked and unmarked Peltier seems to be driven mostly by low responses to the unmarked Peltier. As mosquito populations in all trials showed thermotaxis towards the test 40°C heat at the beginning of the assay (see Methods), this is either due to some previously uncharacterized effect of heat bout sequence on mosquito responses to blank Peltiers, or due to seasonal variation in the behavior. Nevertheless, these shuffled results corroborate the ordered results shown previously, as there are significant differences between marked and unmarked Peltiers at more moderate temperatures. The spatial redistribution caused by the dot is likewise replicated here, with mosquitoes preferentially landing on or around the dot at all non-noxious temperatures when present (Fig 3.7E, F). Overall, these results show that the enhancement of thermotaxis by visual contrast does not depend on order of heat bout presentation.

3.7 Conclusion: Mosquito thermotaxis is enhanced by visual contrast

These results replicate and expand upon a previous finding that visual contrast enhances host-seeking [van Breugel et al., 2015]. We have begun to elucidate the precise mechanisms by which this enhancement occurs by showing that moderate warmth becomes more attractive to mosquitoes when visually marked, and mosquitoes aggregate on areas of high contrast at all attractive temperatures.

Chapter 4: Mosquito thermotaxis requires exposure to CO_2

4.1 Testing the relationship between thermotaxis and CO_2 activation

Previous reports showed that mosquito thermal attraction is enhanced by CO_2 [Burgess, 1959; McMeniman et al., 2014; Krober et al., 2010], which could be through at least two mechanisms.

One possibility is that CO_2 could increase the propensity of mosquitoes to take off and remain in flight, which would increase their probability of coming close enough to a surface to sense its heat. This explanation posits that CO_2 activation and heat-seeking are two separate behavioral modules within the host-seeking sequence. CO_2 links the two by indirectly changing the *external environment* of the mosquitoes, bringing them to heat that they otherwise would not sense. If mosquitoes were to be placed on host heat without elevated CO_2, they would proceed through their independent heat-seeking module, robustly seeking relative warmth.

Alternately, CO_2 could alter mosquito thermal preferences so that they become attracted to temperatures they would ordinarily ignore or avoid. In this case, CO_2 directly changes the *internal state* of mosquitoes, and both CO_2 activation and heat-seeking belong to the same behavioral module. This explanation predicts that even if mosquitoes were to be placed on host heat without elevated CO_2, they would not be interested in pursuing heat.

To distinguish between these two explanations, we needed a CO_2- and heat-independent method of attracting mosquitoes to land on a surface. Serendipitously, mosquito attraction to dark visual contrast is independent of CO_2 and heat attraction, and so the visually marked Peltier can be used to probe the link between CO_2 activation and thermotaxis.

4.2 Wild-type mosquitoes flee heat in the absence of CO_2

In the course of running the experiments of Chapter 3, we discovered that when CO_2 was not puffed into the chamber, mosquitoes aggregated on the visual cue (Fig 4.1A, B). This CO_2-independent attraction to the dot in free flight complemented our observations that the visual responses of magnotethered mosquitoes are not affected by CO_2 concentration (Fig 2.8) and that free flying mosquitoes aggregate on the visually marked Peltier before CO_2 is puffed into the chamber (Fig 3.2C).

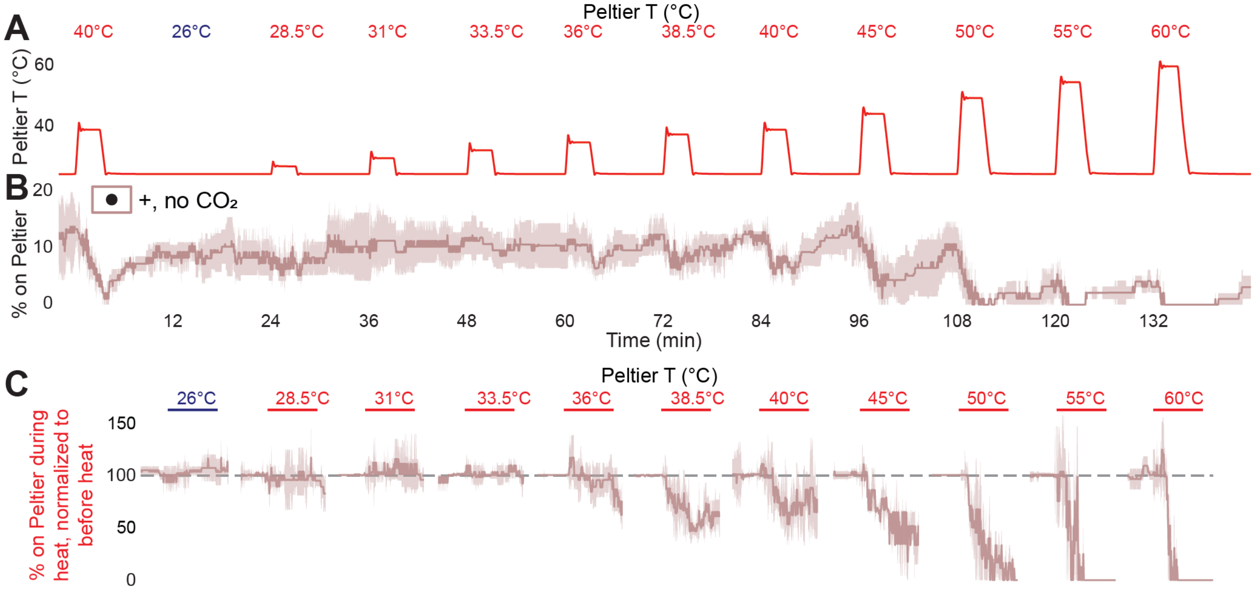

Figure 4.1 Wild-type mosquitoes are not attracted to host-like temperatures without elevated CO_2. **(A)** Peltier temperature. **(B)** Median ± median absolute deviation % of populations of 45-50 wild-type mosquitoes (n = 6) on the visually marked Peltier. **(C)** Median ± median absolute deviation of % residence on Peltier over time, normalized to mean residence 60-0 s before heat. Red horizontal line: heat on.

Further, we found that mosquitoes fled the Peltier at normally attractive temperatures (38.5-50°C, Fig 4.1C). They then reaccumulated on the Peltier, similar to the higher temperatures in experiments described in Chapter 3. These preliminary results suggested that mosquitoes avoided host temperatures in the absence of other host cues and motivated further study.

4.3 *Gr3*$^{ECFP/ECFP}$ mutant mosquitoes, insensitive to CO$_2$, are attracted to visual stimuli

CO$_2$ is a pervasive and naturally-occurring stimulus that is difficult to remove from behavioral assays. In light of this, we used *Gr3*$^{ECFP/ECFP}$ mosquitoes. Wild-type GR3 encodes a putative subunit of the mosquito CO$_2$ receptor. The insertion of constitutively expressed ECFP into the *Gr3* locus disrupts receptor function and completely abolishes CO$_2$ sensation (Fig 4.2) [McMeniman et al., 2014].

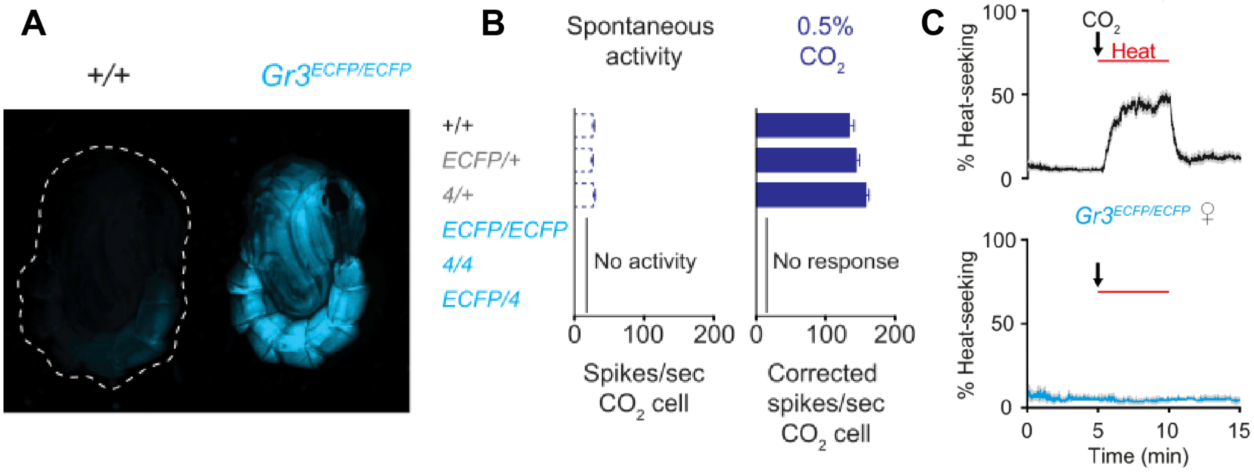

Figure 4.2 *Gr3*$^{ECFP/ECFP}$ mosquitoes cannot sense CO$_2$. Adapted from McMeniman et al., 2014. **(A)** Bright-field fluorescent images of wild-type and *Gr3*$^{ECFP/ECFP}$ pupae, showing ubiquitous expression of ECFP. **(B)** Single-sensillum recordings from *Gr3* mutants. **(C)** % of populations of 15-20 wild-type (black) or *Gr3*$^{ECFP/ECFP}$ (cyan) mosquitoes in response to 40°C heat (red line).

We tested responses of *Gr3*$^{ECFP/ECFP}$ mosquitoes to a heat ramp with a dot-marked Peltier (Fig 4.3A). We ran mutant mosquitoes on the same day as their *Gr3*$^{ECFP/+}$ half-siblings and the wild-type parental strain, both of which retain a functional version of the CO_2 receptor and are sensitive to CO_2 (Fig 4.2). All groups of mosquitoes accumulated on the Peltier between heat bouts (Fig 4.3B), replicating our observation that CO_2 does not alter mosquito visual preferences in the magnotether assay (Fig 2.8). While absolute percentages of *Gr3*$^{ECFP/ECFP}$ mosquitoes between heat bouts diverge from *Gr3*$^{ECFP/+}$ and wild type controls over the course of the experiment, this is likely because the groups of mosquitoes react differently to heat. Qualitatively, the rates of accumulation between heat bouts look similar for all groups mosquitoes.

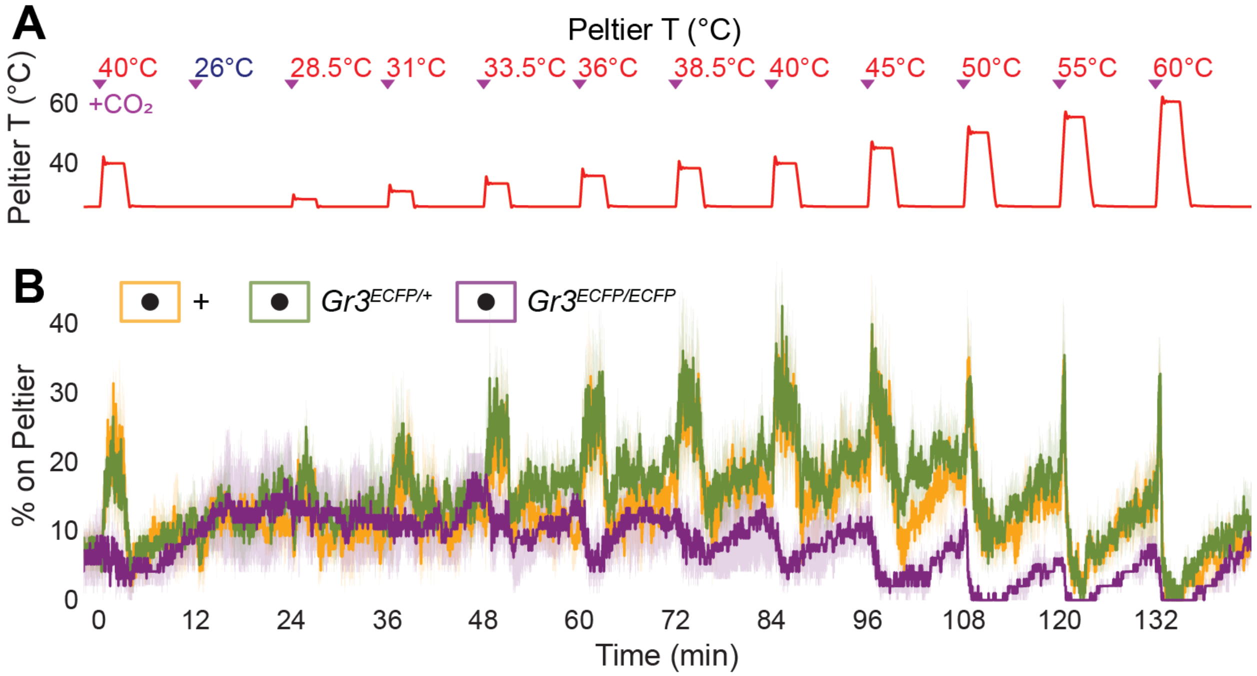

Figure 4.3 *Gr3*$^{ECFP/ECFP}$ mosquitoes accumulate on the Peltier in between bouts of heat. (A) Peltier temperature. CO_2 was pulsed for 20 s at the onset of each heat bout (purple triangle). (B) Median % ± median absolute deviation % of populations of 45-50 mosquitoes on Peltier marked with a visual cue. Genotypes: *Gr3*$^{+/+}$ or wild type (orange, n = 6), *Gr3*$^{ECFP/+}$ (green, n = 6), and *Gr3*$^{ECFP/ECFP}$ (purple, n = 6).

4.4 *Gr3*$^{ECFP/ECFP}$ mutant mosquitoes flee heat

Whereas wild-type and *Gr3*$^{ECFP/+}$ heterozygous mosquitoes increased Peltier occupancy with increasing temperatures, *Gr3*$^{ECFP/ECFP}$ mutant mosquitoes left the Peltier when it was heated to host-like temperatures (Fig 4.4). Because of the diverging numbers of mosquitoes on the Peltier before the heat bout, we analyzed the relative change in occupancy, rather than the absolute occupancy analyzed in Fig 3.3. We normalized the percentage of mosquitoes occupying the Peltier during heat using the mean number of mosquitoes in the 90 s before heat. *Gr3*$^{ECFP/+}$ and wild type controls were statistically indistinguishable from each other at all temperatures. These controls were significantly different from *Gr3*$^{ECFP/ECFP}$ at 36, 45, 50, 55, and 60°C, and approached significance at 40 and 45°C. While the percentages of *Gr3*$^{ECFP/+}$ mosquitoes were very similar to wild type mosquitoes during heat bouts, small differences in their mean occupancy before heat bout were exaggerated in the normalized measure of occupancy, thus increasing the variance between control groups.

Gr3$^{ECFP/ECFP}$ mosquitoes respond very differently to heat than their CO_2-sensitive *Gr3*$^{ECFP/+}$ and wild type counterparts. They never increase their occupancy during heat

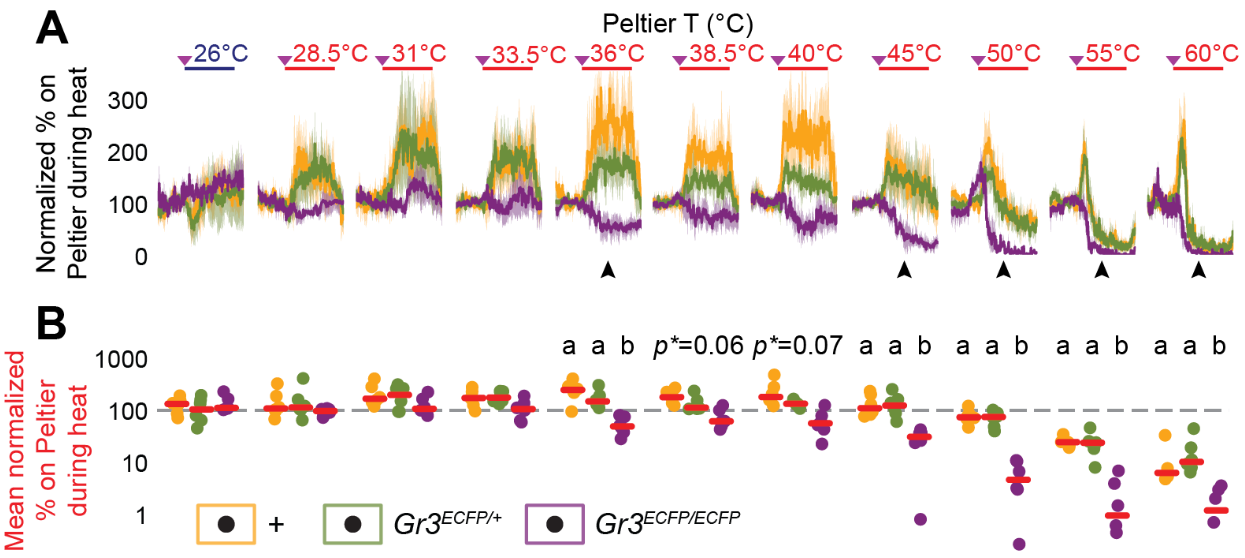

Figure 4.4 *Gr3*$^{ECFP/ECFP}$ mutant mosquitoes flee heat at 36°C and above. (A) Median ± median absolute deviation of % residence on Peltier over time, normalized to mean residence 60-0 s before heat. Purple triangle: CO_2 pulse; red horizontal line: heat on. **(B)** Median % of mosquitoes on the Peltier during heat, normalized as in (A) and plotted on a log10 scale to highlight deviation from 100% (dotted line). Significance ($p < 0.05$) was assessed with Kruskal-Wallis test with Bonferroni correction, then post hoc Mann-Whitney U test with Bonferroni correction. Different letters mark statistically distinct groups.

bouts, and when *Gr3*$^{ECFP/+}$ and wild type mosquitoes increase their occupancy from 36-45°C, they decrease their occupancy. We therefore speculate that CO_2 shifts mosquito thermal preferences in a manner independent of visual stimuli, causing mosquitoes to pursue elevated heat only when they have corroborating evidence that the heat comes from a breathing host.

4.5 *Gr3*$^{ECFP/ECFP}$ mutant mosquitoes do not return to heat after taking off, but wild-type mosquitoes do

CO_2 could act to increase occupancy on host-like temperatures by causing mosquitoes to dwell on heat longer, or to land more frequently on heat. To examine how these rates changed, we manually tracked landings on and take-offs from the Peltier set to 36°C (Fig 4.5). This temperature in combination with CO_2 attracts wild-type and *Gr3*$^{ECFP/+}$ heterozygous mosquitoes but repels *Gr3*$^{ECFP/ECFP}$ mosquitoes (Fig. 4.4), allowing us to compute a population mean dwell time on heat using times of landings and take-offs. We chose to compare dwell times instead of takeoff rates because it allowed us to estimate the amount of time individual mosquitoes persisted on heat.

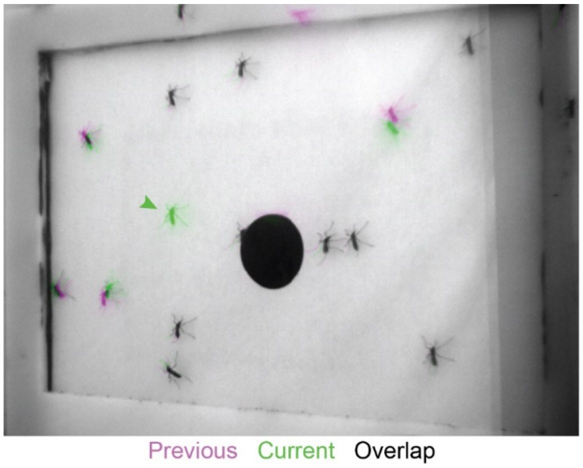

Figure 4.5 Manual scoring of landings and take-offs. Example image of two superimposed frames. Green arrowhead: landing event.

Wild-type and *Gr3*$^{ECFP/+}$ heterozygous mosquitoes did not dwell longer on heat than *Gr3*$^{ECFP/ECFP}$ mosquitoes (Fig 4.6A), perhaps because unlike CO_2-sensitive mosquitoes [McMeniman et al., 2015], CO_2-insensitive mosquitoes do not increase their general motor activity after CO_2 pulses. This suggests that 36°C heat alone is an aversive cue for all landed mosquitoes, replicating previous findings in which mosquitoes walking on a thermal gradient avoided temperatures above 30°C [Corfas & Vosshall, 2015; Blanford et al., 2009]. Instead, the increase in occupancy primarily comes from increased landing of CO_2-sensitive mosquitoes on host-like temperatures (Fig 4.6B). Furthermore, in CO_2-sensitive mosquitoes the number of landings was five to ten times greater than the number of mosquitoes, indicating that individual mosquitoes must be landing and taking off multiple times.

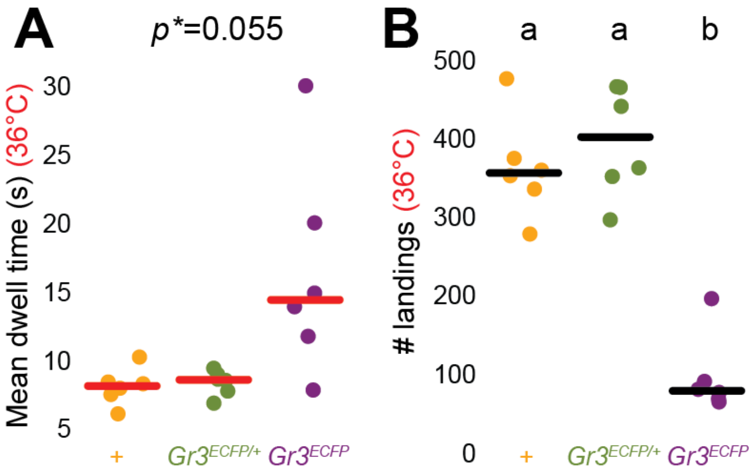

Figure 4.6 Increased occupancy of CO_2-sensitive mosquitoes on 36°C heat is driven by increased landings, not increased dwell times. (A) Mean dwell time and **(B)** number of landings on Peltier wall over the entire heat bout. Significance ($p < 0.05$) was assessed with Kruskal-Wallis test with Bonferroni correction, then post hoc Mann-Whitney U test with Bonferroni correction. Different letters mark statistically distinct groups.

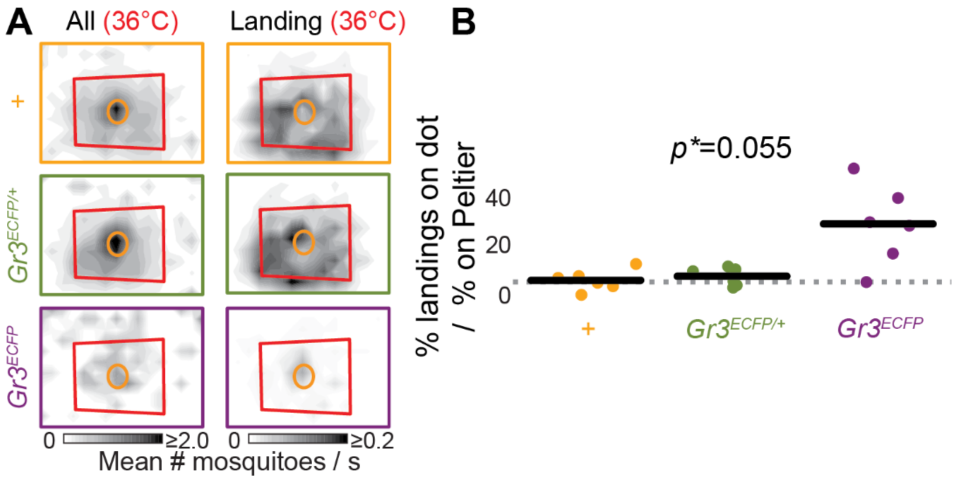

Figure 4.7 *Gr3*$^{ECFP/ECFP}$ landings on the wall may be visually driven. (A, B) Heat maps showing (A) mean mosquito occupancy or (B) landing events on the Peltier (red outline) and surrounding area during entire 36°C heat bout. Visual cue is outlined in orange. **(C)** Ratio of the % of mosquitoes on the area of the dot over the % of mosquitoes on the entire area of the Peltier during 90-180 s of heat. Dotted line indicates expected value from a uniform spatial distribution (5.42%, or the area of the dot over the area of the Peltier). p-value obtained using a Kruskal-Wallis test with Bonferroni correction.

Gr3$^{ECFP/ECFP}$ mosquitoes also still landed on 36°C, but this may be visually driven. While CO_2-sensitive mosquitoes landed evenly across the heated surface, *Gr3*$^{ECFP/ECFP}$ mosquitoes tended to land on the dot, though this effect was not significant (Fig 4.7). Interestingly, while wild-type and *Gr3*$^{ECFP/+}$ mosquitoes aggregated on or around the dot, they did not land preferentially on the dot. This suggests that mosquitoes land on the Peltier and then walk towards the dot afterwards. As walking mosquito visual behavior has not yet been studied, further examination is required to know if this post-landing visual attraction is typical.

All landed mosquitoes dwell only briefly on 36°C, indicating that CO_2 does not act by decreasing an off rate from heat. Instead, *Gr3*$^{ECFP/ECFP}$ uniquely fail to return to heat. Mosquito attraction to host-like temperatures is thus contingent on the perception of elevated CO_2, which drives mosquitoes to repeatedly return to the thermal stimulus.

4.6 Individually tracked mosquitoes return to heat multiple times

In our assay, we posit that an individual CO_2-sensitive wild type mosquito and an individual CO_2-insensitive *Gr3*$^{ECFP/ECFP}$ mosquito begin by sitting on the Peltier surface at ambient temperature, attracted there by the dark visual stimulus. When the surface temperature rises to 36° and CO_2 is puffed into the chamber, both the wild type and the *Gr3*$^{ECFP/ECFP}$ leave. Only then do the two diverge: the *Gr3*$^{ECFP/ECFP}$ mosquito does not return, but the wild type is motivated by elevated CO_2 to return to heat. To verify that individual wild-type mosquitoes are returning to heat multiple times upon CO_2 activation, we used a 3D tracking system to automatically record individual mosquito trajectories as they flew towards a Peltier warmed to 40°C (Fig 4.8).

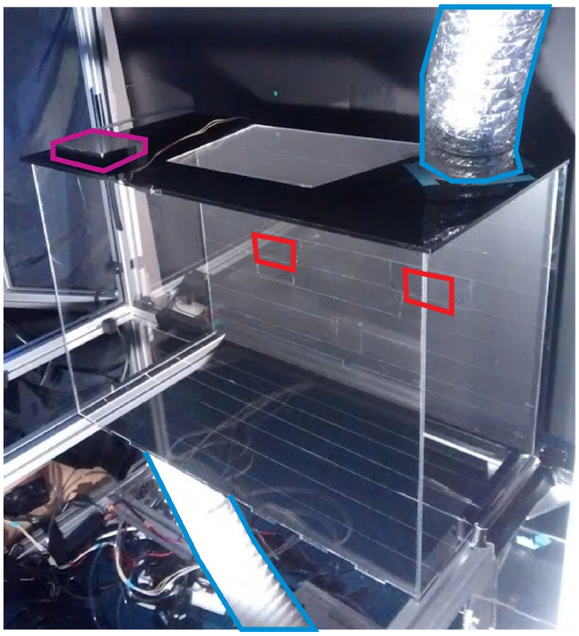

Figure 4.8 Enclosure for 3D tracking of mosquito trajectories (SciTracks). Two cameras at the front triangulate mosquito position. Red outlines: Peltier devices for providing heat. Magenta outline: CO_2 delivered from a FlyPad. Blue outline: Circulating air system for regulating humidity.

We recorded trajectories from 96 individual female mosquitoes and automatically scored their behavior as flying or walking based on their velocity, then subdivided walking into walking on the left Peltier, walking on the right, or walking anywhere else based on position (Fig 4.8). In this preliminary experiment, the left Peltier was maintained at the ambient temperature of 22°C and the right Peltier was heated to 22, 31, 40, and 60°C. These ethograms, though preliminary, show qualitatively that mosquitoes activate flight when CO_2 is puffed into the enclosure and that mosquitoes walk on the Peltier more when it is heated to 40°C.

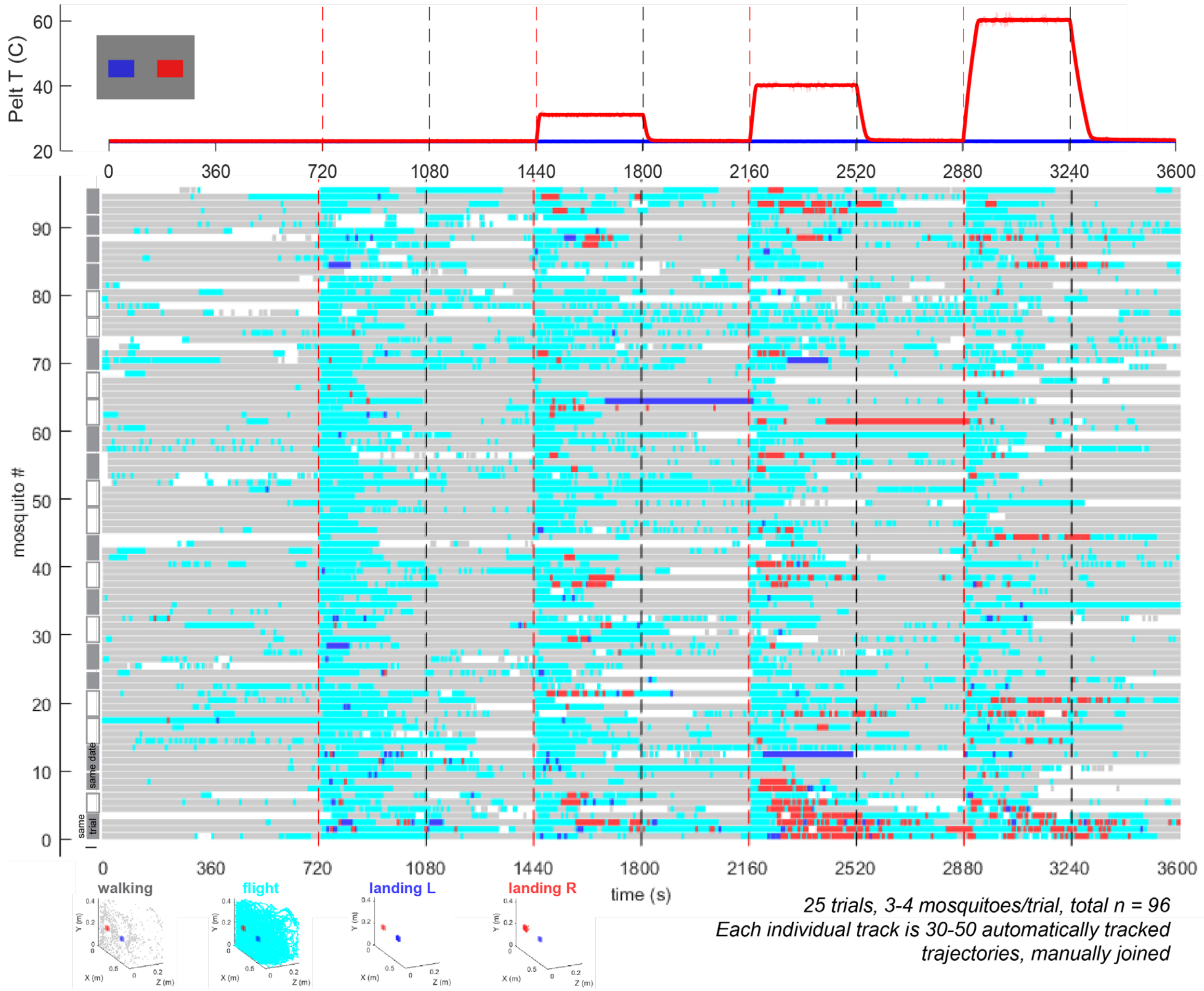

25 trials, 3-4 mosquitoes/trial, total n = 96
Each individual track is 30-50 automatically tracked trajectories, manually joined

Figure 4.9 Preliminary ethograms of 96 individual mosquitoes responding to heat and CO_2. Flights are coded according to flight (cyan), walking (gray), walking on the left Peltier (blue), and walking on the right Peltier (red).

Out of these 96 mosquitoes, 26 landed on 40°C heat at least once (Fig 4.10). Almost all of these mosquitoes left heat and returned multiple times. This preliminary

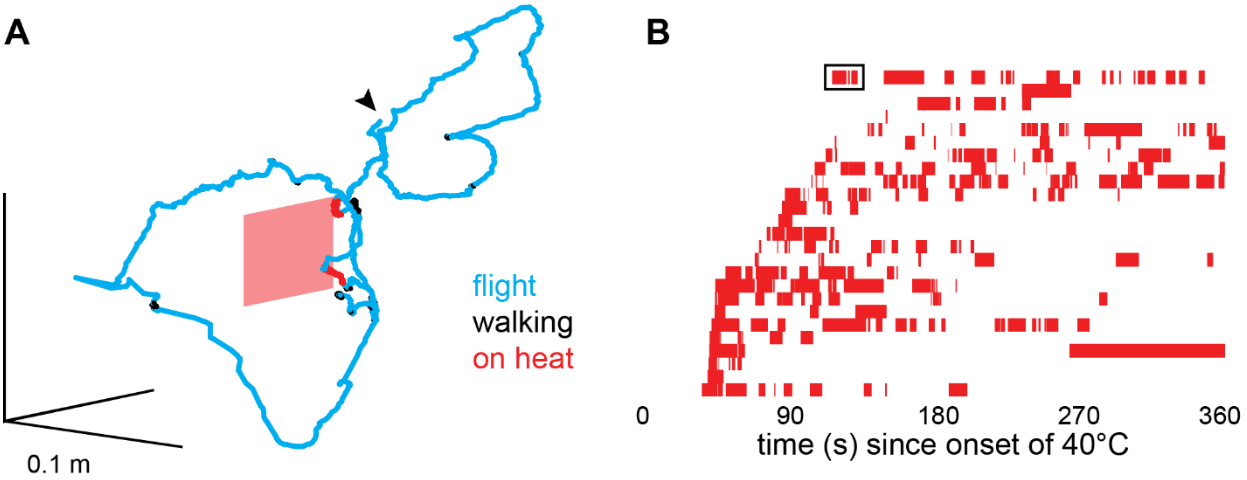

Figure 4.10 Individual mosquitoes return to 40°C heat multiple times. (A) Example trajectory of a female mosquito flying towards a Peltier warmed to 40°C (red filled rectangle). Trajectory is colored based on behavior. Black arrowhead indicates the start of the trajectory in time. **(B)** Raster plots of events where mosquitoes are scored as being on heat. The black box indicates the trajectory highlighted in (A).

evidence verifies that individual mosquitoes are returning to heat multiple times upon CO_2 activation. The mechanisms underlying this return are a ready subject for future inquiry.

4.7 Conclusion: Mosquitoes weigh cues based on certainty of information

Both visual contrast and heat contribute to mosquito attraction. However, whereas visual contrast is generally attractive even outside the context of host-seeking, attraction to heat is contingent upon co-presentation of the chemosensory host-cue CO_2. We speculate that this attraction to visual contrast in flight may be adaptive because flying is an energetically expensive activity [Reinhold, 1999], so finding a dark landing location may provide general respite and camouflage.

However, residence on high heat brings with it threats of damage and desiccation. Indeed, mosquitoes die after 30 min exposures to air temperatures above 42°C [Eisen et al., 2014]. Mosquitoes may balance this thermal threat of heat against the beneficial use of heat as a potent signature of warm-blooded hosts by only thermotaxing when they detect other reliable host cues such as CO_2. Similar to other examples of multisensory integration [Meredith & Stein, 1983; Schumacher et al., 2016], mosquitoes integrate heat and CO_2 to increase their certainty of finding a host.

Chapter 5: Discussion

In this thesis, we have looked at how mosquitoes use vision, then heat and CO_2 in combination to seek hosts at close range. We have shown that *Ae. aegypti* mosquitoes use serial sensory modules in host-seeking. They fly toward visual contrast, and then sense CO_2 to unlock thermotaxis towards potential hosts. These results open many new and exciting inquiries on levels of sensorimotor strategy, neural encoding, and the evolution of complex behavior. We conclude with a series of questions to motivate future discovery.

5.1 Do visual cues signify specific features for mosquitoes?

In this preliminary investigation into mosquito visual responses, we tested only simple shapes with sharp contrasts. Open questions include what visual cues are found in the mosquito natural environment, and if any of them could signify ethologically significant features.

5.1.1 Do host-seeking mosquitoes use visual host cues?

In experiments performed in the magnotether, we could not detect any effects of CO_2 or blood-fed state on mosquito responses to simple shapes. Our free flying data suggest that this attraction to a simple shape, such as a black dot, can sum linearly with thermal and CO_2 attraction. However, our investigations do not exclude the possibility that visual cues could exist which superadditively enhance heat-seeking drives. Such visual cues could be a signature of human hosts to the human-preferring *Ae. aegypti.*

Previous studies have implicated motion as a potential visual host signature [Sippell & Brown, 1979]. In our tethered experiments, we moved our simple shapes sinusoidally. This type of rigid, regular movement is rare in the large vertebrates *Ae. aegypti* pursue, which move phasically as linked sets of body parts. Biological motion, as this is termed, has been studied previously by marking joints and videotaping their movements [Johansson, 1973]. More recent technologies estimate animal pose automatically through deep neural networks [Pereira et al., 2019]. These automated methods could provide a vast trove of simplified biological motion data to rapidly present in the LED arena to tethered mosquitoes. We hypothesize that the human specialist *Ae. aegypti* orients more strongly to typical human motion than to the motion of other vertebrates, such as guinea pigs, in the same way that these mosquitoes prefer human scent [McBride et al., 2014].

We can also find preferred visual stimuli for mosquitoes using adaptive sampling [reviewed in Benda et al., 2007 and DiMattina & Zhang, 2013]. These algorithms were originally developed to generate sensory stimuli that cause a recorded neuron to maximally or most reliably fire action potentials, and could potentially be adapted to automatically design magnotether stimuli. Tuning stimuli requires a set of parameters to vary, such as visual contrast or height-width aspect ratio, and a real-time readout of the behavior to maximize. For intracellular recordings, this behavior is spike rates. For a magnotethered mosquito, the behavior is orientation towards the stimulus. While the magnotether experiments presented in this thesis did not use real-time readouts of orientation, the software platform used (Fig 2.5) is designed to compute flight data “on the fly” and is used in numerous other applications to set stimuli in closed loop [Straw &

Dickinson, 2009]. By profiling optimal visual cues for mosquitoes in air and CO_2, after saline and blood meals, and looking for varying responses, we can screen for potential visual host cues in an unbiased manner.

5.1.2 Do mosquitoes use polarized light for host-seeking or for egg-laying?

Alongside shape and motion cues, *Ae. aegypti* mosquitoes may use polarized light to straighten their flight paths and thus maximize their range while actively host-seeking. The polarization of light refers to the orientation of its waveform, a quality invisible to human eyes but seen by many invertebrates [reviewed in Wehner & Labhart, 2006]. While direct sunlight includes all waveform orientations and is therefore unpolarized, polarized light arises in nature because certain waveforms are selectively scattered. The sky characteristically scatters sunlight in circles around the sun, and this pattern of sky polarization has been used by insects from dung beetles [reviewed in el Jundi et al., 2019] to *Drosophila* [reviewed in Warren et al., 2019] to maintain constant headings during short trips.

The use of polarization vision for host-seeking in *Aedes* and *Culex* mosquitoes has been documented once [Wellington, 1974], and mosquitoes do seem behaviorally capable of detecting polarized light [Bernath et al., 2012]. First, we can ask if *Ae. aegypti* mosquitoes have the specialized eye structures needed to detect polarized light [reviewed in Labhart & Meyer, 1999]. The physical structure of insect photoreceptor cells leads them maximally absorb light with one polarization orientation. Because light comes in multiple orientations, this built-in filter leads to illusory intensity gradients, and so is abolished in most ommatidia by twisting the photoreceptor cells. However, polarization-sensitive insects from crickets to bees have specialized ommatidia in the skyward-facing dorsal rim of their eyes with photoreceptors which are not twisted, and these allow them to sense sky polarization. Polarization sensitivity thus has an anatomical signature, readily seen in electron micrography. The *Ae. aegypti* eye has a dorsal rim area that is genetically patterned with distinct opsins (op2 in Fig 5.1) [Hu et al., 2013]. Does this genetic pattern correlate with an anatomical pattern? We can perform electron micrography on the *Ae. aegypti* dorsal rim ommatidia to see if they possess polarization-sensitive photoreceptor cells.

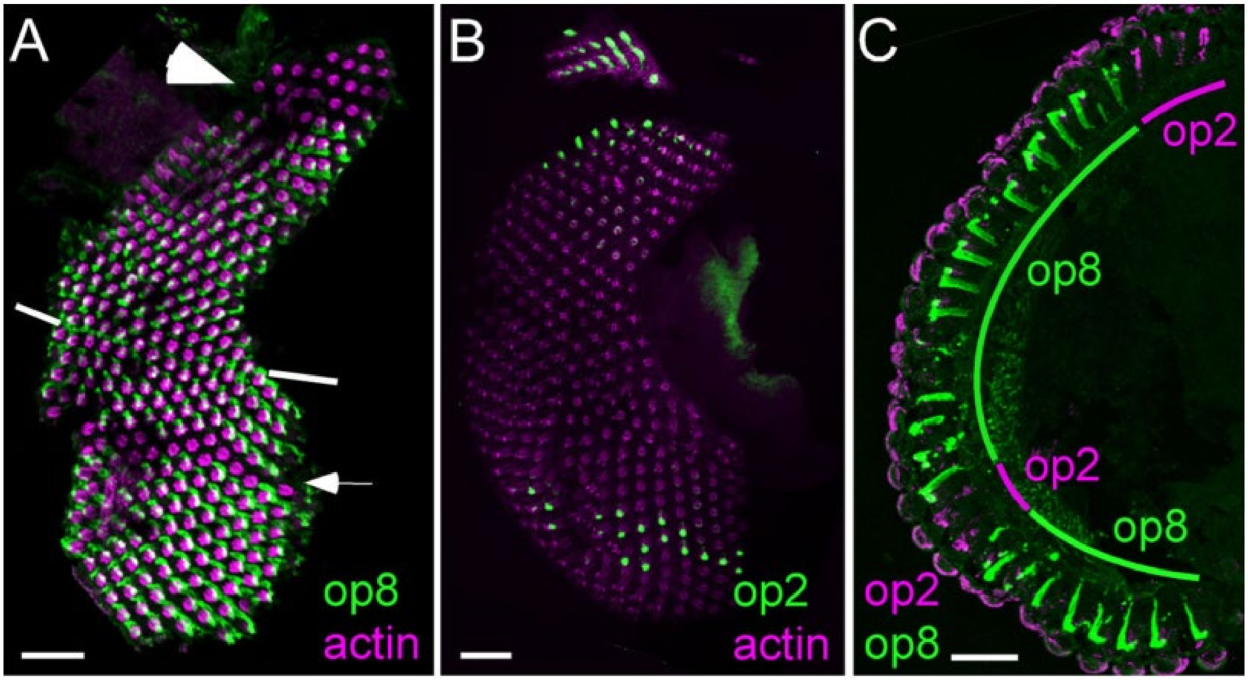

Figure 5.1 Pattern of opsin expressions in the *Ae. aegypti* eye suggests polarization sensitivity in dorsal rim and ventral stripe. A UV-sensitive opsin (op8) and long-range opsin (op2) alternate expression in the eye to define four stereotyped zones. From Hu et al., 2013.

Should *Ae. aegypti* possess suitable optical architecture, the natural next experiment is to tether mosquitoes under a polarized sky and see if they maintain a constant orientation. One of the first applications of the magnotether in *Drosophila melanogaster* performed this experiment and showed that *Drosophila* orient towards sky polarization [Weir & Dickinson, 2012]. The previous study on polarization vision in host-seeking mosquitoes documented ranging flights at dawn and dusk, when skylight polarization is most informative of direction. It will be interesting to investigate if polarization orientation in mosquitoes is increased during these active twilight periods, or after activation by CO_2.

Pools of standing water also scatter light to produce a characteristic pattern of horizontal polarization. These pools of standing water are also highly attractive to female *Ae. aegypti* searching for suitable locations to lay eggs. We may ask if mosquitoes use polarization vision to find water, as has been shown in partially aquatic insects from dragonflies [Wildermuth, 1998] to midges [Horvath et al., 2011] to caddis flies [Kriska et al., 2008]. Intriguingly, mosquito dorsal rim opsins are shared by a ventral stripe in *Ae. aegypti* eyes (op2 in Fig 5.1) [Hu et al., 2009; Hu et al., 2013]. The two regions may also share polarization detection functionality, scanning above for sky direction and below for water. Again, the key experiments are to anatomically examine the ventral stripe for polarization-sensitive photoreceptor cells, then to perform tethered experiments to see if mosquitoes with developed eggs orient towards horizontally polarized light. Complementing the general attraction established by the thesis, these proposed experiments will further elucidate the specialized roles vision may have in the life of a mosquito.

5.2 What motivates activated mosquitoes to return to heat?

While previous assays have examined approach to heated surfaces [Corfas & Vosshall, 2015; van Breugel et al., 2015], in our experiments we were able to examine the responses of landed mosquitoes to heat in a host-seeking context. We showed that both CO_2-sensitive and CO_2-insensitive mosquitoes leave surfaces at host heat, but only CO_2-sensitive mosquitoes return to heat. Many questions remain about how and why this return occurs.

First, why do CO_2-sensitive mosquitoes leave a heated surface, only to fly back? Is heat appetitive to flying mosquitoes but aversive to landed mosquitoes, as it is in thermal gradient assays [Corfas & Vosshall, 2015; Blanford et al., 2005] and for CO_2-insensitive mutants? Flight and walking represent different internal states, and many sensory stimuli have different gains and valences depending on activity state [reviewed in Maimon, 2011]. This is further complicated by differences between heat transfer experienced by a flying mosquito through convection in air and by a landed mosquito through conduction by contact. To test if mosquito responses to heat are dependent on flight state, we can heat tethered mosquitoes in a consistent, directional fashion, such as with a laser with known heat transfer, and see if mosquitoes orients towards or away from the heat depending on whether she is walking on a ball or flying from a tether.

Alternatively, perhaps CO_2-sensitive mosquitoes are not averse to heat like CO_2-insensitive mosquitoes, but are instead hyperactively exploring because they have been activated by CO_2. After all, the Peltier is warm but offers no blood. We can examine this by comparing takeoff rate across different temperatures. If mosquitoes take off at the same rate at ambient as they do on host heat, thermal cues likely do not play a role in the takeoff of activated mosquitoes. If so, then CO_2 truly is shifting thermal preferences of mosquitoes, causing them to disregard otherwise aversive heat, and further study could focus on elucidating the mechanisms behind that shift in internal state.

Activated mosquitoes could return to heat they have left because no other option has been presented in the assay, or because they do not remember that they have previously explored the area. We can distinguish between the two using an assay with two Peltiers, such as in the 3D tracking arena, and alternating which Peltier is warm. If mosquitoes have a memory of a previously unsatisfying place, then we might expect them to explore a novel heated location with shorter latency than the one they have already known. These experiments further define the behavioral relationship between CO_2 and thermosensation.

5.3 Neural hypotheses for integrating vision, heat and CO_2

We have shown that mosquito attraction to dark visual contrast is a behavioral module separate from the integration of CO_2 and thermal cues in host-seeking. This separation bears implications for the neural circuits underlying these sensory computations. We predict that circuits carrying thermal and olfactory information converge to create the synergistic effects we see between CO_2 and host heat. Given the lack of synergy between vision and CO_2, visual circuits mediating the attraction to dark contrast likely converge later, if at all.

5.3.1 How do mosquito brains encode attractive dark features?

How are visual circuits wired? These questions are greatly aided by a rich tradition of fly vision research, where scientists working in advanced flies have untangled much of the circuitry underlying visual processing. Visual information is first received by photoreceptors in the fly retina. It is then relayed through several layers of neural tissue in the optic lobe, from the lamina, to the medulla, then to the lobula and the lobula plate. These layers make primary visual computations, such as motion and feature orientation. [Silies et al., 2014; Borst et al., 2010]

Information then passes from the lobula and lobula plate to optic glomeruli in the inferior lateral protocerebrum (Fig 5.2). The optic glomeruli are argued to be feature detectors, analogous to antennal lobe glomeruli in the olfactory system [Mu et al., 2012; Wu et al., 2017]. Optic glomeruli outputs innervate centers of multisensory integration in the superior lateral protocerebrum, such as the central complex [Seelig & Jayaraman, 2013] and anterior optic tubercle [Homberg et al., 2005], and descending interneurons, which connect to the thoracic ganglion and generate motor output [Strausfeld et al., 2007]. Visual projection neurons also make a few connections in the mushroom body, which may mediate visual learning and is another potential site of convergence between olfactory and visual cues [Vogt et al., 2016].

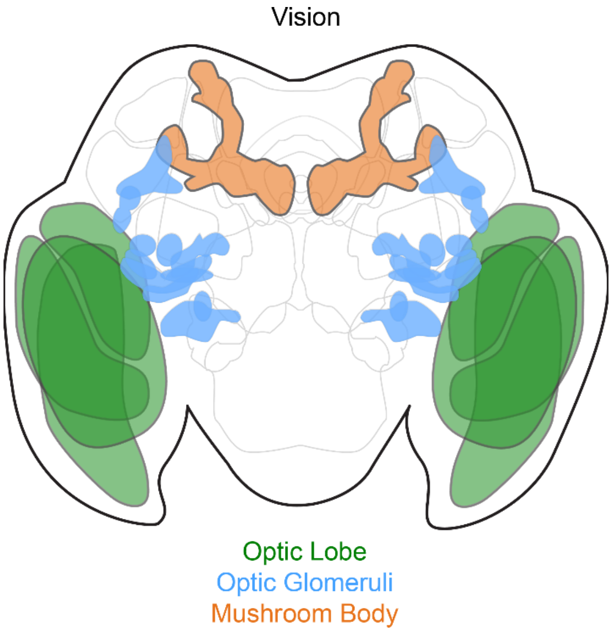

Figure 5.2 Putative first- and second-order visual circuits in the mosquito. Black outlines indicate confirmed anatomy. Shapes without outlines are regions predicted from *Drosophila melanogaster* anatomy. Adapted from Meg Younger, mosquitobrains.org.

Mosquito attraction to dark visual contrast could be due to detection of the presented dark features. Alternately, the attraction we observed could be a negative phototactic reflex. Because objects have edges but attractive darkness need not, we can behaviorally parse object detection from phototaxis by comparing tethered orientation towards an attractive dark tall stripe with orientation towards an edgeless dark gradient comprising of the same luminance as the stripe.

We can also define the attractive visual stimulus by examining the neural circuitry used to encode it. Phototaxis minimally requires comparing light intensities from two points and has been implemented by larval worms with only 8 photoreceptors and 71 neurons [Randel et al., 2014]. Visual object detector neurons have been found in the *Drosophila melanogaster* optic lobe and optic glomeruli [Kim et al., 2015; Wu et al., 2017; Ribeiro et al., 2018]. We can use pan-neuronally encoded calcium indicators to examine if cells in the mosquito optic glomeruli are activated when presented with dark visual features.

If mosquito responses to dark visual shapes are indeed mediated by object vision, then we can begin to make comparisons with known circuits in *Drosophila* object vision. One notable visual behavior difference between the two is that flying *Drosophila* strongly avoid dark small squares (Fig 2.7), thought to signify a predator, while flying *Ae. aegypti* are agnostic or attracted to them (Fig 2.13). This small spot avoidance in *Drosophila* is mediated by visual projection neurons which travel from the lobula to the optic glomeruli [Keles & Frye, 2017; Kim et al., 2015]. Are small squares encoded by equivalent neurons in mosquitoes? If so, then how do they lead to dramatically different responses? We can investigate the synaptic targets of these neurons using photoactivatable GFP to define where an aversive circuit diverges from an agnostic one.

5.3.2 How do mosquito brains integrate heat and olfactory information?

Unlike with visual circuits, heat and olfactory circuits are anatomically close from the periphery to the first stage of processing in the central brain. Peripheral detection of heat begins in the mosquito antennae, an olfactory organ where heat-sensitive sensilla have been characterized at the tip and predicted at the base [McIver, 1973; Davis & Sokolove; 1975; Gingl et al., 2005]. While the downstream targets of these sensilla have not been found in mosquitoes, in *Drosophila* thermal information from the antenna is passed to the proximal antennal protocerebrum (PAP) [Gallio et al., 2011]. Interestingly, some *Drosophila* heat-sensitive neurons which project into the PAP also contain inputs from the antennal lobe (AL) [Liu et al., 2015], the first stage of olfactory processing and directly dorsal to the PAP (Fig 5.3).

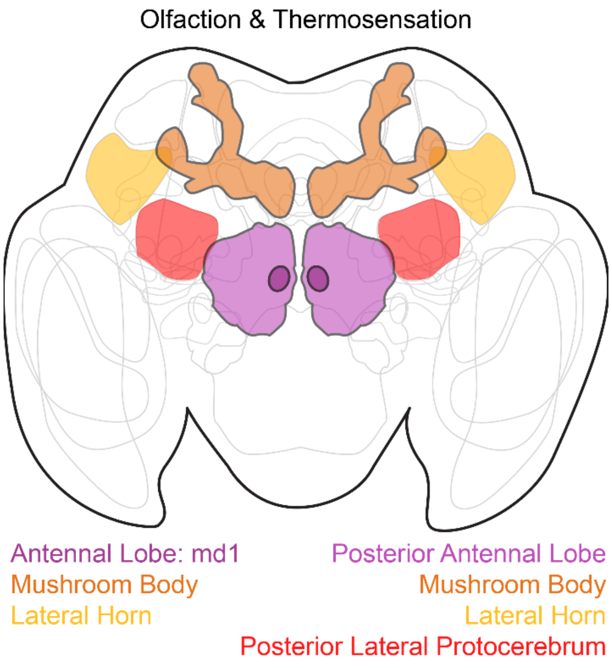

Figure 5.3 Putative first- and second-order olfactory and thermosensory circuits in the mosquito. Black outlines indicate confirmed anatomy. Shapes without outlines are regions predicted from *Drosophila melanogaster* anatomy. Adapted from Meg Younger, mosquitobrains.org.

In mosquitoes, CO_2 receptor genes are expressed in maxillary palp neurons, which projects to one of three medial dorsal glomeruli in the AL [Ignell et al., 2005]. CO_2 detection has been studied in *Drosophila melanogaster*, primarily in the context of innate avoidance behavior. *Drosophila melanogaster* avoid CO_2 at a range of concentrations because it was characterized as a component of a "*Drosophila* stress odorant" [Suh et al., 2004; Suh et al., 2007]. More recent studies have challenged this view, showing that CO_2 also signals *Drosophila* food sources of rotting fruit, and that CO_2 can be attractive in foraging contexts [Lewis et al., 2015; van Breugel et al., 2018]. *Drosophila* CO_2-responsive olfactory receptor neurons, located on the *Drosophila* antennae, project to a single glomerulus in the antennal lobe, which then sends projections to the lateral horn and the mushroom body to mediate both avoidance and attraction [Suh et al., 2004; Lewis et al., 2015; Varela et al., 2019].

We predict that in the mosquito, connections may exist between the AL and PAP that serve to activate mosquito attraction to host heat upon simultaneous exposure to CO_2. We can begin by elucidating the neural circuitry underlying heat detection in *Ae. aegypti*. By dye-filling heat-sensitive sensilla in the antennae, we can identify projection patterns of thermosensitive neurons, predicted to be in the PAP, and then trace the downstream circuits until they reach a potential site of convergence with the mosquito CO_2-detection circuit. We can then image those neurons upon exposure to heat alone, then exposure to heat and CO_2. We expect to see some synergistic boosting of heat response when CO_2 is present. By defining the circuit integrating heat and CO_2, we learn about the mechanism behind a crucial behavioral module in *Ae. aegypti* host-seeking.

5.4 Multimodal integration across mosquito species

Mosquitoes across their evolutionary family display an impressive variety of host choices, from mammals to cold-blooded frogs [Bartlett-Healy et al., 2008] to annelid worms [Reeves et al., 2018], and the algorithms they use to weigh sensory host cues likely vary just as much (Fig 5.4). Our results illustrate how such weighting is performed in one species, providing a first glimpse into how behavioral modules with different sensory inputs can be linked to produce host-seeking behavior in mosquitoes.

Figure 5.4 Examples of diverse host specializations between various mosquito species. (A) Domestic (top) and forest (bottom) interfertile subspecies of *Aedes aegypti*. The domestic form specializes on humans, while the forest form feeds generally on mammals. This divergence is driven in part by the different olfactory bouquet emitted by humans vs. other mammalian hosts. Photo: Lindy McBride. **(B)** *Culex territans*, a frog specialist. These mosquitoes do not exhibit thermotaxis, but they do phonotax towards frog calls. Photo: Ben Matthews. **(C)** *Uranonetaneia sapphirna*, recently found to feed on annelids. Adapted from Reeves et al., 2018.

Multimodal behavior has been proposed to drive speciation more efficiently than unimodal behavior because multiple signals increase variability that selective pressures can act upon [Partan, 2013; Candolin, 2003]. The flexible reweighting of different sensory modules in mosquito host-seeking can allow mosquitoes to rapidly adapt to new hosts and new ecological niches. This process can be seen in action in the specialization of *Ae. aegypti* to humans [McBride et al., 2014]. By learning more about the genetic modules of host-seeking, we can gain insight into the process of behavioral evolution.

5.5 A "mosquitologist" approach to multisensory biology

"I have often been asked why I did not study polarization vision across various groups of animals and instead focused on one group of animals and complemented our studies on the skylight compass with projects on other modes of navigation in the very same animal. My most telling reply was that to really understand what polarized skylight meant to Cataglyphis*, one had to consider the ant's compass as only one part of the animal's entire navigational toolkit…'Discover your own* Cataglyphis*…,' I used to say, '…and get captivated by her.'*

–Rüdiger Wehner, "Life as a cataglyphologist—and beyond" (2013)

Every organism displays many different behaviors with different computational demands, corresponding to different neural architectures. Especially for innate behaviors, brain structures which generate behavior are likely specialized to their input and under stereotyped genetic control, just like different sensory organs. Studying behavior within an organismal context focuses our attention to the calculations animals have to make, their inputs, outputs, and neural transformations. Detailed behavioral assays can parse those calculations into functional modules, and our increasing ability to perturb genes and neurons can confer mechanistic understanding. With the rapid development of genetic and neuroscience tools in mosquitoes [Kokoza & Raikhel, 2011; Riabinina et al., 2018; Matthews et al., 2018], we are poised to uncover the neuronal mechanisms underlying multimodal integration in these charismatic and deadly insects.

Materials and Methods

Fly Rearing and Maintenance

Drosophila melanogaster wild-type laboratory strains (isoD) were maintained and reared with 25°C, with a photoperiod of 12 hr light:12 hr dark on standard corn-meal agar. Flies were sexed and sorted under cold anesthesia (4°C).

Mosquito Rearing and Maintenance

Aedes aegypti wild-type laboratory strains (Orlando) and mutant strains were maintained and reared at 25-28°C, 70%–80% relative humidity with a photoperiod of 14 hr light:10 hr dark (lights on at 7 a.m.) as previously described [DeGennaro et al., 2013]. Briefly, eggs were hatched in deoxygenated, deionized water with powdered Tetramin fish food and larvae were fed Tetramin tablets (Tetra) until pupation. Adult mosquitoes were housed with siblings in BugDorm-1 (Bugdorm) cages and provided constant access to 10% sucrose. Adult females were blood-fed on mice for stock maintenance and blood-fed on human subjects for generation of the $Gr3^{ECFP/ECFP}$ and $Gr3^{ECFP/+}$ mosquitoes used in experiments. Blood-feeding procedures with live mice and humans were approved and monitored by The Rockefeller University Institutional Animal Care and Use Committee and Institutional Review Board, protocols 15772 and LVO-0652, respectively. Human subjects gave their written informed consent to participate.

Gr3 Mutant Strain

Gr3$^{ECFP/ECFP}$ mutants used in this study carry a broadly expressed ECFP marker inserted into the *Gr3* locus as described [McMeniman et al., 2014]. *Gr3*$^{ECFP/+}$ heterozygotes were the offspring of *Gr3*$^{ECFP/ECFP}$ males and wild-type (Orlando) females.

Fly Magnetic Tethering

Flies were magnetically tethered as described [Bender & Dickinson, 2006]. Female flies were collected 1-4 days after eclosion, anesthetized on a Peltier stage at ~4°C for 15-30 min, and attached by the dorsal part of their prothorax to a steel pin using blue-light activated glue (Bondic, Canada). For 1-4 hr after tethering, flies recovered in a dark, humid chamber while holding small squares of tissue paper. Flies were then suspended in a vertically-aligned magnetic field in the center of a cylindrical LED display (570 nm, IORodeo) covering 360 in azimuth and 94 in elevation with each pixel subtending ~3.75°.

LEDs were controlled using PControl in MATLAB [Reiser & Dickinson, 2008]. In each experimental bout, flies were exposed to up to six types of visual stimuli composed of LEDs either off ("dark") or maximally on (luminance 70. cd m^{-2}, "bright"), based on previous work [Maimon et al., 2008]: black horizontally centered rectangles 94° tall x 15° wide ("long stripe"), 46x15° ("medium stripe"), and 15x15° ("square"); a uniform bright field ("blank"); a square wave grating composed of 24 alternating bright and dark 15° stripes; and a randomly composed pattern of shuffled dark and bright pixels ("contour"), not analyzed here. The long stripe, medium stripe, square, blank, and contour were randomly presented in 15 s trials, with every 10-16 trials interspersed by a moving 15 s square wave grating stimulus. Each trial presented the shape at a random position on the arena, moving in a sinusoid of peak-to-peak amplitude 60° and frequency randomly chosen from 0, 0.1, 0.2, 0.5, 1.0, 2.0, 4.0, 6.0, or 8.0 Hz. Flies that failed to follow the direction of wide-field motion or failed to sustain flight were discarded.

Flies were lit from below with IR LEDs (850 nm, DigiKey) and video was captured with an infrared-sensitive camera (AVT-GE680) triggered externally, recording frames (320x240 pixels) at 200 Hz. Fly body orientation was extracted from camera images in real time using FView and FlyTrax [Straw & Dickinson, 2009]. These orientation voltages, alongside the camera frame triggers and information about visual stimuli presented, were digitized at 1 kHz using a Digidata 1440a (Molecular Devices).

Data were processed using custom Python software that extracted the offset of each trial by subtracting the center of stimulus position from fly orientation. “Fixation” was calculated by measuring the percentage of time within 3-15 s of stimulus onset spent with an offset between -45° and 45°, while “antifixation” was calculated by measuring the percentage of time within 3-15 s of stimulus onset spent with an offset greater than -135° or 135°. Scores of all trials of each shape were averaged to obtain one score per shape per fly. Because not all flies experienced all four analyzed shapes, we treated fixation scores of the shapes as independent groups for statistical purposes. Heat maps of offsets from trials, separated by shape, show orientation towards the long stripe and away from the spot. Each sector represents 15° x 1 s and are normalized by column.

Mosquito Magnetic Tethering

Female mosquitoes were collected 4-15 days after eclosion and fasted in the presence of a water source comprising a 60 mL glass bottle (Fisherbrand™ Clear Boston Round Bottles Without Cap Fisher Sci Cat# 02-911-944) filled with deionized water and plugged with a water-soaked cotton wick (Richmond Dental Braided Rolls ½" x 6", Catalogue # 201205) for 18-25 hr. Mosquitoes were anesthetized on ice (4^{o}C) for 5-35 min and were attached by the dorsal part of their prothorax to a steel pin using blue-light activated glue (Bondic, Canada). For 1-4 hr after tethering, mosquitoes recovered in a dark, humid chamber while their legs lightly contacted mesh.

Mosquitoes were then suspended in a vertically-aligned magnetic field in the center of a cylindrical LED display (525 nm, IORodeo) covering 360 in azimuth and 94 in elevation with each pixel subtending ~3.75°. LEDs were controlled using PControl in MATLAB [10]. We generated a textured background consisting of pixels randomly assigned to luminances of 10. or 40. cd m^{-2}, and we used the same background in the same position for all trials. The long stripe, medium stripe, spot, and blank as used in the fly trials were pseudorandomly presented in 10-15 s trials, with every 8 trials interspersed by 10-15 s of moving the background alone. The long stripe, medium stripe, spot, and blank were superimposed on the background at a random position, moving in a sinusoid of peak-to-peak amplitude 60° and frequency randomly chosen from 0, 0.1, 0.5, and 1 Hz. Mosquitoes that failed to follow the direction of wide-field motion or failed to sustain flight were discarded.

To obtain body orientation, mosquitoes were lit from below with IR LEDs (850 nm, DigiKey) were captured with an infrared-sensitive camera (Point Grey FL3-GE-03S1M-C) triggered externally, recording frames (648 x 488 pixels) at 100 Hz. Mosquito body orientation was extracted from camera images in real time using FView and FlyTrax [Straw & Dickinson, 2009]. Camera frame triggers and information regarding the visual stimuli presented were digitized at 1 kHz using a DAQ (Measurement Computing USB-204) and DAQFlex software (Measurement Computing).

Throughout all magnotether experiments, breathing air (~0.04% CO_2, Praxair AI BR-KN) was pumped into the box via a diffusion pad (59-144, Flystuff.com) installed on the ceiling of the enclosure, 20.5 cm directly above the position of the tethered mosquito. In trials labeled "CO_2," the air stream was switched to 10% CO_2 (Praxair AI CD10C-K) via a solenoid valve (Parker-Hannifin) for 10 s. To maintain the same CO_2 concentration throughout the experiment, 1 s of 10% CO_2 was puffed in for every 200 s of air. This regime increased the concentration of CO_2 in the mosquito tethering position 1,250 ppm above baseline and maintained it there for up to 15 min, as measured with a Carbocap Hand-Held CO_2 Meter (model GM70, Vaisala Inc.). Data recording began approximately 1-2 minutes after the initial 10 s pulse of CO_2. After each CO_2 trial, the enclosure was opened for at least 5 minutes, which as measured was sufficient to bring down CO_2 to baseline levels. Because different mosquitoes experienced the air and CO_2 conditions, we treated fixation scores as independent groups for statistical purposes.

Data were processed using custom Python software that synchronized orientation data and DAQ data using computer timestamps, then processed the same way as fly magnetic tether data. Because all mosquitoes experienced all four analyzed shapes, we treated fixation scores of the shapes as dependent groups for statistical purposes. In heat maps of offset, each sector represents 15° x 1 s and are normalized by column. Summary fixation data are shown as median with each data point representing an individual mosquito.

Glytube Blood-Meal Feeding

Females were fed sheep blood or saline in groups of 20–50 using Glytube membrane feeders as described [Duvall et al., 2019]. The protein-free saline meal contained 110 mM NaCl, 20 mM $NaHCO_3$, and 1 mM ATP. Glytubes were placed on top of mesh on the mosquito cage, and females were allowed to feed through the mesh for 15 min. Fed females were scored by eye for complete engorgement. Partially-fed females were treated as non-fed and discarded. Blood-fed and saline-fed females were returned to standard rearing conditions. For the “48 hr post-meal” condition, mosquitoes were fasted in the presence of a water source 20-26 hr before testing and then tested 44-52 hr after Glytube feeding. For the “96 hr post-meal” condition, mosquitoes were fasted without a water source 23-49 hr before testing and tested 94-103 hr after Glytube feeding. Water was not provided because this would stimulate females to lay eggs, and the experimental design required females to be gravid at the time of testing.

Heat-Seeking Assay

Heat-seeking experiments were performed as previously described [Corfas & Vosshall, 2015]. Briefly, the assay apparatus is a 30 x 30 x 30 cm Plexiglass box with a 6 x 9 cm Peltier element (Tellurex) on one vertical wall. To affix a visual stimulus to the Peltier, a 2 cm black dot representing 5.42% of the Peltier area was printed onto a piece of standard white letter size printer paper (extra bright, Navigator; Office Depot/Office

Max), which was cut to 15 x 17 cm and held taut over the Peltier by a magnetic frame such that the center of the dot was 13.97 cm above the ground. Because mosquitoes in free flight can change their perceived angular size of the dot by changing their position, it is difficult to make exact comparisons to the static angular sizes of the stimuli presented in the magnotether. The minimum size of the dot (a mosquito as far away from the dot as possible in the assay) was 2.78°. For a mosquito to experience the dot as the same angular height as the magnotether square (15°), the dot would be 7.60 cm directly ahead of her; for the medium stripe (46°), 2.36 cm; for the long stripe (94°), 0.93 cm.

For blank control trials, the paper was turned over to show the unprinted side. This was done to control for the effect of the Xerox Phaser solid printer ink used to generate the dot, which we speculated might affect heat transfer at that position on the paper. Although the dot was faintly visible to the human eye, mosquitoes showed little or no preference for that position on the paper, and there were no detectable differences in the thermal image of the Peltier when the dot was in place. All stimulus periods lasted 3 min, followed by 9 min of ambient temperature. CO_2 pulses (20 s) accompanied all stimulus period onsets. A second identical control Peltier element was situated on the wall opposite to the stimulus Peltier and was set to ambient temperature during all experiments. Air temperature was measured using a controller and thermocouple identical to that used to measure internal Peltier temperature (Oven Industries 5R7-571, Oven Industries TR-91). The thermocouple was placed at the center of the Peltier and 2 mm from the Peltier surface, approximating the distance of a mosquito’s center of mass from the surface when landed.

Female mosquitoes were separated 8-12 days after eclosion from mixed-sex cages and sorted at 4°C into groups of 45-50. They were kept in custom canisters and sugar-starved in the presence of a water source 13-24 hr before testing. Experiments with mutants were double-blinded to genotype. For each trial, one group was introduced into the enclosure, and only mosquitoes directly on the Peltier area were scored. Due to low contrast between the dark mosquitoes and the black dot, each frame for each heat-seeking experiment was manually inspected to ascertain the number of mosquitoes on the dot.

Summary data are shown as median with individual data points, and timeseries data are shown as median with range of median absolute deviation with normalization constant 1.4826, a robust estimator of dispersion. For the normalized timeseries data shown in Figure 3C, for each heat bout within each trial we computed the mean occupancy on the Peltier during the minute before heat onset and divided the rest of the timeseries by that mean, such that the data are represented as percentages of initial occupancy before heat. Heat maps are smoothed 2D histograms of mean mosquito occupancy during seconds 90–180 of stimulus periods, sampled at 1 Hz and binned into 12 × 16 image sectors.

We quantified positions of landings and takeoffs by superimposing two consecutive frames and manually looking for differences. A still mosquito would appear as a completely overlapped image, whereas a walking mosquito would appear as two adjacent images, defined here as two mosquito images that either shared the same orientation and were less than one mosquito body length apart or had orientations with a difference of less than 90° and shared a center of rotation. A mosquito that was present in the first frame but not in an adjacent image in the second frame was counted as a “takeoff”. Conversely, a mosquito present in the second frame but not the first was counting as a “landing.” Because we sampled at 1 Hz, it is possible that a seemingly walking or still mosquito represents a mosquito that took off in the first frame and then another mosquito that landed within 1 s in the same or an adjacent location. But we expect that such an event would be exceedingly rare. Thus, this manual quantification represents a conservative estimate of landings and takeoffs. Frames were scored blind to genotype.

Because we did not track individual mosquito identity, we could not track duration of individual dwelling events. However, given the times of landing and takeoff events, we reasoned that we could deduce a mean population dwell time as follows. Let A = landing time, B = takeoff time. B – A thus represents dwell time.

$$Mean(B-A) = \frac{\sum_{n=1}^{k}(B_n - A_n)}{k}$$

$$Mean(B-A) = \frac{\sum_{n=1}^{k}(\mathrm{B_n}) - \sum_{n=1}^{k}(\mathrm{A_n})}{k}$$

To make this calculation, we assigned all mosquitoes present at the start of the heat epoch a landing time of 0 s and all mosquitoes present at the end of the heat epoch a takeoff time of 180 s.

3D Trajectory Analysis

Mosquito flight trajectories were collected and processed as previously described [McMeniman et al., 2014]. The assay enclosure was a custom laser-cut acrylic (McMaster Carr) box measuring approximately 65 x 45 x 30 cm, featuring two 4 x 6

Peltier (Tellurex, Adafruit) devices on the vertical back wall linked to two independent controllers (Oven Industries). Throughout experiments, breathing air (~0.04% CO_2, Praxair AI BR-KN) was pumped into the box via a diffusion pad (59-144, Flystuff.com) installed on the ceiling of the enclosure. At the onset of heat bouts, the air stream was switched to 10% CO_2 (Praxair AI CD10C-K) via a solenoid valve (Parker-Hannifin) for 13 s to increase CO_2 by ~1,250 ppm. Humidity was maintained constantly at 40% RH using a UV humidifier controlled by custom Arduino software.

Female mosquitoes were separated 8-12 days after eclosion from mixed-sex cages and sorted at 4°C into groups of 45-50. They were kept in custom canisters and sugar-starved in the presence of a water source 13-24 hr before testing. Trajectories were manually linked to create continuous individual traces. They were then automatically scored into flying (>4 cm away from any surface of the box, or moving at a velocity >10 cm/s) or walking, and walking was further separated into walking and walking on heat based on if the mosquito was positioned on the Peltier surface.

Quantification and Statistical Analysis

All statistical analysis was performed using the Python package scipy.stats. Kruskal-Wallis test with post hoc Mann-Whitney test was used to compare more than 2 independent groups, and Friedman’s test for repeated measures with post hoc Wilcoxon matched-pairs signed-rank test was used to compare more than 2 dependent groups. Mann-Whitney U test was used to compare 2 independent groups. Post hoc tests included Bonferroni correction when multiple comparisons were made. Details of statistical methods are reported in the figure legends.

Data and Software Availability

Data file containing all raw magnotether data, all processed data, and all code used to process data are available at https://github.com/VosshallLab/LiuVosshall2019

Due to file size limitations of online data repositories, raw image files from the heat-seeking assay are available upon request.

References

Agrawal, S., Safarik, S., & Dickinson, M. (2014). The relative roles of vision and chemosensation in mate recognition of *Drosophila melanogaster*. *The Journal of Experimental Biology*, 217(15), 2796–2805. https://doi.org/10.1242/jeb.105817

Allan, S., Day, J. F., & Edman, J. D. (1987). Visual ecology of biting flies*. Annual Review of Entomology*, 32, 297–316. https://doi.org/10.1146/annurev.en.32.010187.001501

Bargmann, C. I. (2012). Beyond the connectome: how neuromodulators shape neural circuits. *BioEssays*, 34(6), 458–465. https://doi.org/10.1002/bies.201100185

Bartlett-Healy, K., Crans, W., & Gaugler, R. (2008). Phonotaxis to amphibian vocalizations in *Culex territans* (Diptera: Culicidae). *Annals of the Entomological Society,* 101(1), 95–103.

Benda, J., Gollisch, T., Machens, C. K., & Herz, A. V. M. (2007). From response to stimulus: adaptive sampling in sensory physiology. *Current Opinion in Neurobiology*, 17(4), 430-436. https://doi.org/10.1016/j.conb.2007.07.009

Bender, J., & Dickinson, M. H. (2006). Visual stimulation of saccades in magnetically tethered *Drosophila*. *The Journal of Experimental Biology*, 209, 3170–3182. https://doi.org/10.1242/jeb.02369

Bernáth, B., Horváth, G., & Meyer-Rochow, V. B. (2012). Polarotaxis in egg-laying yellow fever mosquitoes *Aedes (Stegomyia) aegypti* is masked due to infochemicals. *Journal of Insect Physiology*, 58(7), 1000–1006. https://doi.org/10.1016/j.jinsphys.2012.05.004

Bezares-Calderón, L. A., Verasztó, C., Jékely, G., Shahidi, R., Conzelmann, M., Williams, E. A., … Randel, N. (2014). Neuronal connectome of a sensory-motor circuit for visual navigation. *eLife*, 3, 1–22. https://doi.org/10.7554/elife.02730

Bhatt, S., Gething, P. W., Brady, O. J., Messina, J. P., Farlow, A. W., Moyes, C. L., … Hay, S. I. (2013). The global distribution and burden of dengue. *Nature*, 496(7446), 504–507. https://doi.org/10.1038/nature12060

Blanford, S., Read, A. F., & Thomas, M. B. (2009). Thermal behaviour of *Anopheles stephensi* in response to infection with malaria and fungal entomopathogens. *Malaria Journal*, 8(1), 6–9. https://doi.org/10.1186/1475-2875-8-72

Borst, A., Haag, J., & Reiff, D. (2010). Fly motion vision. *Annual Review of Neuroscience,* 33, 49-70. https://doi.org/10.1146/annurev-neuro-060909-153155

Bowen, M. F. (1991). The sensory physiology of host-seeking behavior in mosquitoes. *Annual Review of Entomology*, 36, 139–158. https://doi.org/10.1146/annurev.en.36.010191.001035

Brown, A. W. A., & Sippell, W. (1953). Studies of the Responses of the female *Aëdes mosquito.* Part V. The Role of Visual Factors. *Bulletin of Entomological Research*, 43(04), 567–574. https://doi.org/10.1017/S0007485300028984

Burgess, L. (1959). Probing behaviour of *ædes ægypti* (L.) in response to heat and moisture. *Nature*, 184(4703), 1968–1969. https://doi.org/10.1038/1841968a0

Bussell, J. J., Yapici, N., Zhang, S. X., Dickson, B. J., & Vosshall, L. B. (2014). Abdominal-B Neurons Control Drosophila Virgin Female Receptivity. *Current Biology*, 24(14), 1584–1595. https://doi.org/10.1016/j.cub.2014.06.011

Candolin, U. (2003). The use of multiple cues in mate choice. *Biological Reviews*, 78(4), 575-595. https://doi.org/10.1017/S1464793103006158

Cardé, R. T., & Willis, M. a. (2008). Navigational strategies used by insects to find distant, wind-borne sources of odor. *Journal of Chemical Ecology*, 34(7), 854–866. https://doi.org/10.1007/s10886-008-9484-5

Choumet, V., Attout, T., Chartier, L., Khun, H., Sautereau, J., Robbe-Vincent, A., … Bain, O. (2012). Visualizing Non Infectious and Infectious *Anopheles gambiae* Blood Feedings in Naive and Saliva-Immunized Mice. *PLoS ONE*, 7(12), e50464. https://doi.org/10.1371/journal.pone.0050464

Clemens, J., Coen, P., Roemschied, F. A., Pereira, T., Mazumder, D., Pacheco, D., & Murthy, M. (2018). Discovery of a new song mode in *Drosophila* reveals hidden structure in the sensory and neural drivers of behavior. *Current Biology,* 28(15), 2400-2412. https://doi.org/10.1016/j.cub.2018.06.011

Clemens, J., Deutsch, D., Thiberge, S. Y., & Murthy, M. (2018). Shared song object detector neurons in *Drosophila* male and female brains drive divergent, sex-specific behaviors. *bioRxiv*, https://doi.org/10.1101/366765

Clements, A. N. (1999). Visual Cues. In *The Biology of Mosquitoes* (pp. 455–456). London: CABI Publishing.

Clowney, E. J., Iguchi, S., Bussell, J. J., Scheer, E., & Ruta, V. (2015). Multimodal Chemosensory Circuits Controlling Male Courtship in *Drosophila*. *Neuron*, 87(5), 1036-1049. https://doi.org/10.1016/j.neuron.2015.07.025

Coen, P., Xie, M., Clemens, J., & Murthy, M. (2016). Sensorimotor Transformations Underlying Variability in Song Intensity during *Drosophila* Courtship. *Neuron*, 89(3), 629–644. https://doi.org/10.1016/j.neuron.2015.12.035

Corfas, R. A. (2016). *The Genetics of Mosquito Heat-Seeking Behavior* (Doctoral dissertation).

Corfas, R. A., & Vosshall, L. B. (2015). The cation channel TRPA1 tunes mosquito thermotaxis to host temperatures. *eLife*, 4, e11750. https://doi.org/10.7554/eLife.11750.001

Cowling, D. E., & Burnet, B. (1981). Courtship songs and genetic control of their acoustic characteristics in sibling species of the *Drosophila melanogaster* subgroup. *Animal Behaviour*, 29(3), 924–935. https://doi.org/10.1016/S0003-3472(81)80030-9

Datta, S. R., Vasconcelos, M. L., Ruta, V., Luo, S., Wong, A., Demir, E., … Axel, R. (2008). The *Drosophila* pheromone cVA activates a sexually dimorphic neural circuit. *Nature*, 452(7186), 473–477. https://doi.org/10.1038/nature06808

Davis, E. E., & Sokolove, P. G. (1975). Temperature responses of antennal receptors of the mosquito,*Aedes aegypti*. *Journal of Comparative Physiol*ogy, 96(3), 223–236. https://doi.org/10.1007/BF00612696

Daykin, P., Kellogg, F., & Wright, R. (1965). Host-Finding and Repulsion of *Aedes Aegypti. The Canadian Entomologist*, 97(3), 239-263. https://doi.org/10.4039/Ent97239-3

DeGennaro, M., McBride, C. S., Seeholzer, L., Nakagawa, T., Dennis, E. J., Goldman, C., … Vosshall, L. B. (2013). *orco* mutant mosquitoes lose strong preference for humans and are not repelled by volatile DEET. *Nature*, 498(7455), 487–491. https://doi.org/10.1038/nature12206

Dekker, T., Geier, M., & Carde, R. T. (2005). Carbon dioxide instantly sensitizes female yellow fever mosquitoes to human skin odours. *Journal of Experimental Biology*, 208(15), 2963–2972. https://doi.org/10.1242/jeb.01736

Dekker, T., & Carde, R. T. (2011). Moment-to-moment flight manoeuvres of the female yellow fever mosquito (*Aedes aegypti* L.) in response to plumes of carbon dioxide and human skin odour. *Journal of Experimental Biology*, 214(20), 3480–3494. https://doi.org/10.1242/jeb.055186

Dickinson, M. H. (2014). Death Valley, *Drosophila*, and the Devonian toolkit. *Annual Review of Entomology*, 59, 51–72. https://doi.org/10.1146/annurev-ento-011613-162041

Dimattina, C., & Zhang, K. (2013). Adaptive stimulus optimization for sensory systems neuroscience. *Front. Neural Circuits,* 7(101), 1–16. https://doi.org/10.3389/fncir.2013.00101

Ding, Y., Lillvis, J. L., Cande, J., Berman, G. J., Arthur, B. J., Xu, M., … Stern, D. L. (2017). Neural Changes Underlying Rapid Fly Song Evolution. *bioRxiv*. https://doi.org/10.1101/238147

Duvall, L. B., Ramos-Espiritu, L., Barsoum, K. E., Glickman, J. F., & Vosshall, L. B. (2019). Small-Molecule Agonists of *Ae. aegypti* Neuropeptide Y Receptor Block Mosquito Biting. *Cell*, 176(4), 687–701. https://doi.org/10.1016/j.cell.2018.12.004

Eisen, L., Monaghan, A. J., Lozano-Fuentes, S., Steinhoff, D. F., Hayden, M. H., & Bieringer, P. E. (2014). The Impact of Temperature on the Bionomics of *Aedes (Stegomyia) aegypti* , With Special Reference to the Cool Geographic Range Margins. *Journal of Medical Entomology*, 51(3), 496–516. https://doi.org/10.1603/ME13214

el Jundi, B., Baird, E., Byrne, M. J., & Dacke, M. (2019). The brain behind straight-line orientation in dung beetles. *The Journal of Experimental Biology*, 222(Suppl 1), jeb192450. https://doi.org/10.1242/jeb.192450

Fenk, L. M., Poehlmann, A., & Straw, A. D. (2014). Asymmetric Processing of Visual Motion for Simultaneous Object and Background Responses. *Current Biology*, 24(24), 2913-2919. https://doi.org/10.1016/j.cub.2014.10.042

Fetsch, C. R., DeAngelis, G. C., & Angelaki, D. E. (2013). Bridging the gap between theories of sensory cue integration and the physiology of multisensory neurons. *Nature Reviews Neuroscience*, 14(6), 429–442. https://doi.org/10.1038/nrn3503

Frei, J., Guerin, P. M., Kessler, S., Bourquin, M., & Kröber, T. (2010). An In Vitro Assay for Testing Mosquito Repellents Employing a Warm Body and Carbon Dioxide as a Behavioral Activator. *Journal of the American Mosquito Control Association*, 26(4), 381–386. https://doi.org/10.2987/10-6044.1

Gallio, M., Ofstad, T. A., Macpherson, L. J., Wang, J. W., & Zuker, C. S. (2011). The coding of temperature in the *Drosophila* brain. *Cell*, 144(4), 614–624. https://doi.org/10.1016/j.cell.2011.01.028

Galun, R. (1963). Feeding Response in *Aedes aegypti* : Stimulation by Adenosine Ribosomes and Ribonucleic Acids in Three Morphological States of Neurospora. *Science*, 142(3600), 1674–1675.

Gillies, M. T. (1980). The role of carbon dioxide in host-finding by mosquitoes (Diptera: Culicidae): a review. *Bulletin of Entomological Research*, 70(4), 525–532. https://doi.org/10.1017/S0007485300007811

Gingl, E., Hinterwirth, A., & Tichy, H. (2005). Sensory Representation of Temperature in Mosquito Warm and Cold Cells. *Journal of Neurophysiology*, 94(1), 176–185. https://doi.org/10.1152/jn.01164.2004

Götz, K. (1987). Course-control, metabolism and wing interference during ultralong tethered flight in *Drosophila melanogaster. Journal of Experimental Biology*, 128(1), 35–46. http://jeb.biologists.org/content/128/1/35.short

Greenwood, A. K., Wark, A. R., Yoshida, K., & Peichel, C. L. (2013). Genetic and neural modularity underlie the evolution of schooling behavior in threespine sticklebacks. *Current Biology*, 23(19), 1884–1888. https://doi.org/10.1016/j.cub.2013.07.058

Harris, G., Wu, T., Linfield, G., Choi, M., Liu, H., & Zhang, Y. (2019). Molecular and cellular modulators for multisensory integration in *C. elegans. PLoS Genetics*, 15(3), e1007706. https://doi.org/10.1371/journal.pgen.1007706

Hecht, S., & Wald, G. (1934). The visual acuity and intensity discrimination of *Drosophila. The Journal of General Physiology*, 17(4), 517–547. https://doi.org/10.1085/jgp.17.4.517

Hirsch, J., & Curcio, C. A. (1989). The spatial resolution capacity of human foveal retina. *Vision Research*, 29(9), 1095–1101. https://doi.org/10.1016/0042-6989(89)90058-8

Holmes, S. (1911). The reactions of mosquitoes to light in different periods of their life history. *Journal of Animal Behavior*, 1(1), 29–32. Retrieved from http://psycnet.apa.org/journals/jab/1/1/29/

Homberg, U., Hofer, S., Pfeiffer, K., & Gebhardt, S. (2003). Organization and neural connections of the anterior optic tubercle in the brain of the locust*, Schistocerca gregaria. Journal of Comparative Neurology*, 462(4), 415–430. https://doi.org/10.1002/cne.10771

Horváth, G., Móra, A., Bernáth, B., & Kriska, G. (2011). Polarotaxis in non-biting midges: Female chironomids are attracted to horizontally polarized light. *Physiology and Behavior*, 104(5), 1010–1015. https://doi.org/10.1016/j.physbeh.2011.06.022

Hu, C. K., & Hoekstra, H. E. (2017). Peromyscus burrowing: A model system for behavioral evolution. In *Seminars in cell & developmental biology*, 61, 107–114. https://doi.org/10.1016/j.semcdb.2016.08.001

Hu, X., England, J. H., Lani, A. C., Tung, J. J., Ward, N. J., Adams, S. M., … O'Tousa, J. E. (2009). Patterned rhodopsin expression in R7 photoreceptors of mosquito retina: Implications for species-specific behavior. *Journal of Comparative Neurology*, 516(4), 334–342. https://doi.org/10.1002/cne.22114

Hu, X., Leming, M. T., Whaley, M. a, & O'Tousa, J. E. (2013). Rhodopsin coexpression in UV photoreceptors of *Aedes aegypti* and *Anopheles gambiae* mosquitoes. *The Journal of Experimental Biology,* 217(6), 1003–1008. https://doi.org/10.1242/jeb.096347

Ignell, R., Dekker, T., Ghaninia, M., & Hansson, B. S. (2005). Neuronal architecture of the mosquito deutocerebrum. *The Journal of Comparative Neurology*, 493(2), 207–240. https://doi.org/10.1002/cne.20800

Jiang, W., Wallace, M. T., Jiang, H., Vaughan, J. W., & Stein, B. E. (2017). Two Cortical Areas Mediate Multisensory Integration in Superior Colliculus Neurons. *Journal of Neurophysiology*, 85(2), 506–522. https://doi.org/10.1152/jn.2001.85.2.506

Johansson, G. (1973). Visual perception of biological motion and a model for its analysis. *Perception & Psychophysics*. https://doi.org/10.3758/BF03212378

Jones, J. L. (2006). Robots at the tipping point: the road to iRobot Roomba. *IEEE Robotics & Automation Magazine*, 13(1), 76–78. https://doi.org/10.1109/mra.2006.1598056

Keleş, M. F., & Frye, M. A. (2017). Object-Detecting Neurons in *Drosophila. Current Biology*, 27(5), 680-687. https://doi.org/10.1016/j.cub.2017.01.012

Kennedy, J. S. (1940). The visual responses of flying mosquitoes. *Proceedings of the Zoological Society of London*, 109, 221–242. https://doi.org/10.1111/j.1096-3642.1940.tb00831.x

Kim, A. J., Fitzgerald, J. K., & Maimon, G. (2015). Cellular evidence for efference copy in *Drosophila* visuomotor processing. *Nature Neuroscience*, 15(August). https://doi.org/10.1038/nn.4083

Klowden, M. (1995). Blood, sex, and the mosquito. *Bioscience*, 45(5), 326–331. Retrieved from http://www.jstor.org/stable/10.2307/1312493

Kohatsu, S., & Yamamoto, D. (2015). Visually induced initiation of *Drosophila* innate courtship-like following pursuit is mediated by central excitatory state. *Nature Communications*, 6, 6457. https://doi.org/10.1038/ncomms7457

Kokoza, V. a, & Raikhel, A. S. (2011). Targeted gene expression in the transgenic *Aedes aegypti* using the binary Gal4-UAS system. *Insect Biochemistry and Molecular Biology*, 41(8), 637–644. https://doi.org/10.1016/j.ibmb.2011.04.004

Kowalko, J. E., Rohner, N., Rompani, S. B., Peterson, B. K., Linden, T. A., Yoshizawa, M., … Tabin, C. J. (2013). Loss of schooling behavior in cavefish through sight-dependent and sight-independent mechanisms. *Current Biology*, 23(19), 1874–1883. https://doi.org/10.1016/j.cub.2013.07.056

Kriska, G., Malik, P., Szivák, I., & Horváth, G. (2008). Glass buildings on river banks as “polarized light traps” for mass-swarming polarotactic caddis flies. *Naturwissenschaften*, 95(5), 461–467. https://doi.org/10.1007/s00114-008-0345-4

Kuehn, B. M. (2014). Chikungunya Virus Transmission Found in the United States. *JAMA,* 312(8), 2–3.

Labhart, T., & Meyer, E. P. (1999). Detectors for polarized skylight in insects: a survey of ommatidial specializations in the dorsal rim area of the compound eye. *Microscopy Research and Technique*, 47(6), 368–379. https://doi.org/10.1002/(SICI)1097-0029(19991215)47:6

Lee, R. M. K. W., & Craig, D. A. (2010). Cibarial sensilla and armature in mosquito adults (Diptera: Culicidae). *Canadian Journal of Zoology*, 61(3), 633–646. https://doi.org/10.1139/z83-085

Lewis, L. P. C., Siju, K. P., Aso, Y., Friedrich, A. B., Bulteel, A. J. B., Rubin, G. M., & Grunwald Kadow, I. C. (2015). A Higher Brain Circuit for Immediate Integration of Conflicting Sensory Information in *Drosophila. Current Biology*, 25(17), 2203–2214. https://doi.org/10.1016/j.cub.2015.07.015

Liesch, J., Bellani, L. L., & Vosshall, L. B. (2013). Functional and Genetic Characterization of Neuropeptide Y-Like Receptors in *Aedes aegypti. PLoS Neglected Tropical Diseases*, 7(10), e2486. https://doi.org/10.1371/journal.pntd.0002486

Liu, W. W., Mazor, O., & Wilson, R. I. (2015). Thermosensory processing in the *Drosophila* brain. *Nature*, 519(7543), 353–357. https://doi.org/10.1038/nature14170

Lorenz, K. Z. (1981). *The Foundations of Ethology*. Vienna: Springer Vienna.

Maimon, G. (2011). Modulation of visual physiology by behavioral state in monkeys, mice, and flies*. Current Opinion in Neurobiology*, 21(4), 559–564. https://doi.org/10.1016/j.conb.2011.05.001

Maimon, G., Straw, A. D., & Dickinson, M. H. (2008). A simple vision-based algorithm for decision making in flying *Drosophila. Current Biology*, 18(6), 464–470. https://doi.org/10.1016/j.cub.2008.02.054

Manning, A., & Bastock, M. (1955). The Courtship of *Drosophila Melanogaster. Behaviour,* 8(2), 85–110. https://doi.org/10.1163/156853955X00184

Matthews, B. J., Dudchenko, O., Kingan, S. B., Koren, S., Antoshechkin, I., Crawford, J. E., … Vosshall, L. B. (2018). Improved reference genome of *Aedes aegypti* informs arbovirus vector control. *Nature*, 563(7732), 501–507. https://doi.org/10.1038/s41586-018-0692-z

Matthews, B. J., McBride, C. S., DeGennaro, M., Despo, O., & Vosshall, L. B. (2016). The neurotranscriptome of the *Aedes aegypti* mosquito. *BMC Genomics*, 17(1), 32. https://doi.org/10.1186/s12864-015-2239-0

Mayer, M. S., & James, J. D. (1969). Attraction of *Aedes aegypti* (L.): responses to human arms, carbon dioxide, and air currents in a new type of olfactometer. *Bulletin of Entomological Research*, 58(03), 629–642.

McBride, C. S., Baier, F., Omondi, A. B., Spitzer, S. a., Lutomiah, J., Sang, R., … Vosshall, L. B. (2014). Evolution of mosquito preference for humans linked to an odorant receptor. *Nature*, 515(7526), 222–227. https://doi.org/10.1038/nature13964

McIver, S. B. (1973). Fine structure of antennal sensilla coeloconica of culicine mosquitoes. *Tissue and Cell*, 5(1), 105–112. https://doi.org/10.1016/S0040-8166(73)80009-6

McMeniman, C. J., Corfas, R. A., Matthews, B. J., Ritchie, S. a, & Vosshall, L. B. (2014). Multimodal integration of carbon dioxide and other sensory cues drives mosquito attraction to humans. *Cell*, 156(5), 1060–1071. https://doi.org/10.1016/j.cell.2013.12.044

Meredith, M. A., & Stein, B. E. (1983). Interactions among converging sensory inputs in the superior colliculus. *Science*, 221(4608), 389–391. Retrieved from http://www.ncbi.nlm.nih.gov/pubmed/6867718

Mongeau, J. M., & Frye, M. A. (2017). *Drosophila* Spatiotemporally Integrates Visual Signals to Control Saccades. *Current Biology*, 27(19), 2901–2914.e2. https://doi.org/10.1016/j.cub.2017.08.035

Mongeau, J.-M., Cheng, K. Y., Aptekar, J., & Frye, M. A. (2019). Visuomotor strategies for object approach and aversion in *Drosophila melanogaster. The Journal of Experimental Biology*, 222(3), jeb193730. https://doi.org/10.1242/jeb.193730

Mu, L., Ito, K., Bacon, J. P., & Strausfeld, N. J. (2012). Optic Glomeruli and Their Inputs in *Drosophila* Share an Organizational Ground Pattern with the Antennal Lobes. Journal of Neuroscience, 32(18), 6061–6071. https://doi.org/10.1523/JNEUROSCI.0221-12.2012

Muir, L. E., Thorne, M. J., & Kay, B. H. (1992). *Aedes aegypti* (Diptera: Culicidae) vision: spectral sensitivity and other perceptual parameters of the female eye. Journal of Medical Entomology, 29(2), 278–281. Retrieved from http://www.ncbi.nlm.nih.gov/pubmed/1495042

Ohyama, T., Schneider-Mizell, C. M., Fetter, R. D., Aleman, J. V., Franconville, R., Rivera-Alba, M., … Zlatic, M. (2015). A multilevel multimodal circuit enhances action selection in *Drosophila. Nature*, 520(7549), 633–639. https://doi.org/10.1038/nature14297

Partan, S. R. (2013). Ten unanswered questions in multimodal communication. *Behavioral Ecology and Sociobiology*, 67(9), 1523–1539. https://doi.org/10.1007/s00265-013-1565-y

Pereira, T. D., Aldarondo, D. E., Willmore, L., Kislin, M., Wang, S. S.-H., Murthy, M., & Shaevitz, J. W. (2019). Fast animal pose estimation using deep neural networks. *Nature Methods*, 16(1), 117–125. https://doi.org/10.1038/s41592-018-0234-5

Raposo, D., Sheppard, J. P., Schrater, P. R., & Churchland, A. K. (2012). Multisensory Decision-Making in Rats and Humans*. Journal of Neuroscience*, 32(11), 3726–3735. https://doi.org/10.1523/JNEUROSCI.4998-11.2012

Reeves, L. E., Holderman, C. J., Blosser, E. M., Gillett-Kaufman, J. L., Kawahara, A. Y., Kaufman, P. E., & Burkett-Cadena, N. D. (2018). Identification of *Uranotaenia sapphirina* as a specialist of annelids broadens known mosquito host use patterns. *Communications Biology*, 1(1), 92. https://doi.org/10.1038/s42003-018-0096-5

Reiser, M. B., & Dickinson, M. H. (2008). A modular display system for insect behavioral neuroscience. *Journal of Neuroscience Metho*ds, 167(2), 127–139. https://doi.org/10.1016/j.jneumeth.2007.07.019

Riabinina, O., Task, D., Marr, E., Lin, C.-C., Alford, R., O'Brochta, D. A., & Potter, C. J. (2016). Organization of olfactory centres in the malaria mosquito *Anopheles gambiae. Nature Communications*, 7, 13010. https://doi.org/10.1038/ncomms13010

Ribeiro, I. M. A., Drews, M., Bahl, A., Machacek, C., Borst, A., & Dickson, B. J. (2018). Visual Projection Neurons Mediating Directed Courtship in *Drosophila. Cell*, 174(3), 607–621. https://doi.org/10.1016/j.cell.2018.06.020

Ruta, V., Datta, S. R., Vasconcelos, M. L., Freeland, J., Looger, L. L., & Axel, R. (2010). A dimorphic pheromone circuit in *Drosophila* from sensory input to descending output. *Nature*, 468(7324), 686–690. https://doi.org/10.1038/nature09554

Schrum, J., & Miikkulainen, R. (2014). Evolving multimodal behavior with modular neural networks in Ms. Pac-Man. In *Proceedings of the 2014 annual conference on genetic and evolutionary computation* (pp. 325–332). ACM. https://doi.org/10.1145/2576768.2598234

Schumacher, S., Burt de Perera, T., Thenert, J., & von der Emde, G. (2016). Cross-modal object recognition and dynamic weighting of sensory inputs in a fish. *Proceedings of the National Academy of Sciences*, 113(27), 7638-7643. https://doi.org/10.1073/pnas.1603120113

Seelig, J. D., & Jayaraman, V. (2013). Feature detection and orientation tuning in the *Drosophila* central complex. *Nature,* 503(7475), 262–266. https://doi.org/10.1038/nature12601

Seilheimer, R. L., Rosenberg, A., & Angelaki, D. E. (2014). Models and processes of multisensory cue combination. *Current Opinion in Neurobiology*, 25, 38–46. https://doi.org/10.1016/j.conb.2013.11.008

Silies, M., Gohl, D. M., & Clandinin, T. R. (2014). Motion-detecting circuits in flies: coming into view. *Annual Review of Neuroscience*, 37, 307–327. https://doi.org/10.1146/annurev-neuro-071013-013931

Smith, A. (1978). An investigation of the mechanisms underlying nest construction in the mud wasp *Paralastor sp.*(Hymenoptera: Eumenidae). *Animal Behaviour*, 26, 232–240. Retrieved from http://www.sciencedirect.com/science/article/pii/0003347278900234

Stein, B. E., & Stanford, T. R. (2008). Multisensory integration: Current issues from the perspective of the single neuron. *Nature Reviews Neuroscience*, 9(4), 255–266. https://doi.org/10.1038/nrn2331

Strausfeld, N. J., Sinakevitch, I., & Okamura, J.-Y. (2007). Organization of local interneurons in optic glomeruli of the dipterous visual system and comparisons with the antennal lobes. *Developmental Neurobiology*, 67(10), 1267–1288. https://doi.org/10.1002/dneu.20396

Straw, A. D., & Dickinson, M. H. (2009). Motmot, an open-source toolkit for realtime video acquisition and analysis. *Source Code for Biology and Medicine*, 4(1), 5. https://doi.org/10.1186/1751-0473-4-5

Sturtevant, A. H. (1915). Experiments on sex recognition and the problem of sexual selection in *Drosoophilia. Journal of Animal Behavior*, 5(5), 351–366. https://doi.org/10.1037/h0074109

Suh, G. S. B., Wong, A. M., Hergarden, A. C., Wang, J. W., Simon, A. F., Benzer, S., … Anderson, D. J. (2004). A single population of olfactory sensory neurons mediates an innate avoidance behaviour in *Drosophila. Nature*, 431(7010), 854–859. https://doi.org/10.1038/nature02980

Suh, G. S. B., Ben-Tabou de Leon, S., Tanimoto, H., Fiala, A., Benzer, S., & Anderson, D. J. (2007). Light Activation of an Innate Olfactory Avoidance Response in *Drosophila. Current Biology*, 17(10), 905–908. https://doi.org/10.1016/j.cub.2007.04.046

Takken, W. (1991). The Role of Olfaction in Host-seeking of Mosquitoes: A Review. *International Journal of Tropical Insect Science*, 12(1-2-3), 287–295.

Taylor, B., & Jones, M. D. R. (1969). The circadian rhythm of flight activity in the mosquito *Aedes aegypti* (L.): the phase-setting effects of lights-on and light-off. *Journal of Experimental Biology*, 51(1), 59–70.

Theobald, J. C., Duistermars, B. J., Ringach, D. L., & Frye, M. A. (2004). Flies see second-order motion. *Current Biology*, 18(11), 1761–1765. https://doi.org/10.1016/j.cub.2004.09.050

Tinbergen, N. (1951). *The study of instinct*. New York: Clarendon Press.

van Breugel, F., Huda, A., & Dickinson, M. H. (2018). Distinct activity-gated pathways mediate attraction and aversion to CO_2 in *Drosophila. Nature*, 564(7736), 420–424. https://doi.org/10.1038/s41586-018-0732-8

van Breugel, F., Riffell, J., Fairhall, A., & Dickinson, M. H. (2015). Mosquitoes Use Vision to Associate Odor Plumes with Thermal Targets. *Current Biology*, 25(16), 2123–2129. https://doi.org/10.1016/j.cub.2015.06.046

Varela, N., Gaspar, M., Dias, S., & Vasconcelos, M. L. (2019). Avoidance response to CO_2 in the lateral horn. *PLoS Biology*, 17(1), e2006749. https://doi.org/10.1371/journal.pbio.2006749

Verhulst, N. O., Beijleveld, H., Qiu, Y. T., Maliepaard, C., Verduyn, W., Haasnoot, G. W., … Smallegange, R. C. (2013). Relation between HLA genes, human skin volatiles and attractiveness of humans to malaria mosquitoes. *Infection, Genetics and Evolution*, 18, 87–93. https://doi.org/10.1016/j.meegid.2013.05.009

Vinauger, C., Breugel, F. Van, Locke, L. T., Tobin, K. K. S., Michael, H., Fairhall, A., … Riffell, J. A. (2019). Visual-olfactory integration in the human disease vector mosquito, *Aedes aegypti*. *bioRxiv.* https://doi.org/10.1101/512996

Vogt, K., Aso, Y., Hige, T., Knapek, S., Ichinose, T., Friedrich, A. B., … Tanimoto, H. (2016). Direct neural pathways convey distinct visual information to *Drosophila* mushroom bodies. e*Life,* 5, e14009. https://doi.org/10.7554/eLife.14009

von Philipsborn, A. C., Liu, T., Yu, J. Y., Masser, C., Bidaye, S. S., & Dickson, B. J. (2011). Neuronal Control of *Drosophila* Courtship Song. *Neuron*, 69(3), 509–522. https://doi.org/10.1016/j.neuron.2011.01.011

Warren, T. L., Giraldo, Y. M., & Dickinson, M. H. (2019). Celestial navigation in *Drosophila. The Journal of Experimental Biology*, 222(Suppl 1), jeb186148. https://doi.org/10.1242/jeb.186148

Weber, J. N., Peterson, B. K., & Hoekstra, H. E. (2013). Discrete genetic modules are responsible for complex burrow evolution in *Peromyscus* mice. *Nature,* 493(7432), 402–405. https://doi.org/10.1038/nature11816

Wehner, R. (2013). Life as a cataglyphologist--and beyond. *Annual Review of Entomology*, 58, 1–18. https://doi.org/10.1146/annurev-ento-120811-153641

Wehner, R., & Labhart, T. (2006). Polarisation vision. In *Invertebrate Vision* (pp. 291–348).

Weir, P. T., & Dickinson, M. H. (2012). Flying *Drosophila* orient to sky polarization. *Current Biology*: CB, 22(1), 21–27. https://doi.org/10.1016/j.cub.2011.11.026

Wellington, W. G. (1974). Changes in Mosquito Flight Associated With Natural Changes in Polarized Light. *The Canadian Entomologist*, 106(9), 941–948. https://doi.org/10.4039/Ent106941-9

Wilkinson, L. K., Meredith, M. A., & Stein, B. E. (1996). The role of anterior ectosylvian cortex in cross-modality orientation and approach behavior. *Experimental Brain Research*, 112(1). https://doi.org/10.1007/BF00227172

Wu, M., Card, G. M., Morimoto, M. M., Reiser, M. B., Nern, A., Williamson, W. R., & Rubin, G. M. (2016). Visual projection neurons in the *Drosophila* lobula link feature detection to distinct behavioral programs. *eLife*, 5, e21022. https://doi.org/10.7554/elife.21022